(NASA-CR-166012) FULL-SCALE TESTING, PRODUCTION AND COST ANALYSIS DATA FOR THE ADVANCED COMPOSITE STABILIZER FOR BOEING 737 AIRCRAFT, VOLUME 2 Final Report (Boeing Commercial Airplane Co.) 102 p

N85-13915

Unclas

G3/24 24826

NASA Contractor Report 166012

FULL-SCALE TESTING, PRODUCTION, AND COST ANALYSIS DATA FOR THE ADVANCED COMPOSITE STABILIZER FOR BOEING 737 AIRCRAFT

VOLUME II—FINAL REPORT

MAR 1983
RECEIVED
NASA STI FACILITY
ACCESS DEPT.

R. B. Aniversario
S. T. Harvey
J. E. McCarty
J. T. Parsons
D. C. Peterson
L. D. Pritchett
D. R. Wilson
E. R. Woguli s

BOEING COMMERCIAL AIRPLANE COMPANY
P.O. BOX 3707, SEATTLE, WA 98124

CONTRACT NAS1-15025
December 1982

PUBLICLY RELEASED ON
JAN 1985

NASA
National Aeronautics and
Space Administration

Langley Research Center
Hampton Virginia 23665

1. Report No.
NASA CR-166012

2. Government Accession No.

3. Recipient's Catalog No.

4. Title and Subtitle
FULL-SCALE TESTING, PRODUCTION, AND COST ANALYSIS DATA FOR THE ADVANCED COMPOSITE STABILIZER FOR BOEING 737 AIRCRAFT, VOLUME II–FINAL REPORT

5. Report Date
December 1982

6. Performing Organization Code

7. Author(s)
R.B. Aniversario, S.T. Harvey, J.E. McCarty, J.T. Parsons, D.C. Peterson, L.D. Pritchett, D.R. Wilson, and E.R. Wogulis

8. Performing Organization Report No.
D6-46038-2

9. Performing Organization Name and Address
Boeing Commercial Airplane Company
P.O. Box 3707
Seattle, Washington 98124

10. Work Unit No.

11. Contract or Grant No.
NAS1-15025

12. Sponsoring Agency Name and Address
National Aeronautics and Space Administration
Washington, D.C. 20546

13. Type of Report and Period Covered
Contractor Report

14. Sponsoring Agency Code

15. Supplementary Notes
Langley Technical Monitor: A.J. Chapman
Final Report

16. Abstract
This report defines and discusses the development, testing, production activities, and associated costs that were required to produce five-and-one-half advanced-composite stabilizer shipsets for Boeing 737 aircraft.

17. Key Words (Suggested by Author(s))
advanced composites
long-term durability
structural integrity
weight savings

18. Distribution Statement
[redacted]

19. Security Classif. (of this report)	20. Security Classif. (of this page)	21. No. of Pages	22. Price
Unclassified	Unclassified	108	

N 305

[redacted]

NASA Contractor Report 166012

FULL-SCALE TESTING, PRODUCTION, AND COST ANALYSIS DATA FOR THE ADVANCED COMPOSITE STABILIZER FOR BOEING 737 AIRCRAFT

VOLUME II—FINAL REPORT

R. B. Aniversario
S. T. Harvey
J. E. McCarty
J. T. Parsons
D. C. Peterson
L. D. Pritchett
D. R. Wilson
E. P. Wogulis

BOEING COMMERCIAL AIRPLANE COMPANY
P.O. BOX 3707, SEATTLE, WA 98124

CONTRACT NAS1-15025

National Aeronautics and
Space Administration

Langley Research Center
Hampton, Virginia 23665

PRECEDING PAGE BLANK NOT FILMED

FOREWORD

This final technical report (vol. II) and a technical summary (vol. I, ref. 1) were prepared by the Boeing Commerical Airplane Company, Renton, Washington, under NASA Contract NAS1-15025. They cover work performed between July 1977 and December 1981. The program was sponsored by the National Aeronautics and Space Administration, Langley Research Center (NASA-LRC). Dr. H. A. Leybold, Marvin B. Dow, and Andrew J. Chapman were the NASA-LRC project managers.

The following Boeing personnel were principal contributors to the program:

Program Director
    S. T. Harvey

Design
    G. Ohgi
    R. J. Nicoli
    E. R. Wogulis
    W. C. Brown

Structural Analysis
    D. R. Wilson
    R. W. Johnson
    J. E. McCarty

Weight and Balance Analysis
    G. Nishimura
    J. T. Parsons
    R. E. Baum

Manufacturing Technology
    M. C. Garvey
    V. S. Thompson
    E. S. Jamison

Production Manager
    J. E. Gallant
    W. D. Grant

Technical Operations Manager
    L. D. Pritchett

Business Management
    C. M. Lytle
    M. R. Wiebe
    D. V. Chovil

ORIGINAL PAGE IS
OF POOR QUALITY

SUMMARY

This is the final report for the full-scale testing, production, and cost analysis data for the advanced composite stabilizer for the Boeing 737 aircraft. It covers, along with References 1, 2, and 3, all work performed on the program from its inception in July 1977 through its conclusion in December 1981.

The principal program objective was to design, produce, and test an advanced composite 737 stabilizer that would meet the same functional criteria as the existing metal stabilizer. A full-scale left-hand ground test article was chosen that was structurally complete with elevator, balance panels, leading edge, trailing edge, closure rib, and associated hardware. The upper and lower skins and stringers, front and rear spars, ribs, and trailing-edge beam were fabricated from graphite-epoxy materials. The test stabilizer was supported in a horizontal position by using a structural steel test fixture. The composite stabilizer initially was subjected to four static load cases. It sustained design limit (67% ultimate) load for these cases. Afterwards, cyclic spectrum loads equivalent to 120 000 flights or one-and-one-half lifetimes were applied to the test article. Included as part of the cyclic loading were 80 000 spectrum flights with simulated service and/or maintenance damage. No structural damage or flaw growth of inflicted damage was found. It also was subjected to a number of fail-safe tests, one of which indicated that additional reinforcement using a plate integral with the fail-safe lug strap, the lower lug strap, and the spar web was necessary.

At the successful conclusion of all ground testing, the composite stabilizer was exposed to lightning strike tests. The full-scale test program met all FAA certification requirements.

Ground vibration and flight tests were performed using a production 737 aircraft with a graphite-epoxy stabilizer installed. In both cases, the composite stabilizer functioned completely within the counterpart aluminum-stabilizer-required envelope. The Federal Aviation Regulation 25 (FAR 25) was completely satisfied, and FAA certification was achieved during August 1982 (ref. 4).

Another prime program objective was to gain simulated production experience. This was accomplished by producing five-and-one-half shipsets of stabilizers using advanced composite materials. Experience was gained in estimating, tool development, and fabrication processes. The graphite subcomponents were produced by Boeing's Fabrication Division at Auburn, Washington. Assembly was accomplished at the Boeing facility in Wichita, Kansas, using conventional tools. The production assembly tools could not be used because the graphite assembly had fewer parts. Overall production problems were minimal.

The final objective of the program was to obtain realistic production cost data for the five-and-one-half shipset production run. Of the total production expenditures, labor was 85%, and nonlabor was 15%. Production labor was 64% for fabrication, 30% for assembly, and 6% for manufacturing, research, and development. Material usage factors for the program were 2.8 lb for fabric and 1.8 lb for tape for each pound of flyaway weight. With automation, these factors could be appreciably reduced. Recurring costs for 200 shipsets of advanced composite 737 stabilizers are estimated to be $40.3 million.

The program was successful and well timed. The results will provide the necessary confidence for the company to commit use of graphite-composite structure in similar applications on future aircraft.

CONTENTS

Page

1.0 INTRODUCTION 1

2.0 SYMBOLS AND ABBREVIATIONS 3

3.0 ANALYSIS AND TEST 5

- 3.1 Full-Scale Ground Test 5
  - 3.1.1 Description of Test Article 5
  - 3.1.2 Description of Test Setup 5
  - 3.1.3 Test Loads 5
  - 3.1.4 Description of Tests Conducted 13
  - 3.1.5 Test Results. 21
- 3.2 Ground Vibration Test 33
- 3.3 Flight Tests 35
- 3.4 FAA Certification 40
- 3.5 Weights. 40
  - 3.5.1 Production Analysis 40
  - 3.5.2 Conclusions 41

4.0 PRODUCTION 45

- 4.1 Detail Tooling 45
- 4.2 Assembly Tooling 45
- 4.3 Component Manufacturing 46
  - 4.3.1 Component Statistics. 48
  - 4.3.2 Skin Panel Fabrication 48
  - 4.3.3 Spar Fabrication 51
  - 4.3.4 Fabrication Problems and Solutions. 58

Page

4.4 Assembly Operations 61

4.4.1 Assembly Schedules 68

4.4.2 Assembly Problems. 69

5.0 COST ANALYSIS 71

5.1 Labor Costs 72

5.2 Usage Factors 77

5.3 Conclusions 79

6.0 CONCLUSIONS. 81

7.0 REFERENCES 83

APPENDIX: FATIGUE SPECTRUM A-1

FIGURES

Page

1 Full-Scale Ground Test 6

2 Test Support Fixture—Full-Scale Ground Test 7

3 Test Setup—Full-Scale Ground Test. 7

4 Stabilizer Ground Test Setup—Bonded Pads and Evener System 8

5 Load Case 3710—Load Comparison 9

6 Load Case 4430—Load Comparison 10

7 Load Case 4761—Load Comparison 11

8 Load Case 4010—Load Comparison 12

9 Test Spectrum General Loading Sequence 13

10 Induced Damage Locations 16

11 Overall View of the Full-Scale Ground Test Stabilizer Used for Lightning Discharge Tests 17

12 Lightning Strike Zones 18

13 Lightning Test Waveform and Test Values—Zone 1A 19

14 Lightning Test Waveform and Test Values—Zone 1B 20

15 Lightning Test Discharge Positions—737 Horizontal Stabilizer Tip Section. 21

16 Lower Surface Skin Repair—Station 111.1, Stringer 10 23

17 Graphite Fiber Breakage—Upper Rear-Spar Lug 24

18 Strain Comparison Zones 25

19 Skin Panel Shear Strains—Station 75.1 26

Page

20 Skin Panel Shear Strains Between Rear Spar and Stringer 1 27

21 Spanwise Strain Comparisons 28

22 Spar Deflections—Calculated (ATLAS) Versus Measured (Test) 29

23 Failure Description. 30

24 Web Cracks—Forward Face 31

25 Web Cracks—Aft Face 31

26 Through-Thickness Cracks. 32

27 Through-Thickness Cracks—Edge View 32

28 Tensile Failure of Inboard Web. 33

29 Delamination of Face Plies 33

30 Finite Element and Strain Comparison 34

31 Rear-Spar Fail-Safe Steel Reinforcement Plate 35

32 Lightning Discharge Damage (Tests 1 and 2) 36

33 Lightning Discharge Damage (Tests 3 and 4) 36

34 Ground Vibration Test Setup. 38

35 Speed and Altitude Test Points. 38

36 Flutter Vane Installation 39

37 Weight and Time History 42

38 Bagging Procedure—No-Bleed Material 46

39 Cure Cycle—No-Bleed Material 47

40 Stabilizer Skin Panel in Layup 49

41 Closeup of I-Stiffeners Located on Skin Layup 49

42 I-Stiffened Skin Panel in Fabrication 50

Page

43 I-Stiffened Skin Panel After Cure 50

44 I-Stiffened Skin Panel Showing Spanwise Warp 51

45 Front-Spar Channel Layup Mandrel 52

46 Front-Spar Layup of Fillers in Lug Area 52

47 Front-Spar Halves After Cure 53

48 Front-Spar Caps After Cure 53

49 Front-Spar Final Bond Preparations 54

50 Front-Spar After Final Bond 54

51 Front-Spar Inboard End After Trim 55

52 Rear-Spar Channel Halves 55

53 Rear-Spar Closeup of Lug Area 56

54 Rear-Spar Preparation for Final Bond 56

55 Rear Spar After Final Bond and Chord Trim 57

56 Rear-Spar Preparation for Inboard End Trim 57

57 Spar Warpage 58

58 Delamination in Stabilizer Upper Skin Panel 59

59 Stabilizer Typical Skin Panel/Stringer Layup 59

60 Spar Bonding 60

61 Left-Hand Rear-Spar Assembly—Aft Side View 62

62 Left-Hand Rear-Spar Assembly—Forward Side View 62

63 Left-Hand Rear Spar Located in Trailing-Edge Assembly Tool 63

64 Left-Hand Rear-Spar/Trailing-Edge Assembly 63

Page

65 Left-Hand Rear-Spar/Trailing-Edge Assemblies—Inboard End View of Advanced Composites (Left) and Metal (Right) 64

66 Left-Hand Rear-Spar/Trailing-Edge Assemblies—Outboard End View of Advanced Composites (Right) and Metal (Left) 64

67 Stabilizer During Fit Check to Production Elevator/Balance Panels 65

68 Left-Hand Trailing-Edge, Front-Spar, and Inspar Ribs in Major Assembly Tool—Inboard End View 66

69 Left-Hand Trailing-Edge, Front-Spar, and Inspar Ribs in Major Assembly Tool—Outboard End View. 66

70 Left-Hand Stabilizer Box With Lower Skin Panel in Place 67

71 Left-Hand Stabilizer Box With Upper Skin Panel in Place 67

72 Completed Stabilizers 68

73 Operation Phasing Summary 69

74 Total Recurring and Nonrecurring Production Costs by Major Element—5½ Shipsets. 71

75 Total Recurring and Nonrecurring Component Production Labor Hours—5½ Shipsets 73

76 Total Recurring and Nonrecurring Fabrication Labor Hours 75

77 Total Recurring and Nonrecurring Assembly Labor Hours—5½ Shipsets 77

78 Fabrication and Assembly Recurring Costs (Percentage of Labor Hours)—5 Shipsets. 78

79 Relative Composite Stabilizer Cost Comparison—Initial 200 Shipsets 79

TABLES

Page

1 Damage Location and Description 15

2 Fail-Safe Load Cases 17

3 Inspection Schedule 22

4 Aluminum Versus Graphite-Epoxy Stabilizer Mode Comparison 37

5 Metal and Graphite-Epoxy Horizontal Stabilizers—Inspar Structure Weight Comparison 41

6 Predicted and Actual Composite Stabilizer Inspar Structure Component Weights 43

7 Recurring Labor Hours—5 Shipsets 72

8 Component Production Labor Expenditures—Total Recurring and Nonrecurring (Excludes Tooling and Engineering) 74

9 Production Tooling 76

ORIGINAL PAGE IS
OF POOR QUALITY

1.0 INTRODUCTION

The escalation of aircraft fuel prices has motivated assessment of new technology concepts for designing and building commercial aircraft. Advanced composite materials, if used extensively in airframe components, offer high potential for reducing structural weight and thereby direct operating costs of commercial transport aircraft. To achieve the goal of production commitments to advanced composite structures, there is a need to convincingly demonstrate that these structures save weight, possess long-term durability, and can be fabricated at costs competitive with conventional metal structures.

To meet this need, NASA has established a program for composite structures under the Aircraft Energy Efficiency (ACEE) program. As part of this program, Boeing has redesigned and fabricated the horizontal stabilizer of the 737 transport using composite materials, has submitted data to FAA, and has obtained certification. Five shipsets of composite stabilizers have been manufactured to establish a firm basis for estimating production costs and to provide sufficient units for evaluation in airline service. This work has been performed under NASA Contract NAS1-15025.

The broad objective of the ACEE Composite Structures program is to accelerate the use of composite structures in new transport aircraft by developing technology and processes for early progressive introduction of composite structures into production commercial transport aircraft. Specific objectives of the 737 Composite Horizontal Stabilizer program were to:

- Provide structural weight at least 20% less than the metal stabilizer
- Fabricate at least 40% by weight of the stabilizer constituent parts from advanced composite materials
- Demonstrate cost competitiveness with the metal stabilizer
- Obtain FAA certification for the composite stabilizer
- Evaluate the composite stabilizer on aircraft in airline service

To achieve these objectives, Boeing concentrated efforts on conceiving, developing, and analyzing alternative stabilizer design concepts. After design selection, the following were performed: materials evaluation, ancillary tests to determine material design allowables, structural elements tests, and full-scale ground and flight tests to satisfy FAA certification requirements. Specific program activities to achieve objectives included:

- Program management and plan development
- Establishing design criteria
- Conceptual and preliminary design
- Manufacturing process development
- Material evaluation and selection
- Verification testing
- Detail design
- FAA certification

Work accomplished in each of these areas is described in detail in this document and summarized in Reference 1.

NOTE: Certain commercial products are identified in this document in order to specify adequately the characteristics of the material and components under investigation. In no case does such identification imply recommendation or endorsement of the product by NASA or Boeing, nor does it imply that the materials are necessarily the only ones available for the purpose.

2.0 SYMBOLS AND ABBREVIATIONS

ACEE	aircraft energy efficiency
ATLAS	computer program
℄	centerline
DUL	design ultimate load
EDI	electronic deflection indicators
FAA	Federal Aviation Administration
FAR	Federal Aviation Regulation
FEP	fluorinated ethylene propylene (Teflon)
LC	load case
MEK	methyl ethyl ketone
M_D	flight boundary, design dive speed, Mach number
MR&D	manufacturing research and development
MSCR	manufacturing specification and coordination record
V_D	flight boundary, design dive speed, knots equivalent air speed (keas)

PRECEDING PAGE BLANK NOT FILMED

3.0 ANALYSIS AND TEST

3.1 FULL-SCALE GROUND TEST

3.1.1 Description of Test Article

The test article was a left-hand, full-scale, Boeing model 737 graphite-epoxy horizontal stabilizer that was structurally complete with elevator, balance panels, leading edge, trailing edge, closure rib, and associated hardware. The upper and lower skins, front and rear spars, ribs, and trailing-edge beams were fabricated from graphite-epoxy material. Removable portions of the leading edge, trailing edge, tip, and elevator were existing 737 metal stabilizer components. A thermal compensation linkage also was added to the existing stabilizer structure to minimize thermal growth mismatch between the aluminum-fiberglass elevator and the graphite-epoxy inspar box. A detail description of the 737 graphite-epoxy stabilizer is included in Section 3.0 of Reference 3.

3.1.2 Description of Test Setup

The test stabilizer was supported in a horizontal position by a structural steel test fixture. The graphite-epoxy stabilizer assembly (test article) was attached to a metal production center section at the front- and rear-spar inboard terminal lug locations. A dummy right-hand stabilizer box was attached to the right-hand side of the center section and was used for symmetrical loading. The center section was supported by a structural test fixture at its aft support hinges and front dummy jackscrew fitting. The test setup is shown in Figures 1, 2, and 3.

Stabilizer airloads were applied to the lower and upper surface through pads bonded to the surface panels. The stabilizer inspar section, trailing-edge, and elevator surface areas were divided into sector areas with a load pad or fitting for each sector. Pad loads were applied through a series of evener systems and hydraulic actuators. The load pad locations and pad load distributions were optimized to match spanwise shear, moment, and torsion for each load case tested. Required leading-edge and balance panel loads matched shear and torsion about the front-spar and elevator hinge line respectively. Figure 4 shows the bonded pads and evener system used to apply loads to the lower panel.

Rosette strain gages (195) and axial strain gages (62) were installed to measure strains at critical areas and to verify internal load distributions. Structural deflections were measured at 18 locations along the front and rear spars by electronic deflection indicators (EDI).

Hydraulic jacks (16) were used to apply the tension and compression pad loads, leading-edge loads, and balance panel loads. A load cell was installed in series with each hydraulic jack to measure applied load.

3.1.3 Test Loads

3.1.3.1 Static Loads

The composite stabilizer was subjected to five static load cases (LC):

PAGE 4 INTENTIONALLY BLANK

ORIGINAL PAGE IS
OF POOR QUALITY

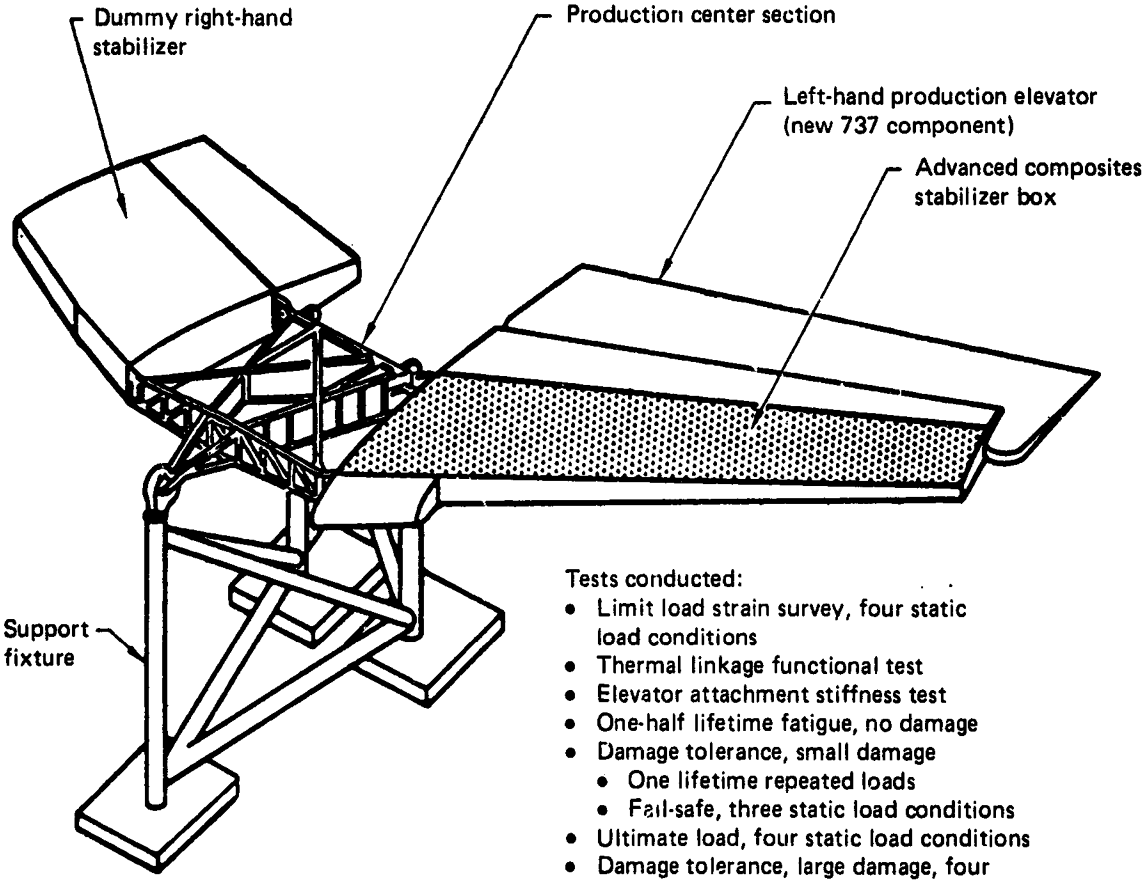
Dummy right-hand stabilizer
Production center section
Left-hand production elevator (new 737 component)
Advanced composites stabilizer box
Support fixture

Tests conducted:

- Limit load strain survey, four static load conditions
- Thermal linkage functional test
- Elevator attachment stiffness test
- One-half lifetime fatigue, no damage
- Damage tolerance, small damage
    - One lifetime repeated loads
    - Fail-safe, three static load conditions
- Ultimate load, four static load conditions
- Damage tolerance, large damage, four static load conditions
- Tip section subjected to lightning test

Figure 1. Full-Scale Ground Test

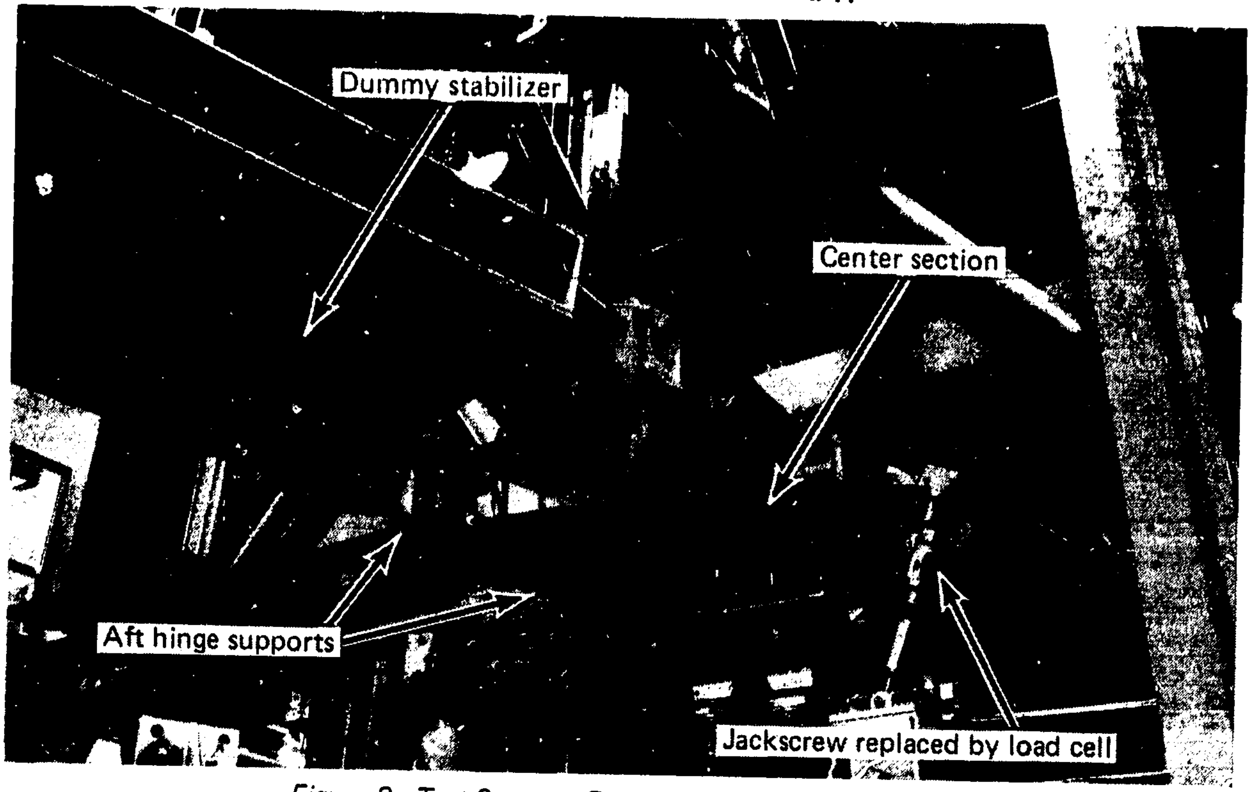
Dummy stabilizer
Center section
Aft hinge supports
Jackscrew replaced by load cell

Figure 2. Test Support Fixture—Full-Scale Ground Test

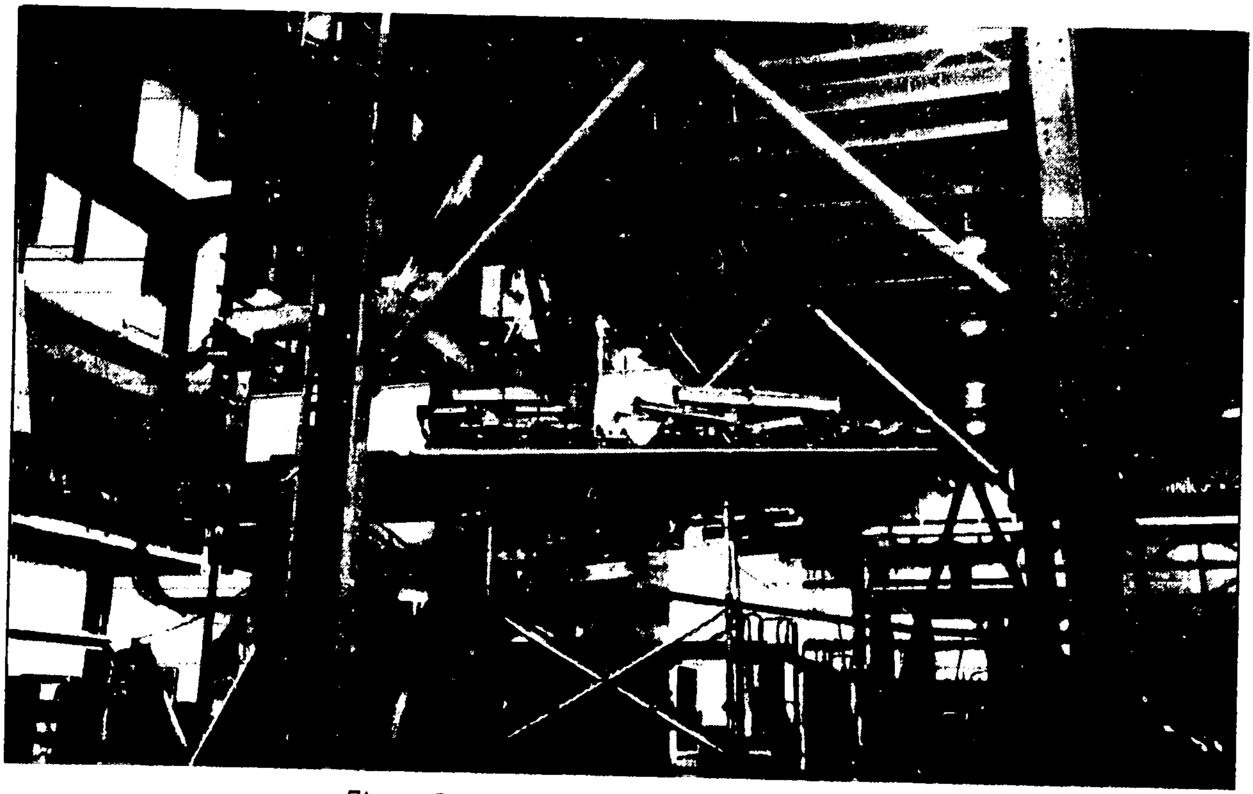

Figure 3. Test Setup—Full-Scale Ground Test

ORIGINAL PAGE
BLACK AND WHITE PHOTOGRAPH

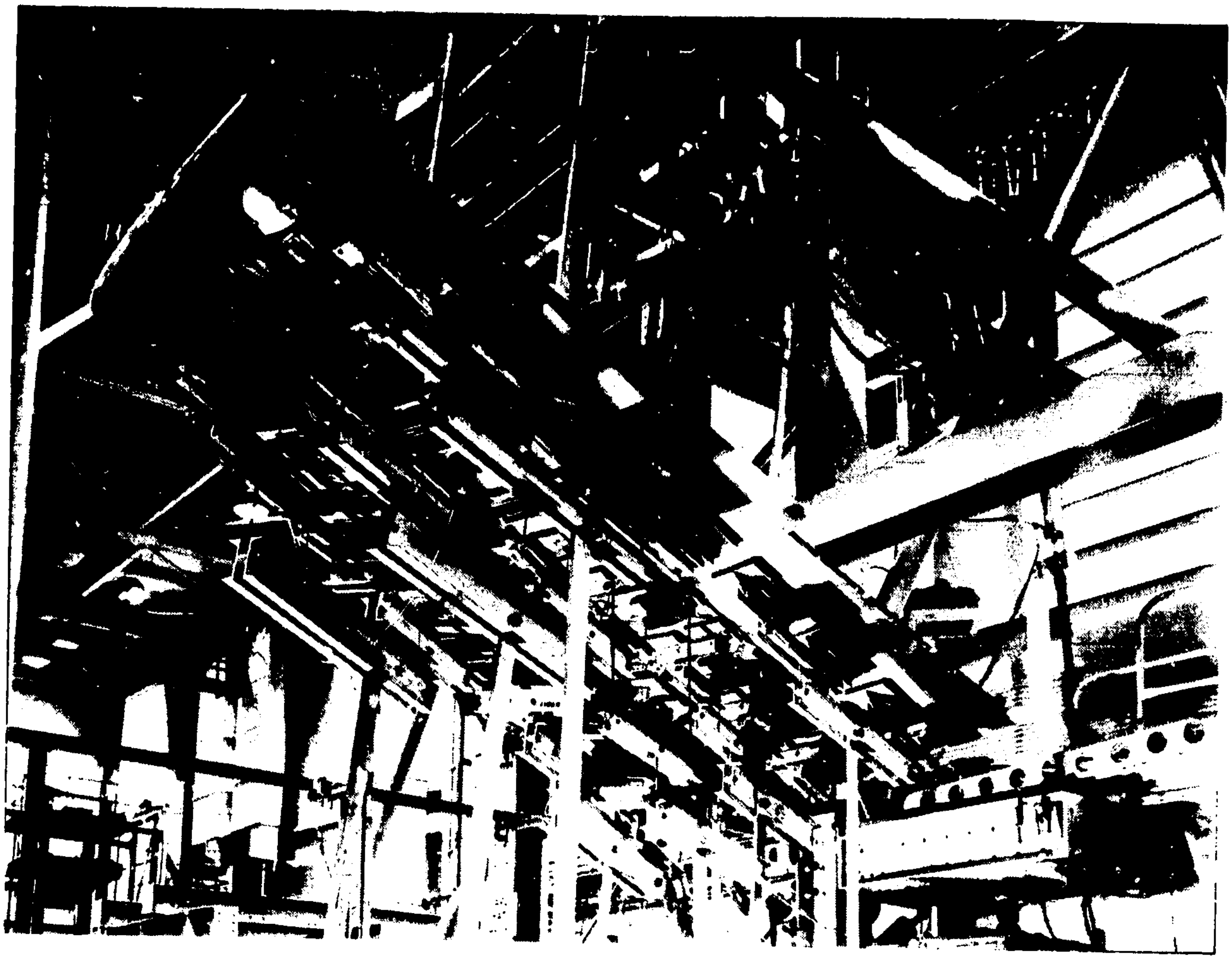

Figure 4. Stabilizer Ground Test Setup--Bonded Pads and Evener System

- Load case 5: positive maneuver at 648 km/hr (350 kn) at 7163m (23 500 ft); (load case 5 is at V_C and replaces load case 3710 as the torsion condition for damage tolerance tests.)
- Load case 3710: positive maneuver at 814 km/hr (440 kn) at 3018m (9900 ft) (maximum torsion, ultimate load test)
- Load case 4430: positive gust at 518 km/hr (280 kn) at sea level (maximum positive bending)
- Load case 4761: negative gust at 814 km/hr (440 kn) at 3962m (13 000 ft) (maximum negative bending and surface pressure, ultimate load test)
- Load case 4010: flaps down maneuver at 352 km/hr (190 kn) at sea level (maximum negative bending, ultimate and damage tolerance tests)

Comparisons of the applied test loads versus design loads are shown in Figures 5 through 8.

ORIGINAL PAGE IS
OF POOR QUALITY

ORIGINAL PAGE IS
OF POOR QUALITY

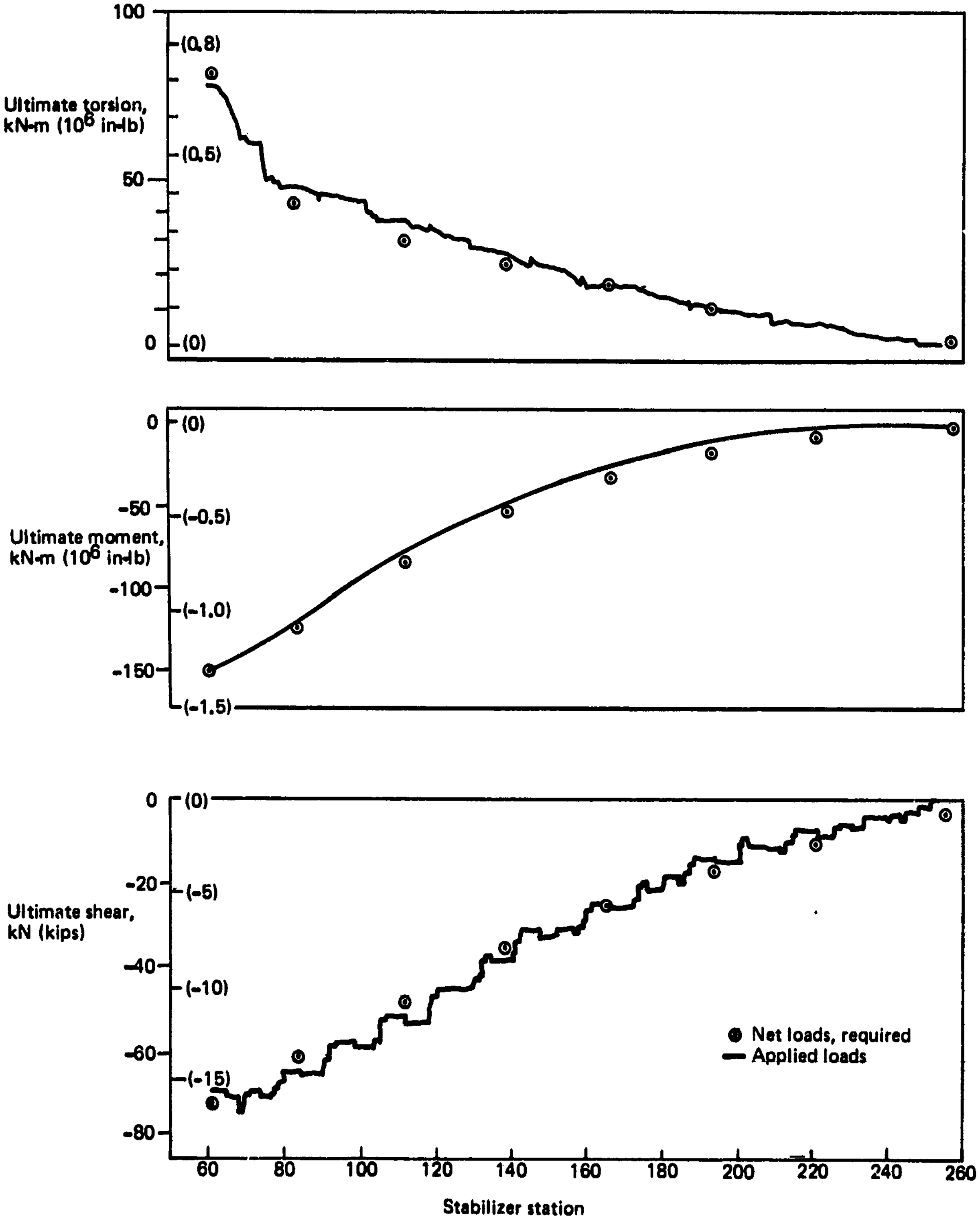

Figure 5. Load Case 3710—Load Comparison

ORIGINAL PAGE IS
OF POOR QUALITY

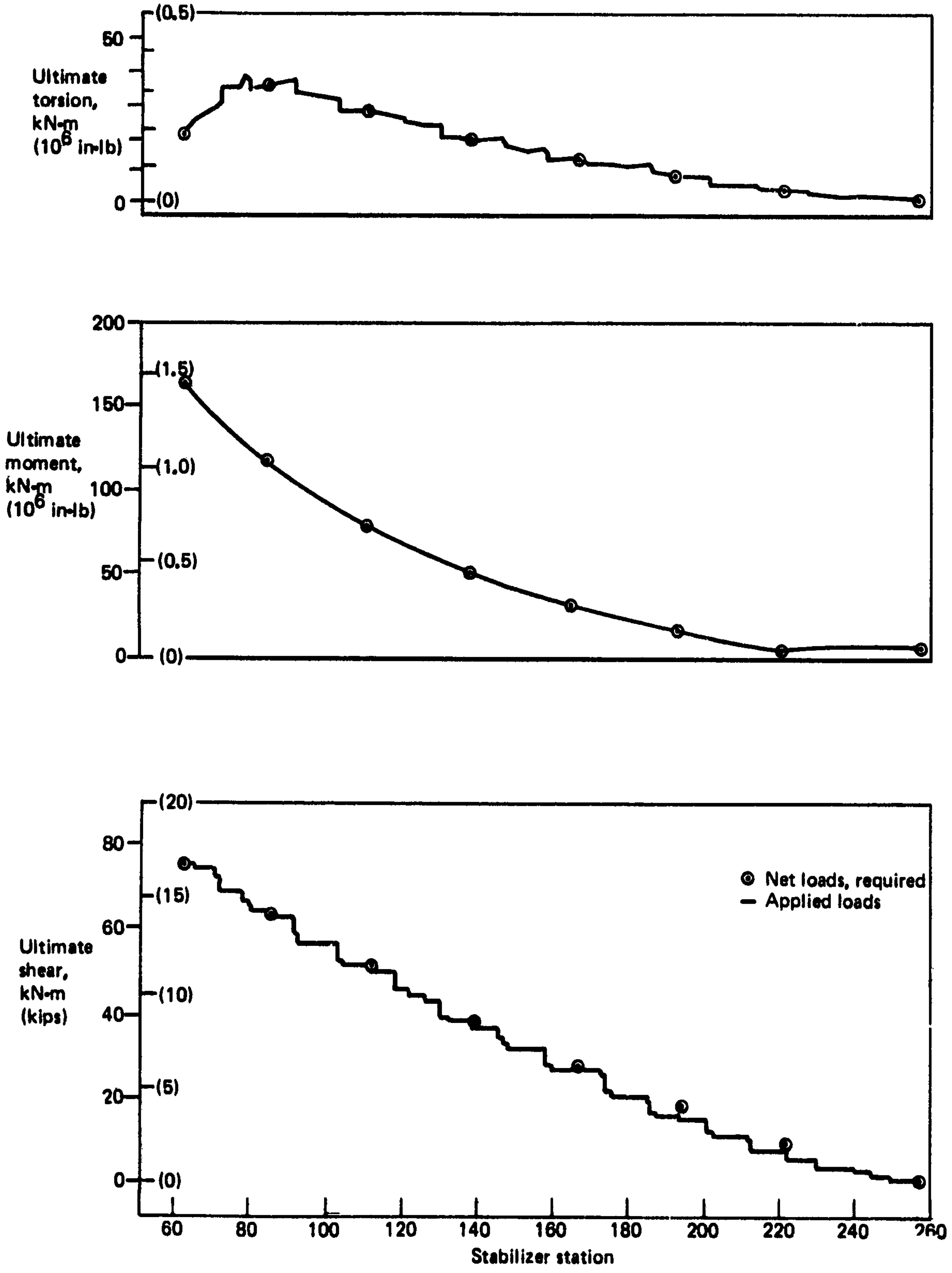

Figure 6. Load Case 4430—Load Comparison

ORIGINAL PAGE IS
OF POOR QUALITY

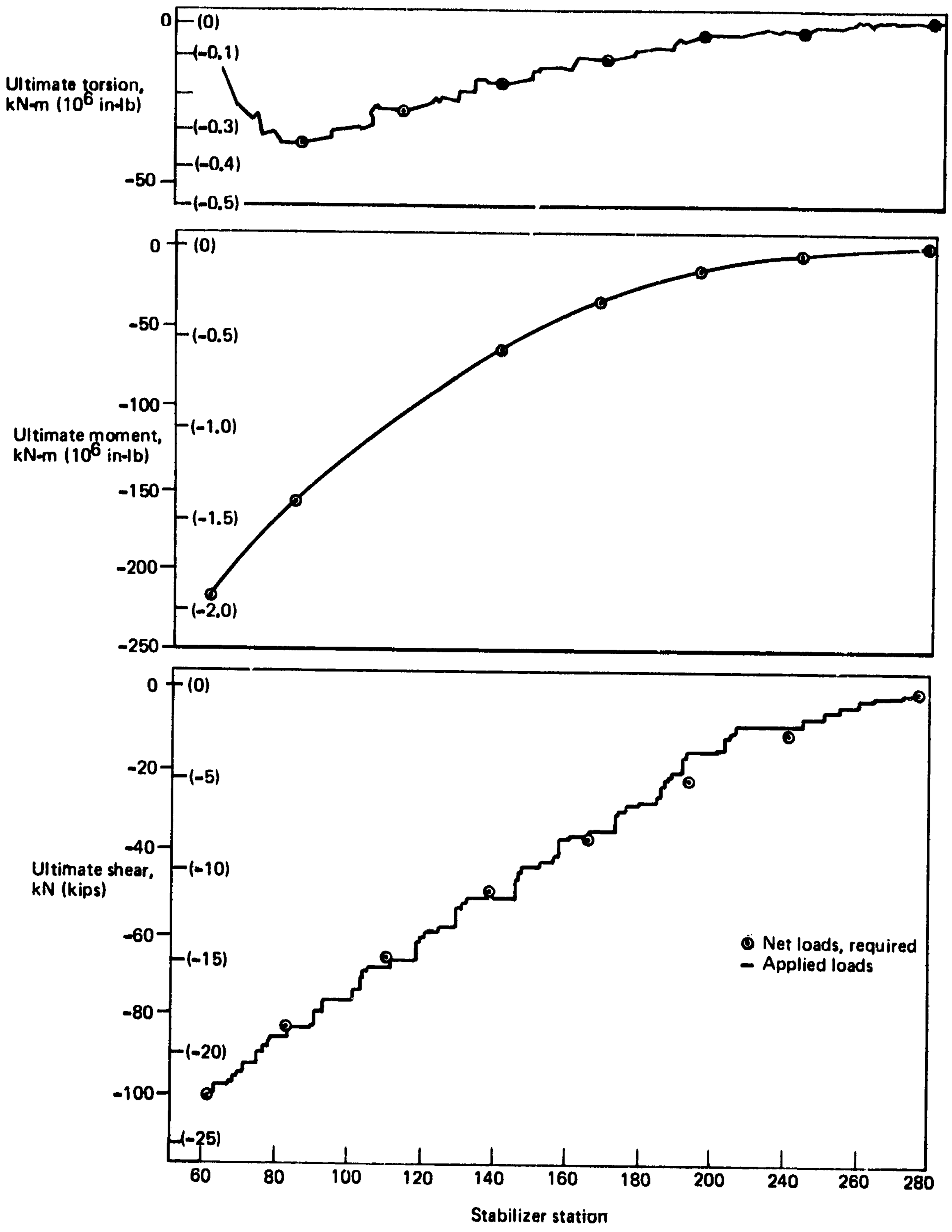

Figure 7. Load Case 4761 – Load Comparison

ORIGINAL PAGE IS
OF POOR QUALITY

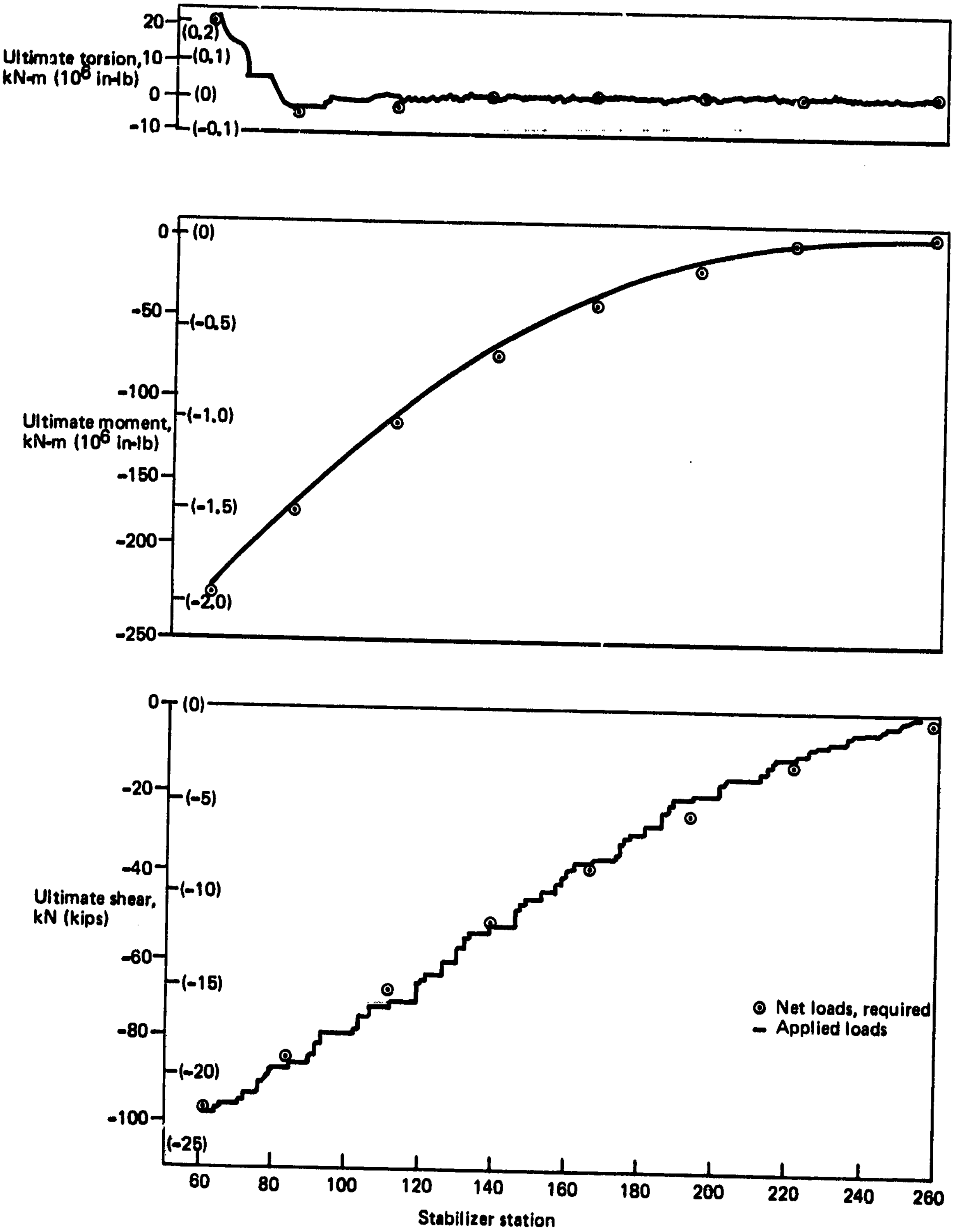

Figure 8. Load Case 4010—Load Comparison

ORIGINAL PAGE IS
OF POOR QUALITY

3.1.3.2 Cyclic Loads

The test flight profile was reduced to six major flight phases defined as taxi, takeoff, climb, cruise, descent, and landing. The taxi, takeoff, and landing phase alternating loads are of a relatively small magnitude and are represented by single excursions of the 1g load plus the secondary cycle excursion. Significant alternating load activity exists during climb, cruise, and descent phases, so these test phases contain an appropriate number of alternating load peaks about the 1g load levels. The resulting general load sequence is shown in Figure 9. A detailed description of the test flight profile loads can be found in the Appendix.

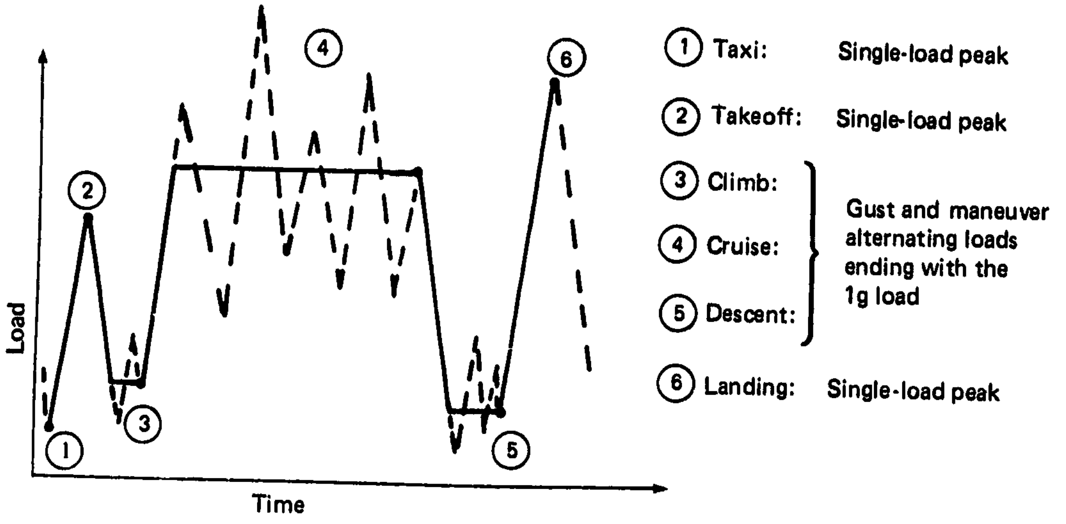
Load
Time
①
②
③
④
⑤
⑥
① Taxi: Single-load peak
② Takeoff: Single-load peak
③ Climb:
④ Cruise:
⑤ Descent:
Gust and maneuver alternating loads ending with the 1g load
⑥ Landing: Single-load peak

Figure 9. Test Spectrum General Loading Sequence

3.1.4 Description of Tests Conducted

The following tests were conducted (in the sequence listed) on the 737 graphite-epoxy stabilizer.

3.1.4.1 Design Limit Load Test

Design limit loads (67% of design ultimate loads) were applied to the stabilizer in each of four design load cases (3710, 4010, 4761, and 4430) to obtain strain and deflection data for correlation with the limit load requirements.

3.1.4.2 Elevator Stiffness Test

This test was performed to determine the lateral stiffness capability of the elevator hinge fitting at elevator station 121.59 with the primary hinge fitting at elevator station 39.02 failed. Load was applied parallel to the elevator hinge line at the elevator. The applied hinge line load and the amount of deflection between the elevator and stabilizer at the hinge line were measured and recorded.

3.1.4.3 Thermal Linkage Functional Test

This test was performed to measure the internal loads and determine the adequacy of the thermal compensation linkage to minimize thermal growth mismatch between the aluminum-fiberglass elevator and the graphite-epoxy inspar box. Radiant heat lamps and liquid nitrogen were used to heat and cool the thermal cavity up to 68°C (155°F) and down to -54°C (-65°F) respectively. This temperature range represented the maximum ground-air-ground thermal cycle. During the thermal cycle, temperatures in the cavity area and forces required to initiate elevator rotation were recorded.

3.1.4.4 One-Half Lifetime Fatigue Test

A total of 40 000 spectrum load flights, representing one-half lifetime of aircraft service, were applied to the stabilizer. Visual and ultrasonic inspections were performed at routine intervals, and strain and deflection data were recorded at specific flight intervals.

3.1.4.5 Damage Tolerance Tests—Small Damage

With simulated service and/or maintenance damage inflicted in selected areas, a total of 80 000 spectrum load flights representing one lifetime of aircraft service were applied to the stabilizer. The damage is defined in Table 1 and shown in Figure 10. Visual, ultrasonic, and X-ray inspections were performed at routine intervals, and strain and deflection data were recorded at specific flight intervals.

3.1.4.6 Ultimate Load Tests

Design ultimate loads were applied to the stabilizer in each of four design load cases (3710, 4430, 4761, 4010) to obtain strain and deflection data for comparison with the finite element ATLAS model generated strains and deflections.

3.1.4.7 Fail-Safe and Damage Tolerance Tests

Fail-safe tests, simulating failed spar-to-center-section attachment points, were performed by removing one of the spar attachment pins or bolts and applying the critical design limit load as a fail-safe load. The fail-safe load conditions are defined in Table 2. The damage tolerance capability of the stabilizer with large, simulated discrete damage (simulated failure of primary structural member in a major load path) was evaluated during the ancillary test program (sec. 4.2, ref. 3).

3.1.4.8 Lightning Discharge Test

This test was conducted to determine the type and extent of damage that would be sustained by a full-scale stabilizer and its flame spray lightning protection system when exposed to simulated lightning discharges. The test was performed with the full-scale ground test article after all structural testing was completed. The test article is shown in Figure 11. The lightning strike protection system was developed during the ancillary test program and is described in Section 4.2 of Reference 3.

The lightning strike zone locations for the 737 aircraft are defined in Section 3.2.9 of Reference 3. The outboard tip of the stabilizer is in a zone 1A area and was

ORIGINAL PAGE IS
OF POOR QUALITY

Table 1. Damage Location and Description

Damage ID No.	Location	Description
LS-1	Lower skin at stabilizer station 77 between the rear spar and stringer 1	Cut skin 12.7 mm (0.5 in) long at 45 deg to the rear spar. Simulates service damage
LS-2 and LS-3	Lower skin at stringer 1 and stabilizer station 111.1 rib intersection	Damaged skin in fastener countersink. Simulates delamination caused by improper fastener installation
LS-4	Lower skin to rear spar fastener at stabilizer station 80	(Same as LS-2)
LS-5	Lower skin at stringer 2 and stabilizer station 111.1 rib intersection	Impact damage. Simulates service damage ▷
LS-6	Lower skin stringer 2 inner chord between stabilizer stations 83.5 and 111.1	Impact damage. Simulates dropped tool during assembly ▷
LS-7	Lower skin along rear spar at stabilizer station 97.3	Impact damage. Simulates service damage ▷
LS-8	Lower skin along front spar at stabilizer station 97.3	Impact damage. Simulates service damage ▷
LS-9	Lower skin at the intersection of the rib at stabilizer station 111.1 and stringer 10	Impact damage. Simulates service damage ▷
US-1	Upper skin (same as LS-1)	Impact damage. Simulates dropped tool or hail damage ▷
US-2 and US-3	Upper skin (same as LS-2 and -3)	(Same as LS-2 and -3)
US-4	Upper skin (same as LS-4)	(Same as LS-2 and -3)
US-5	Upper skin (same as LS-7)	(Same as LS-7) ▷
US-6	Upper skin (same as LS-8)	(Same as LS-8) ▷
RS-1	Rear spar, edge of web cut out at stabilizer station 90	Impact damage. Simulates fabrication or service damage ▷
RS-2	Rear spar, edge of web cut out at stabilizer station 86	Web cut 6.4 mm (0.25 in) long. Simulates fatigue or service damage
RS-3	Rear spar chord forward flange at stabilizer station 72.5	Cut from flange edge to fastener hole. Simulates fatigue or service damage
RS-4	Rear spar web at stabilizer station 96	Impact damage. Simulates fatigue or service damage ▷
RS-5	Rear spar web at stabilizer station 99	Cut web 12.7 mm (0.5 in) long. Simulates fatigue or service damage
RS-6	Rear spar, lower chord, forward flange at stabilizer station 72, in radius adjacent to lug plate	Impact damage. Simulates fatigue or fabrication damage ▷
RS-7	Rear spar web at stabilizer station 170.5, 25.4 mm (1.0 in) above lower flange	Impact damage. Simulates fatigue or fabrication damage ▷
RS-8	Rear spar at stabilizer station 164, 25.4 mm (1.0 in) above lower flange	(Same as RS-7) ▷

▷ Impact damage. Detectable by visual inspection.

ORIGINAL PAGE IS
OF POOR QUALITY

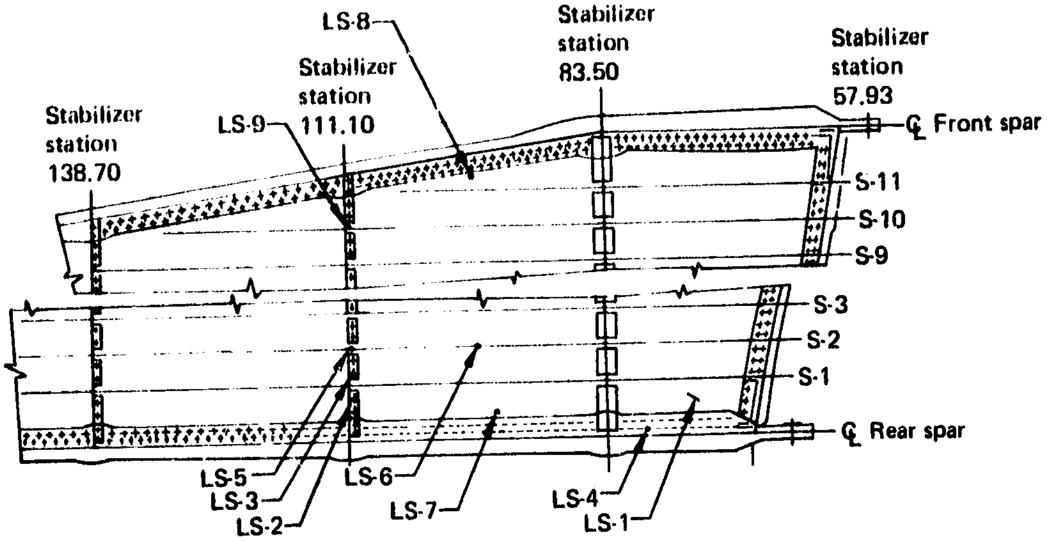
LS-8
Stabilizer station 83.50
Stabilizer station 57.93
Front spar
Stabilizer station 111.10
Stabilizer station 138.70
LS-9
S-11
S-10
S-9
S-3
S-2
S-1
Rear spar
LS-5
LS-3
LS-2
LS-6
LS-7
LS-4
LS-1

Lower Surface Damage Location

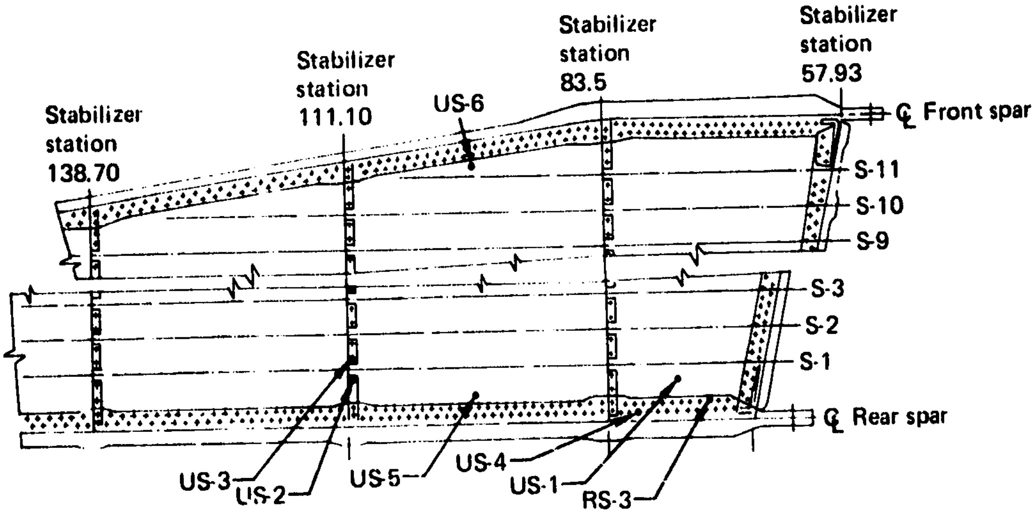
Stabilizer station 83.5
Stabilizer station 57.93
Stabilizer station 111.10
US-6
Front spar
Stabilizer station 138.70
S-11
S-10
S-9
S-3
S-2
S-1
Rear spar
US-3
US-2
US-5
US-4
US-1
RS-3

Upper Surface Damage Location

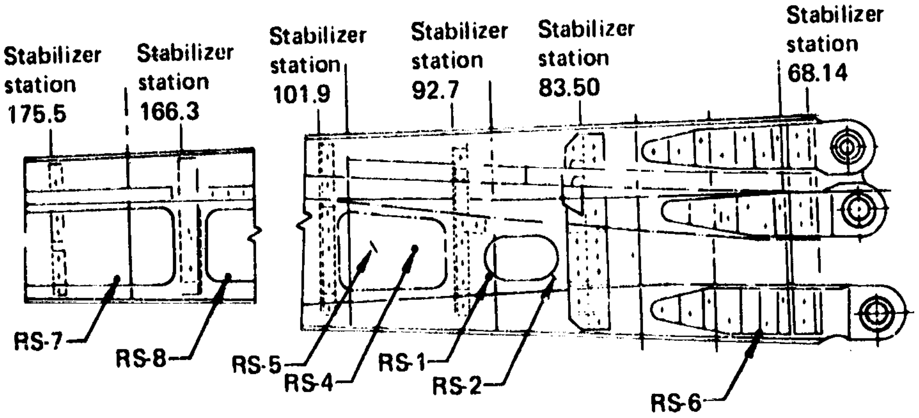
Stabilizer station 68.14
Stabilizer station 175.5
Stabilizer station 166.3
Stabilizer station 101.9
Stabilizer station 92.7
Stabilizer station 83.50
RS-7
RS-8
RS-5
RS-4
RS-1
RS-2
RS-6

Rear Spar Damage Location

Figure 10. Induced Damage Locations

ORIGINAL PAGE
BLACK AND WHITE PHOTOGRAPH

Table 2. Fail-Safe Load Cases

Test number	Bolt or pin removed	Load case applied
1	Front spar, lower	4430
2	Rear spar, lower	4430
3	Front spar, upper	4010
4	Rear spar, upper	4010

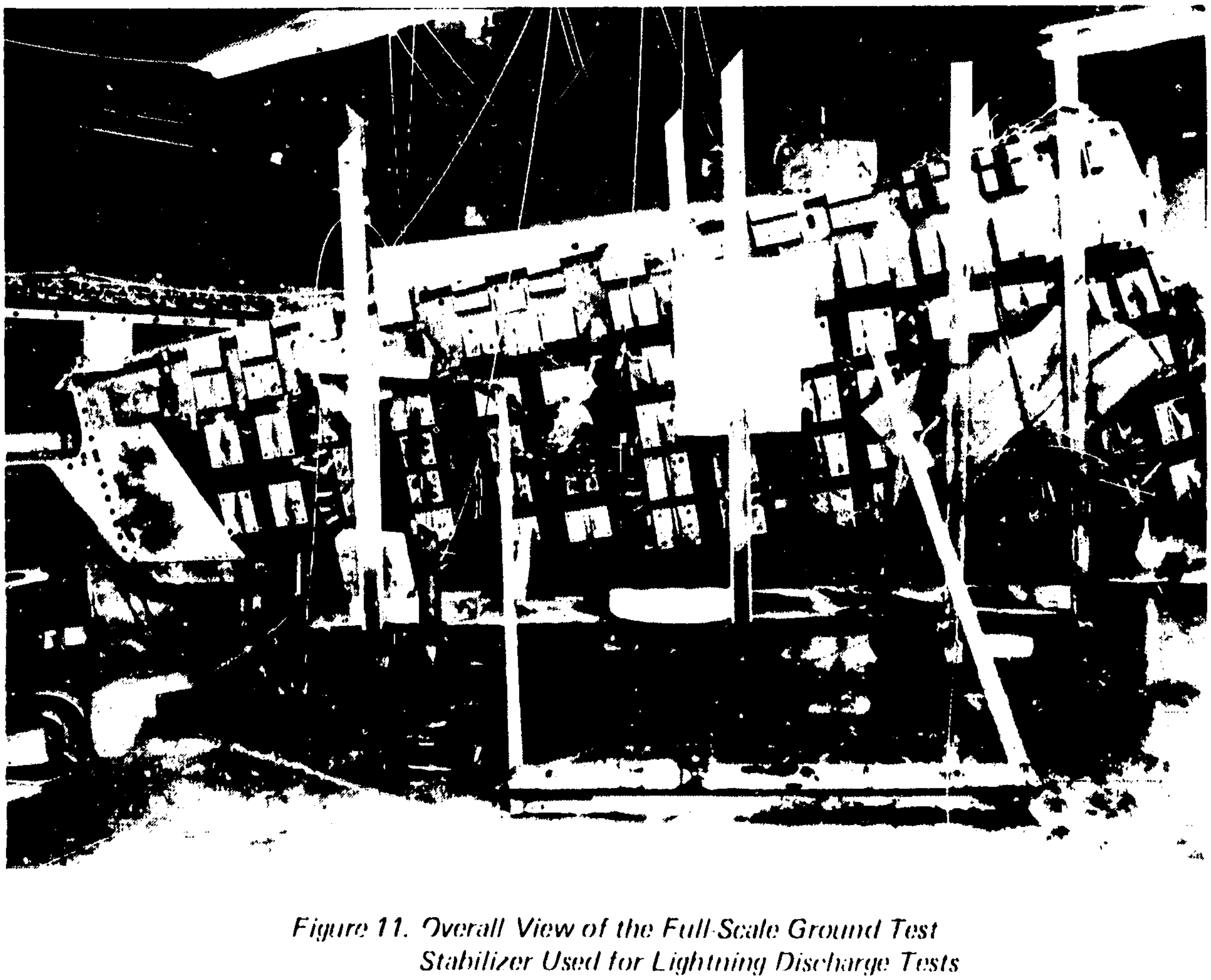

Figure 11. Overall View of the Full-Scale Ground Test Stabilizer Used for Lightning Discharge Tests

ORIGINAL PAGE IS
OF POOR QUALITY

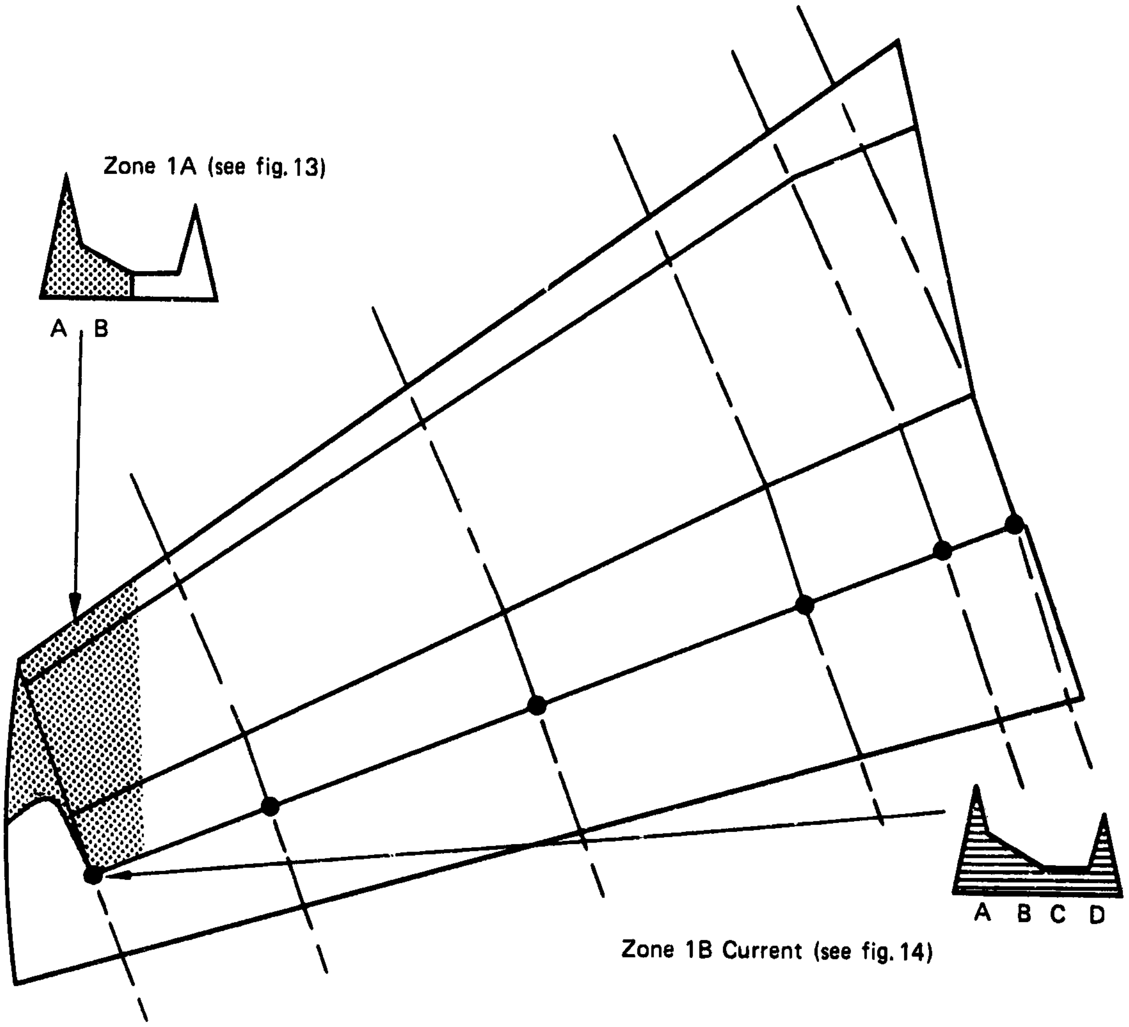

Figure 12. Lightning Strike Zones

tested accordingly. The outboard stabilizer hinge fittings for the elevator have to conduct zone 1B lightning current from the elevator into the stabilizer and were included in the test. Figure 12 defines the lightning strike zones for the stabilizer, and Figures 13 and 14 define the lightning test waveforms used.

A 7.62-cm (3-in) air gap was established between the discharge probe and the stabilizer tip for zone 1A discharges. Zone 1B lightning current was supplied by a hard-wired entry point through a hinge fitting location. The four attachment points (1 through 4) for the zone 1A lightning discharges and the hard-wired current entry point for the zone 1B lightning discharge current (5) are shown in Figure 15.

ORIGINAL PAGE IS OF POOR QUALITY

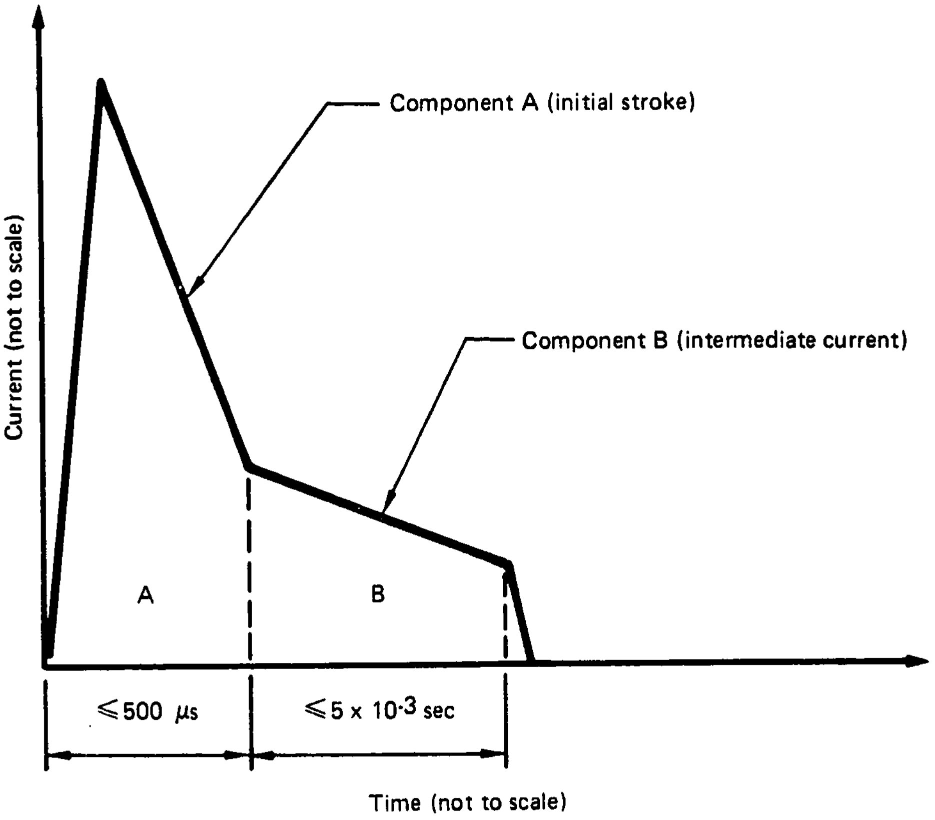
Component A (initial stroke)
Component B (intermediate current)
Current (not to scale)
A
B
≤500 μs
≤5 x 10-3 sec
Time (not to scale)

Test waveform	Parameter	Recommended test values*	Boeing test values			
			Test 1	Test 2	Test 3	Test 4
Component A	I_{peak} (amphere)	200 000 ±10%	154 690	171 880	187 500	189 060
	A (kiloamphere^2-sec)	2 000 ±20%	1 690	2 161	2 366	2 435
Component B	I_{avg} (amphere)	2 000 ±10%	1 701	1 924	1 893	1 916
	Q (coulomb)	10	8.5	9.6	9.5	9.6

*MIL-STD-1757

Figure 13. Lightning Test Waveform and Test Values—Zone 1A

ORIGINAL PAGE IS
OF POOR QUALITY

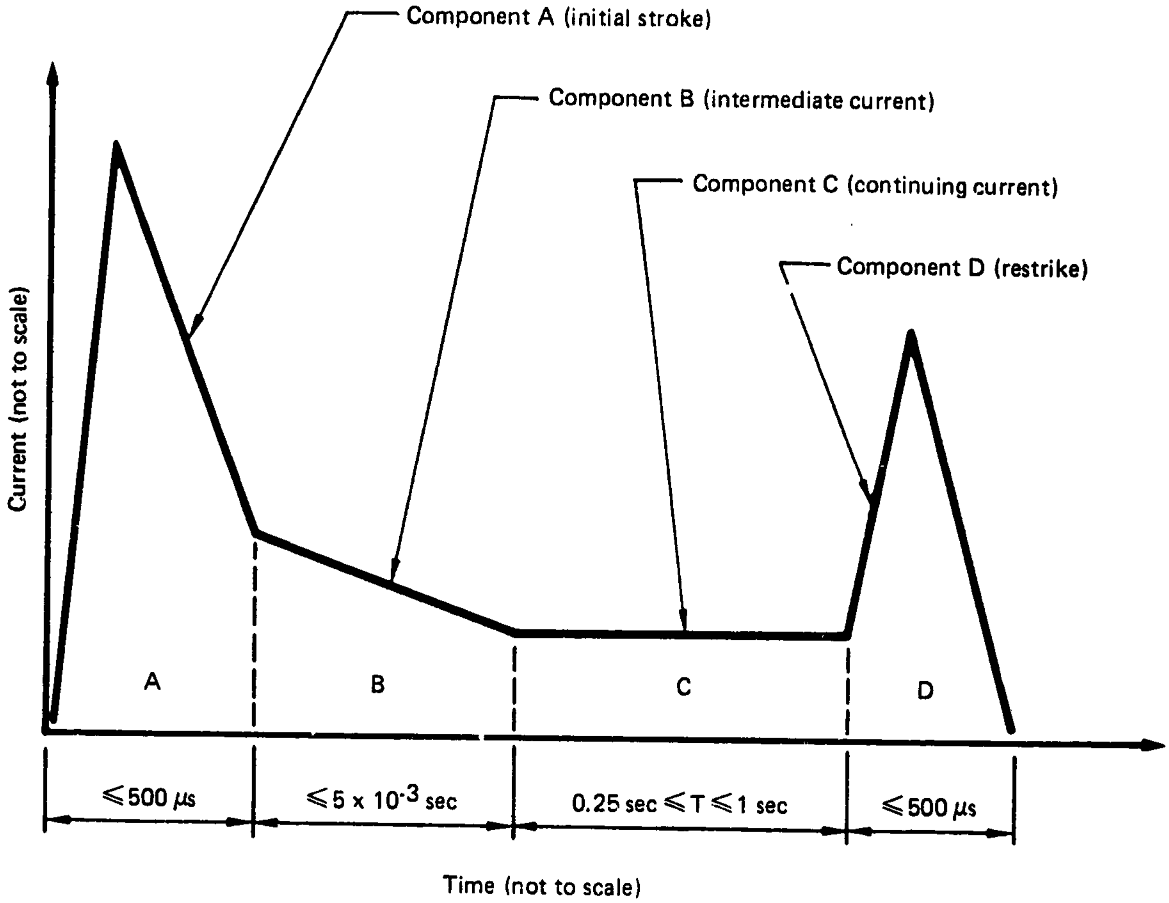
Component A (initial stroke)
Component B (intermediate current)
Component C (continuing current)
Component D (restrike)
Current (not to scale)
A
B
C
D
≤500 μs
≤5 x 10-3 sec
0.25 sec ≤T≤1 sec
≤500 μs
Time (not to scale)

Test waveform	Parameter	Recommended test values*	Boeing test value, test 5
Component A	I_{peak}(amphere)	200 000 ±10%	175 780
	A (kiloamphere^2-sec)	2 000 ±20%	2 551
Component B	I_{avg}(amphere)	2 000 ±10%	1 839
	Q (coulomb)	10	9.2
Component C	I_{avg}(amphere)	200 to 300	252
	Q (coulomb)	200 ±20%	205
Component D	I_{peak}(amphere)	100 000 ±10%	89 063
	A (kiloamphere^2-sec)	250 ±20%	243

*MIL-STD-1757

Figure 14. Lightning Test Waveform and Test Values—Zone 1B

ORIGINAL PAGE IS
OF POOR QUALITY

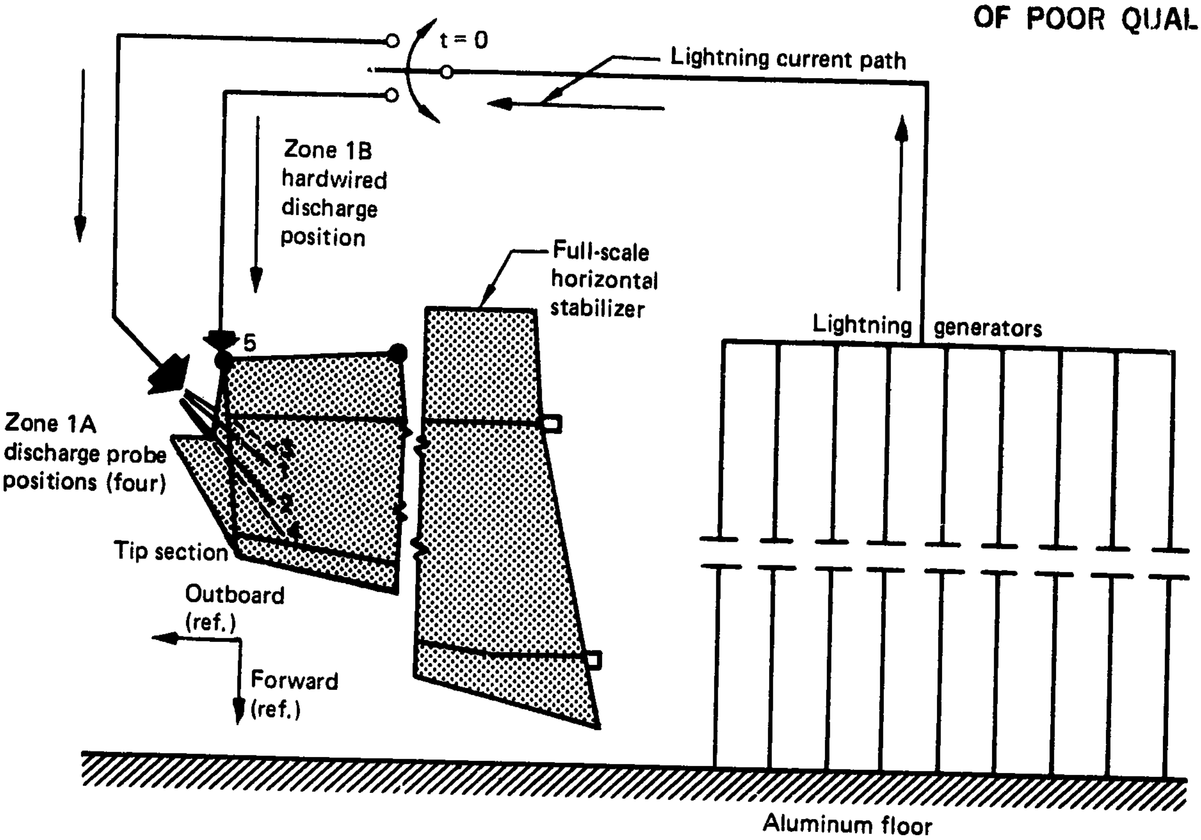

t = 0
Lightning current path
Zone 1B
hardwired
discharge
position
Full-scale
horizontal
stabilizer
Lightning generators
5
Zone 1A
discharge probe
positions (four)
1
2
3
4
Tip section
Outboard
(ref.)
Forward
(ref.)
Aluminum floor

Figure 15. Lightning Test Discharge Positions—737 Horizontal Stabilizer Tip Section

3.1.5 Test Results

3.1.5.1 Limit Load Test

The stabilizer was successfully tested to 67% of design ultimate load (DUL) for load cases 3710, 4010, 4761, and 4430 with no damage to the specimen. Strain, deflection, and load readings were recorded. Examination of measured strains and deflections showed agreement with the finite element ATLAS model values.

3.1.5.2 Elevator Stiffness Test

Analysis showed that with the primary hinge fitting at elevator station 39.02 failed, the secondary load path at station 121.59 must provide a stiffness of at least 0.88 MN/m (5000 lb/in). From the load versus deflection data recorded during this test, it was found that the elevator hinge line deflected 0.216 mm (0.0085 in) with a 3.8-kN (855-lb) load applied. Stiffness equals 17.6 MN/m (100 000 lb/in) or 20 times greater than required.

3.1.5.3 Thermal Linkage Functional Test

Test results showed that the load required to initiate rotation of the elevator varied by no more than 5% throughout the thermal cycle, thus demonstrating that the thermal linkage performed its design function.

ORIGINAL PAGE IS
OF POOR QUALITY

Table 3. Inspection Schedule

1000 flights	No [2] damage	0	10	20	30	[1] 40								
	With [3] damage					0	10	20	30	40	50	60	70	[1] 80
Visual inspection		X	X	X	X	X	X	X	X	X	X	X	X	X
Ultrasonic				X		X	X	X		X		X		X
X-ray						X				X				X
Strain survey		X		X		X	X	X		X		X		X

[1] Spectrum loading is applied in blocks of 10 000 flights. The half-life (37 500 flights) is exceeded in order to apply all loads included in the fourth block

[2] Fatigue test, half-life

[3] Damage tolerance test, one life with damage

3.1.5.4 One-Half-Lifetime Fatigue Test

The stabilizer was subjected to spectrum loads equivalent to 40 000 flights, representing one-half lifetime of aircraft service. During the testing, structural inspections were performed per the schedule shown in Table 3. A review of the strain gage and deflection data recorded during test showed no change, and no apparent damage was detected during the structural inspections.

3.1.5.5 Damage Tolerance Tests—Small Damage

The stabilizer was subjected to one full lifetime (80 000 flights) of spectrum loads with the simulated service and/or maintenance damage present as described in Section 3.1.4.5. During the testing, structural inspections were performed according to the schedule shown in Table 3. Results of inspections conducted before, during, and after application of one full lifetime of cyclic loads showed no flaw growth because of spectrum loading to any of the damaged areas or no change in original baseline inspections. Strain and deflection surveys were conducted, and comparisons with values from earlier surveys showed close agreement.

Upon completion of the repeated load and durability tests, residual strength with the induced damage as described in Section 3.1.4.5 was tested. The test article withstood application of limit load for load cases 4010, 4430, and 5 with the induced damage.

ORIGINAL PAGE
BLACK AND WHITE PHOTOGRAPH

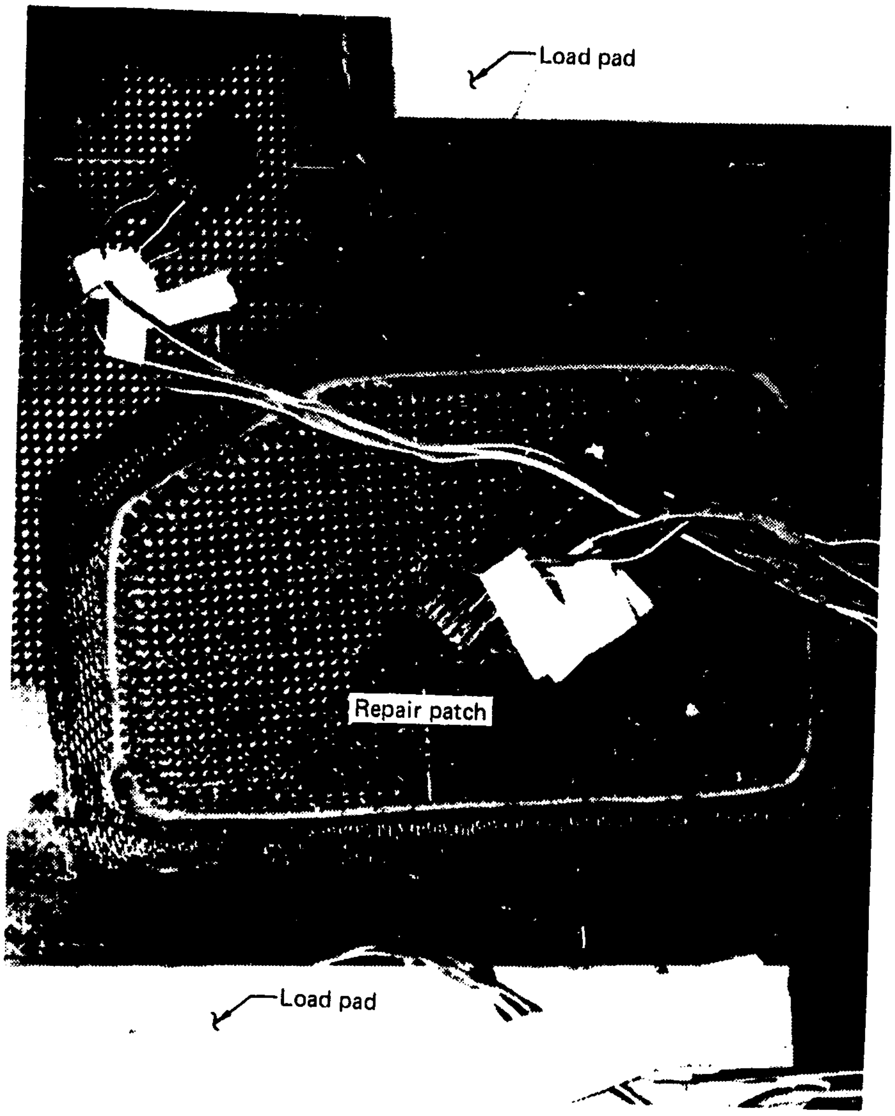

Figure 16. Lower Surface Skin Repair—Station 111.1, Stringer 10

3.1.5.6 Ultimate Load Tests

Load cases 3710 and 4430 were applied to 100% design ultimate load with no damage or failures occurring.

Loading was stopped at 67% of ultimate load case 4761 when high strain readings were noted in the area of inflicted damage at the skin lower surface, stabilizer station 111.10, and stringer 10 (LS 9, fig. 10). Damage in this area was repaired as shown in Figure 16. After the repair was made, ultimate load case 4761 was applied again. Test loading was halted when graphite fiber breakage occurred to the rear-spar upper terminal lug at 94.4% of design ultimate load. Graphite fiber

ORIGINAL PAGE
BLACK AND WHITE PHOTOGRAPH

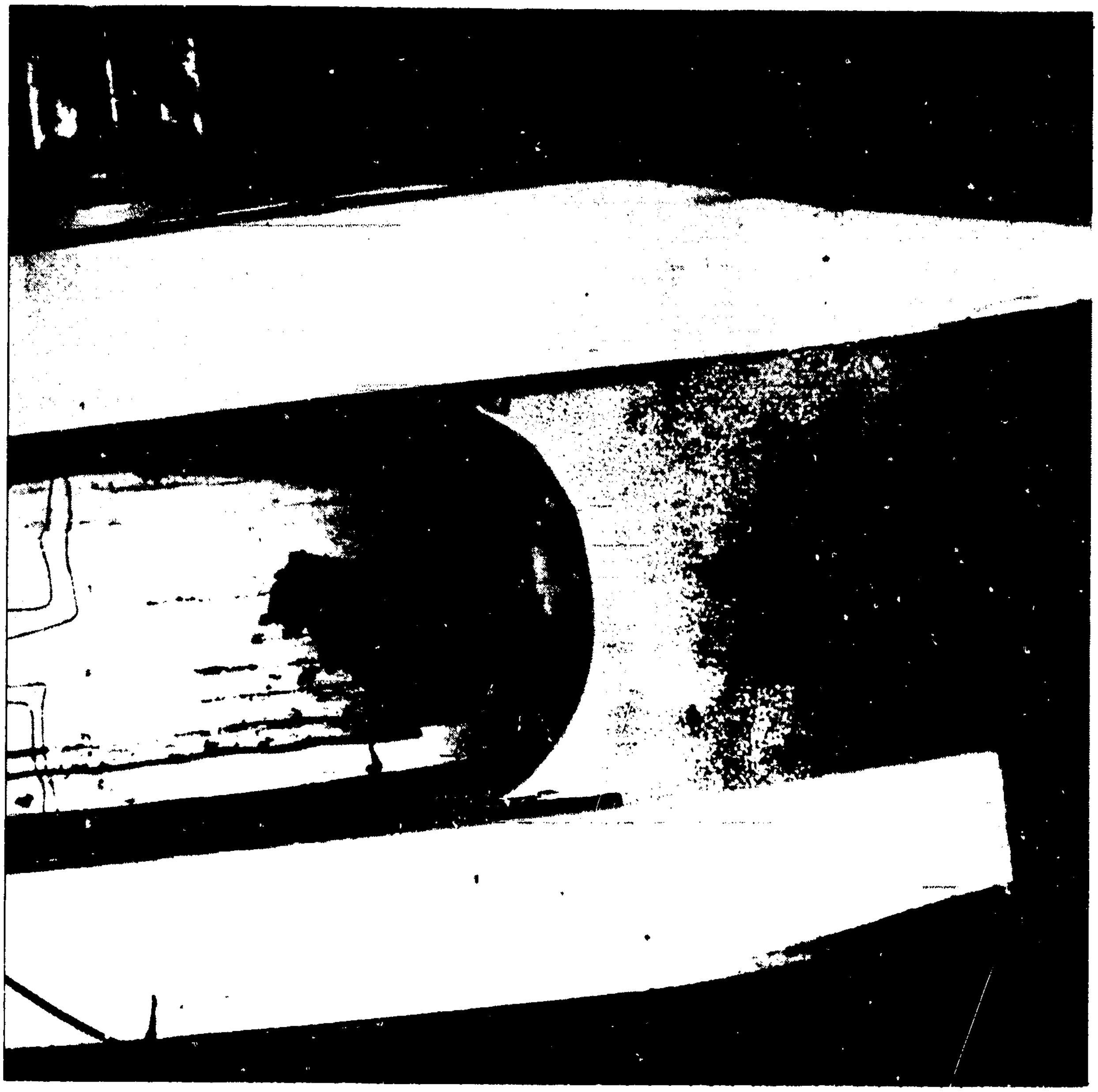

Figure 17. Graphite Fiber Breakage—Upper Rear-Spar Lug

breakage at this load level is predicted by component tests. The design includes lug reinforcement to sustain ultimate loads with the graphite damaged. The damaged area is shown in Figure 17. No repair was made to the rear-spar lug, and load case 4761 was applied to 100% of design ultimate load without failure.

Finally, ultimate load case 4010 was applied to 100% of design ultimate load, and no additional damage occurred.

**ORIGINAL PAGE IS
OF POOR QUALITY**

Figures 18 through 21 show strain comparisons, and Figure 22 shows deflection comparisons between the test stabilizer and the predicted finite element model values for load case 4010. Comparisons of test strains and deflections versus predicted finite element model strains and deflections for the other load conditions tested are similar to those shown for load case 4010.

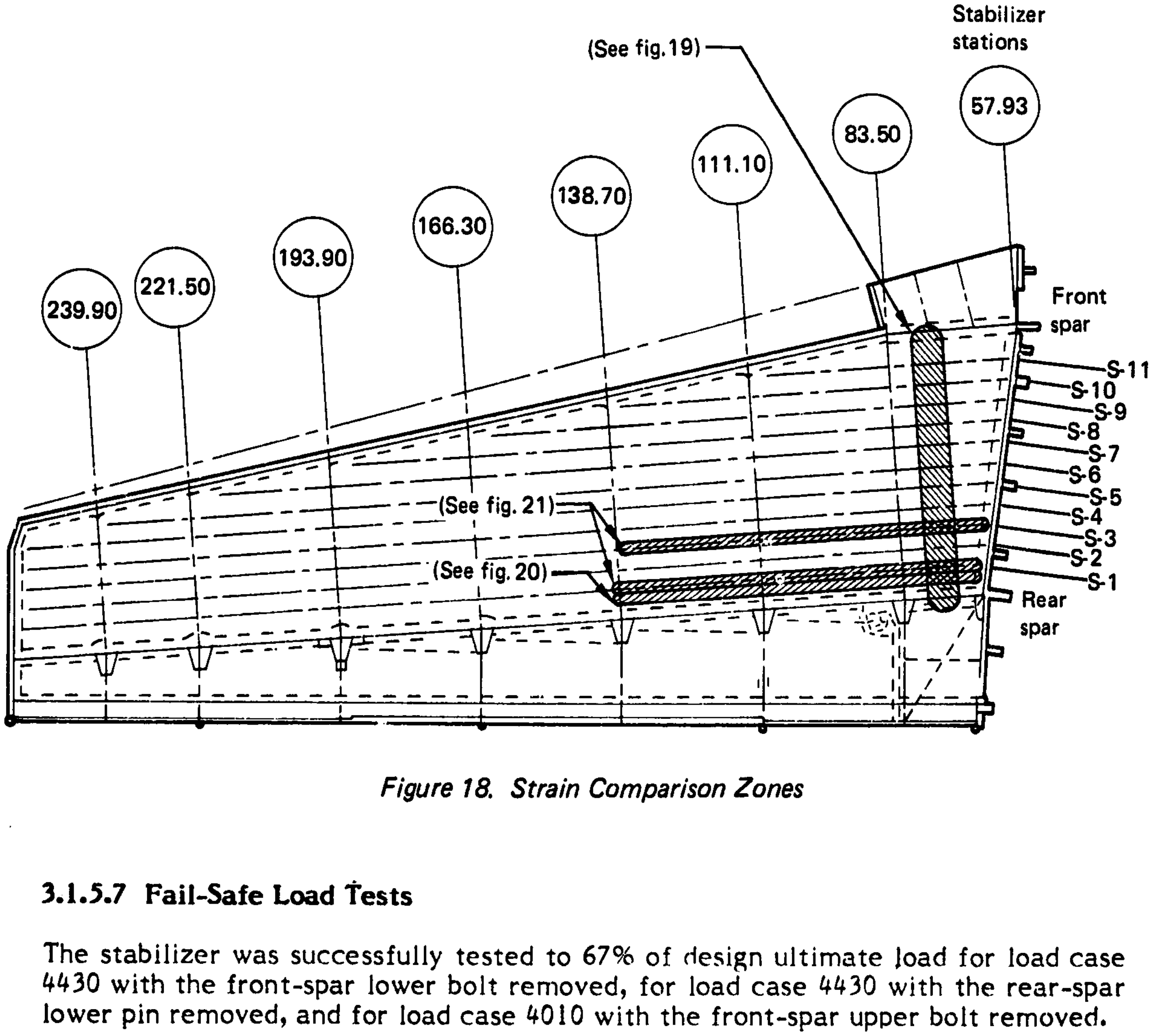
Stabilizer stations
57.93
83.50
111.10
138.70
166.30
193.90
221.50
239.90
(See fig. 19)
Front spar
S-11
S-10
S-9
S-8
S-7
S-6
S-5
S-4
S-3
S-2
S-1
Rear spar
(See fig. 21)
(See fig. 20)

Figure 18. Strain Comparison Zones

3.1.5.7 Fail-Safe Load Tests

The stabilizer was successfully tested to 67% of design ultimate load for load case 4430 with the front-spar lower bolt removed, for load case 4430 with the rear-spar lower pin removed, and for load case 4010 with the front-spar upper bolt removed.

During application of load case 4010 with the rear-spar upper pin removed, a shear failure of the rear-spar web between stabilizer station 68.14 and 96.0 occurred at 61% of design ultimate load (91% design limit load). The rear-spar failure was initiated by a tension failure of graphite-epoxy fibers in a direct line between the upper fail-safe lug and the lower lug. A description of the failure is summarized in Figure 23, and photos of the details are shown in Figures 24 through 29.

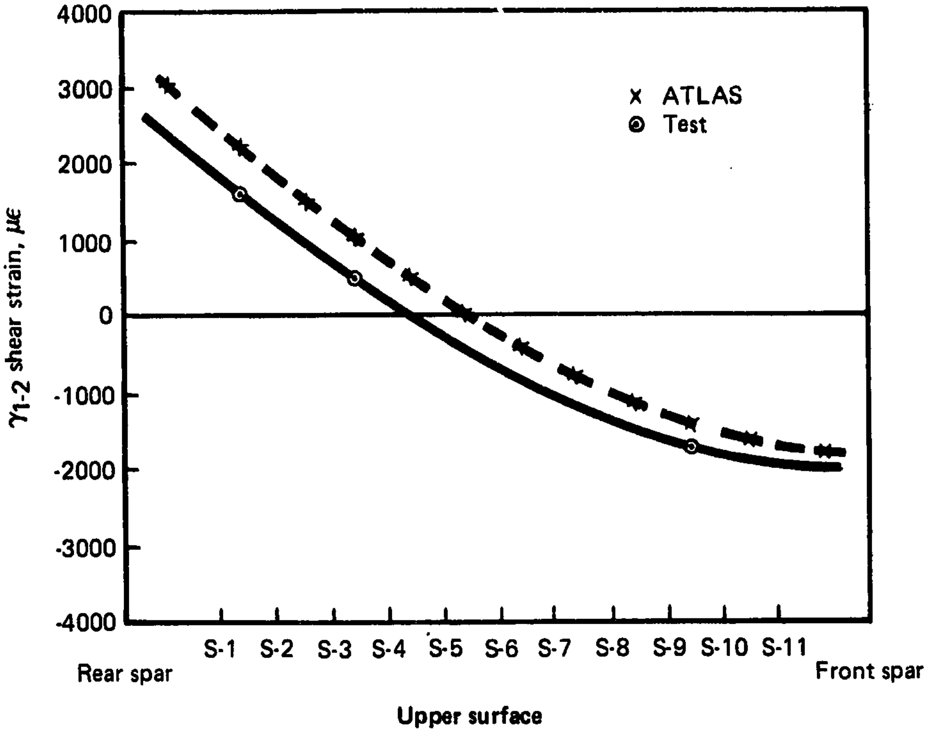

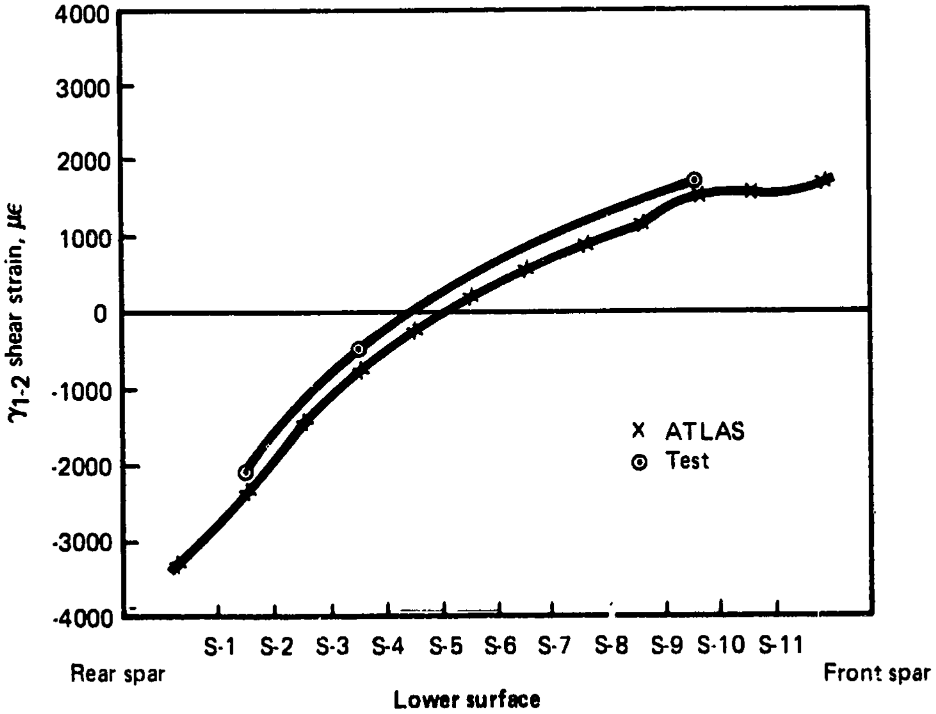

- Load condition 4010 (100% design ultimate load)

Figure 19. Skin Panel Shear Strains—Station 75.1

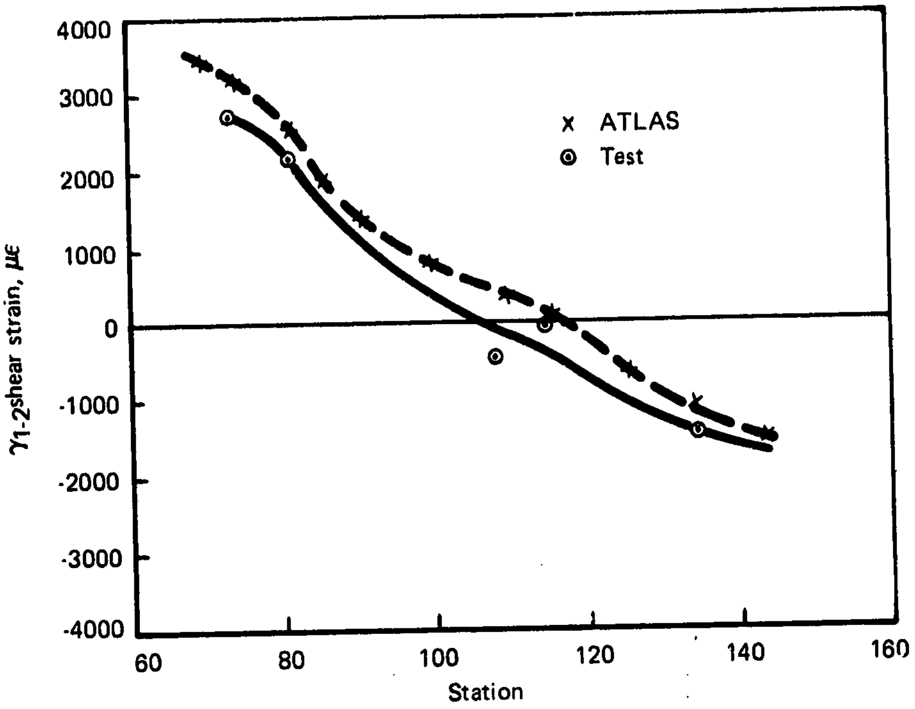

Upper surface

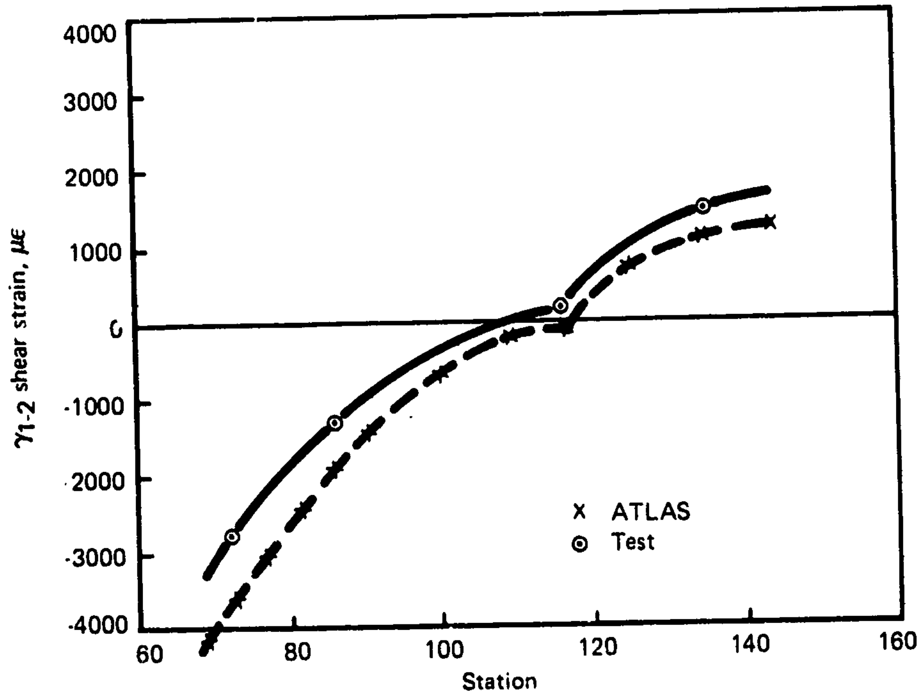

Lower surface

- Load condition 4010 (100% design ultimate load)

Figure 20. Skin Panel Shear Strains Between Rear Spar and Stringer 1

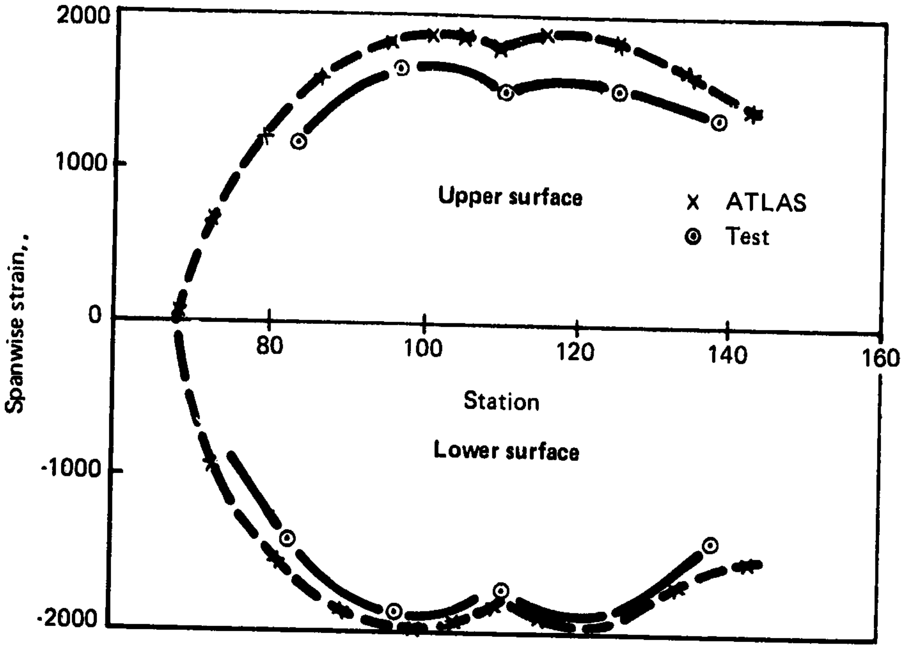

Spanwise strain along ℄ of stringer 1

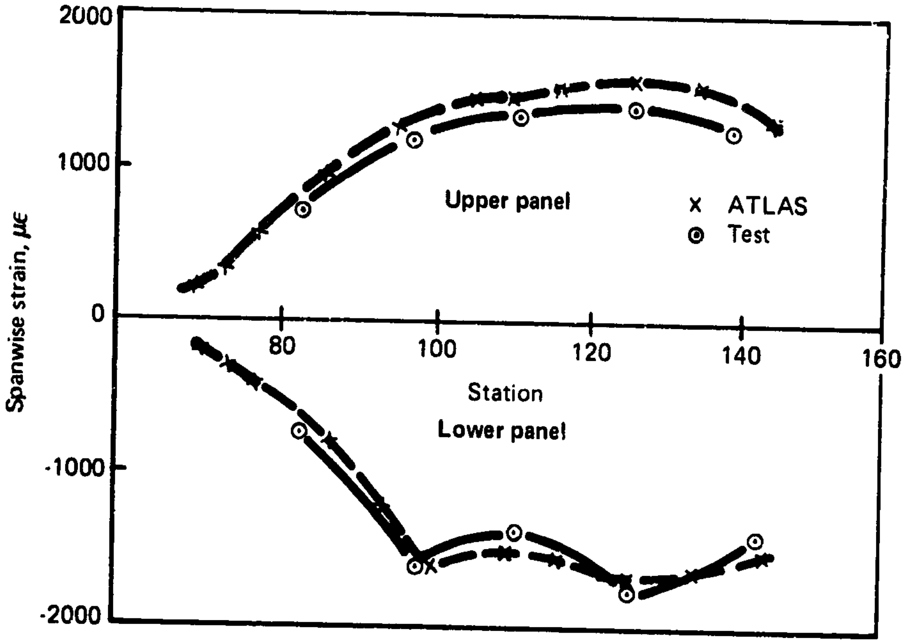

Spanwise strain along ℄ of stringer 3

- Load condition 4010 (ultimate)

Figure 21. Spanwise Strain Comparisons

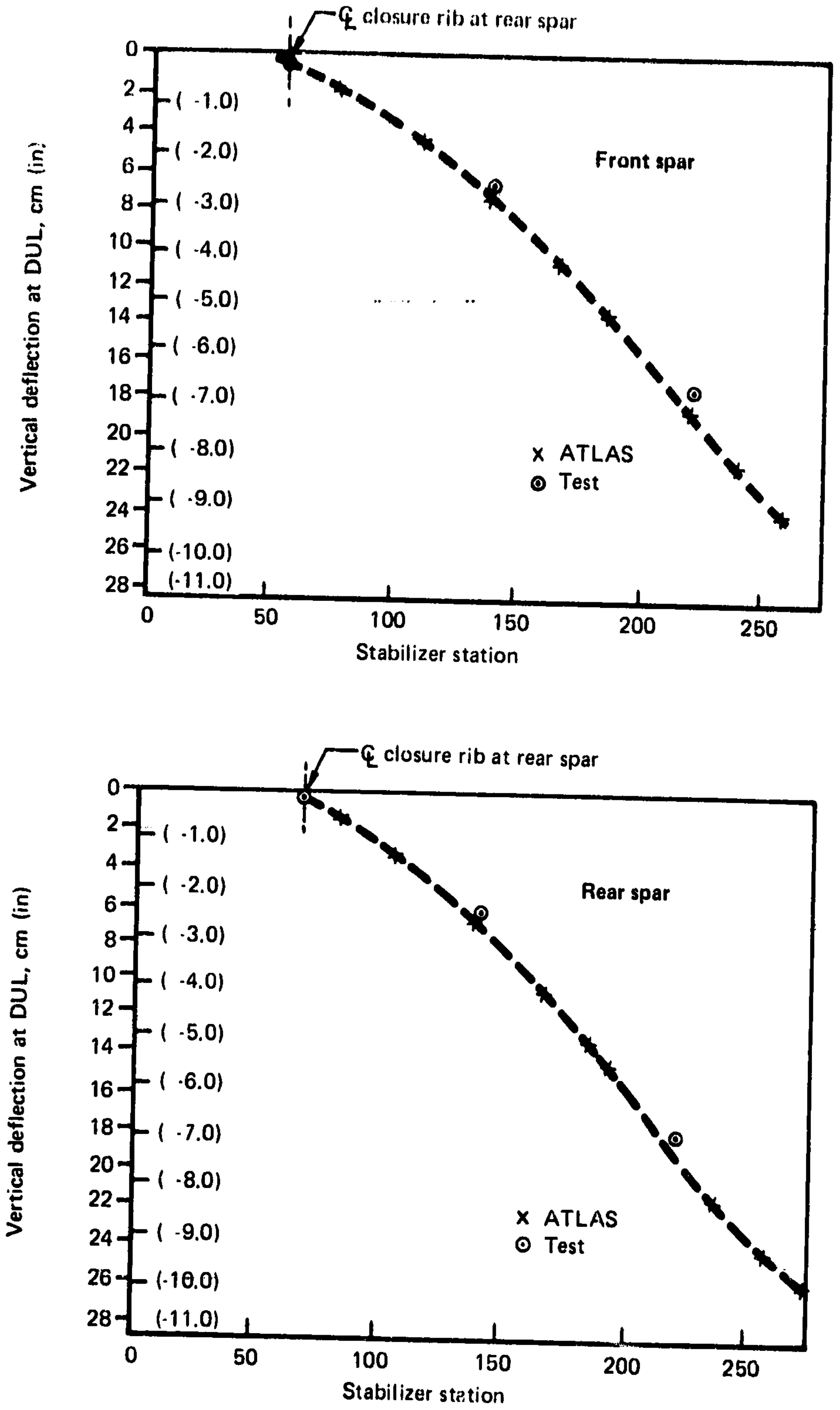

- Load condition 4010 (ultimate)

Figure 22. Spar Deflections—Calculated (ATLAS) Versus Measured (Test)

ORIGINAL PAGE IS
OF POOR QUALITY

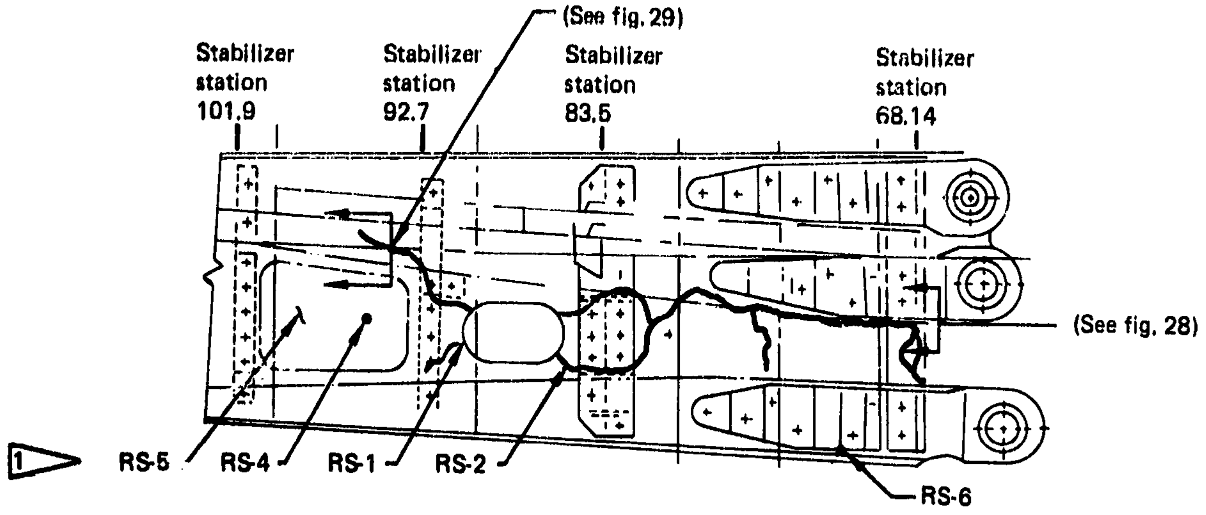
(See fig. 29)
Stabilizer station 101.9
Stabilizer station 92.7
Stabilizer station 83.5
Stabilizer station 68.14
(See fig. 28)
1
RS-5
RS-4
RS-1
RS-2
RS-6

Web cracks—forward face (see fig. 24)

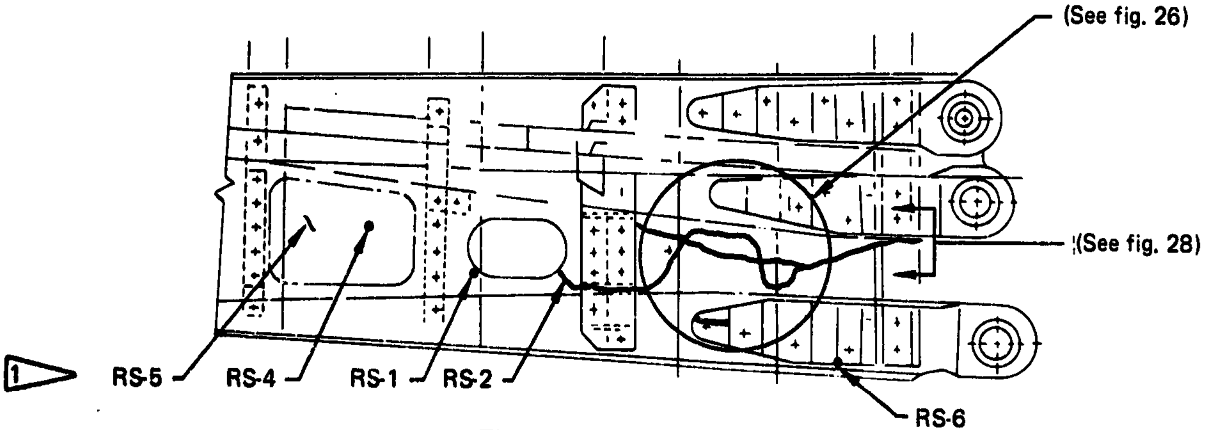
(See fig. 26)
(See fig. 28)
1
RS-5
RS-4
RS-1
RS-2
RS-6

Through-thickness crack

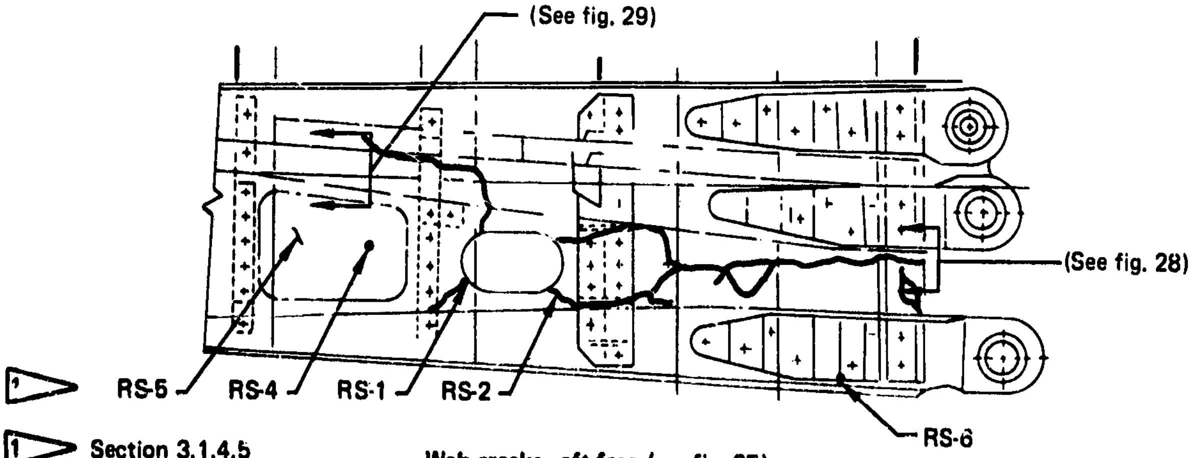
(See fig. 29)
(See fig. 28)
1
RS-5
RS-4
RS-1
RS-2
RS-6
1 Section 3.1.4.5

Web cracks—aft face (see fig. 25)

Figure 23. Failure Description

ORIGINAL PAGE
BLACK AND WHITE PHOTOGRAPH

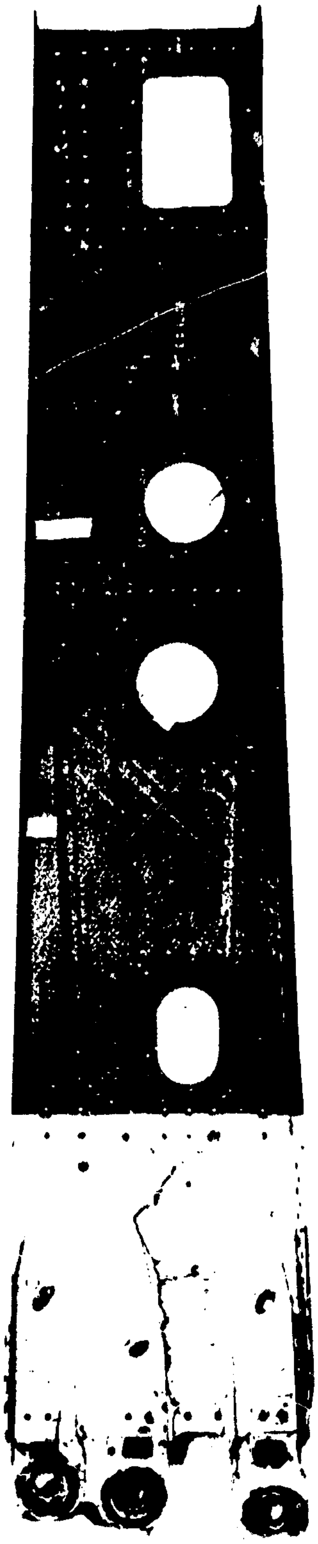

Figure 24. Web Cracks – Forward Face

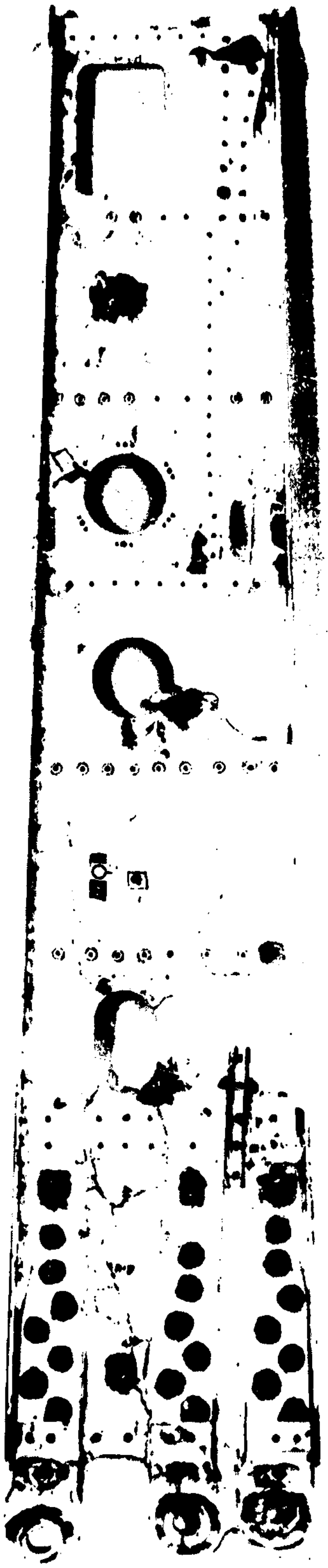

Figure 25. Web Cracks – Aft Face

ORIGINAL PAGE
BLACK AND WHITE PHOTOGRAPH

ORIGINAL PAGE IS
OF POOR QUALITY

Figure 26. Through Thickness Cracks

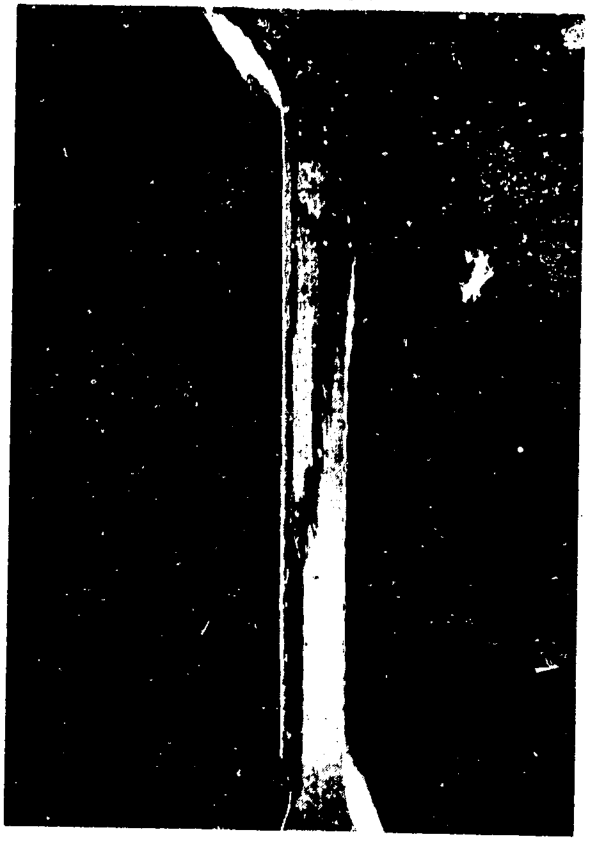

Figure 27. Through Thickness Cracks Edge View

Visual inspection of the forward and aft surfaces showed different crack patterns (figs. 24 and 25). Macroscopic inspection showed tensile failure of the inboard edge of the web (fig. 28), delamination of the forward and aft face plies (fig. 29), and a shear failure at the neutral axis (figs. 26 and 27).

The ATLAS finite element model analysis results for the spar web shear are compared with the linear extrapolated strain gage data in Figure 30. This comparison shows close agreement. Figure 30 also shows close agreement between the axial strains in the spar chords.

Using this information from the visual inspection with the test and predicted strain data, the failure initiation was pinpointed at the inboard edge of the web adjacent to the fail-safe lug (fig. 28). Deflection data extracted from ATLAS analysis confirmed a tension load between the lugs. Combined with the shear, this tension load produced excessive strains at the fail-safe lug-web intersection. This load and load path combination produced the failure initiation, as noted, which then propagated to produce the shear failure at the web center. This area was fixed by the addition of a steel reinforcement plate integral with the fail-safe lug strap, the lower lug strap, and the spar web (fig. 31).

ORIGINAL PAGE
BLACK AND WHITE PHOTOGRAPH

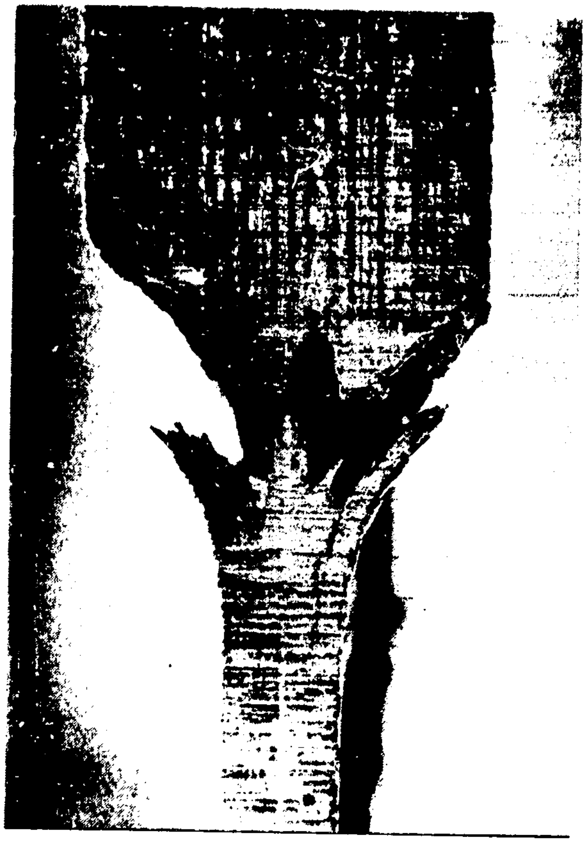

Figure 28. Tensile Failure of Inboard Web

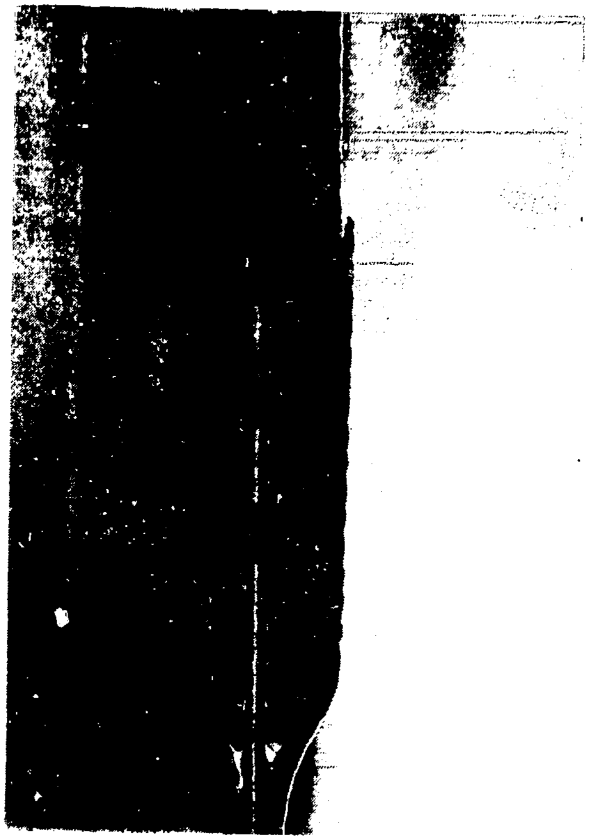

Figure 29. Delamination of Face Plies

3.1.5.8 Lightning Discharge Tests

Figures 32 and 33 show the lightning discharge damage produced at points 1 through 4. The lightning discharge tests at points 3 and 4 produced punctures in the tip section skin and stiffeners delaminated from the skin. All four of the lightning discharge damage areas exhibit the characteristic vaporization of flame spray coating and charring of the outer laminate epoxy resin.

Even though the damage to the stabilizer because of lightning discharge would not affect flight safety, an additional rib was added (see table 5 in sec. 3.5.2) to control damage even further.

3.2 GROUND VIBRATION TEST

Ground vibration testing was performed on a production 737 aircraft with a graphite-epoxy horizontal stabilizer installed. The purpose of the test was to measure the natural frequencies and modes of the graphite-epoxy stabilizer/elevator/tab. These frequencies and modes were compared with those used in the flutter analysis.

ORIGINAL PAGE IS
OF POOR QUALITY

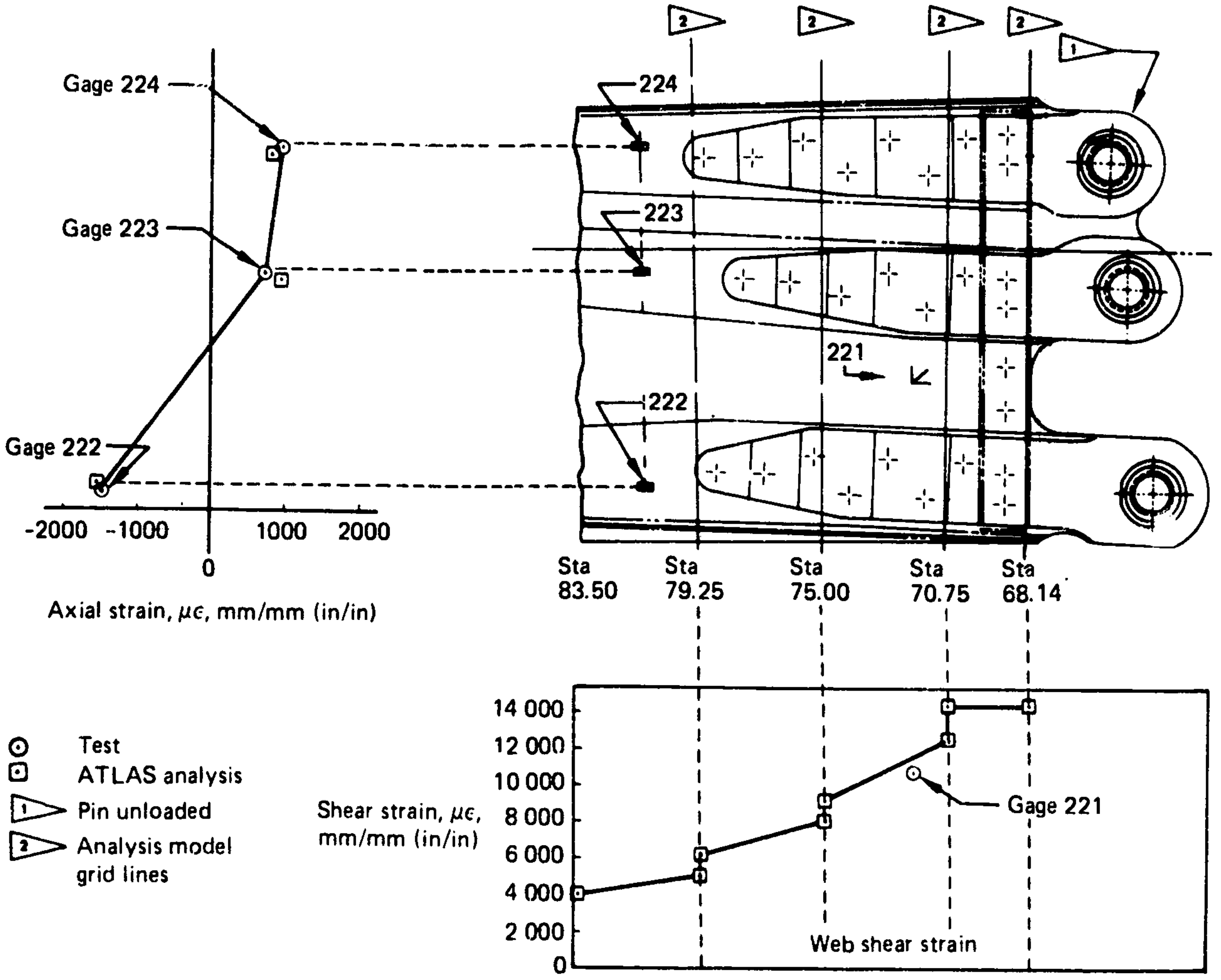

- Load case 4010, limit load fail-safe condition

Figure 30. Finite Element and Strain Gage Comparison

The test airplane was positioned on a level surface in an operating-empty weight configuration. The airplane was supported on the main and nose gears with reduced tire pressure. A portable vibration shaker was used to excite the stabilizer at several locations and directions. Tests were conducted with hydraulic power on and off. The test setup is shown in Figure 34.

Accelerometers, located on both right- and left-hand stabilizers, elevators, tabs, and control columns, were used to measure control system natural frequencies, mode shapes, and damping characteristics. In addition, accelerometer data was recorded on the fin/rudder, wingtip, and stabilizer support structure. The measured natural frequencies of the graphite-epoxy stabilizer were in close agreement with those of the aluminum stabilizer, demonstrating similar dynamic characteristics. A mode comparison of the aluminum and graphite-epoxy structures is shown on Table 4.

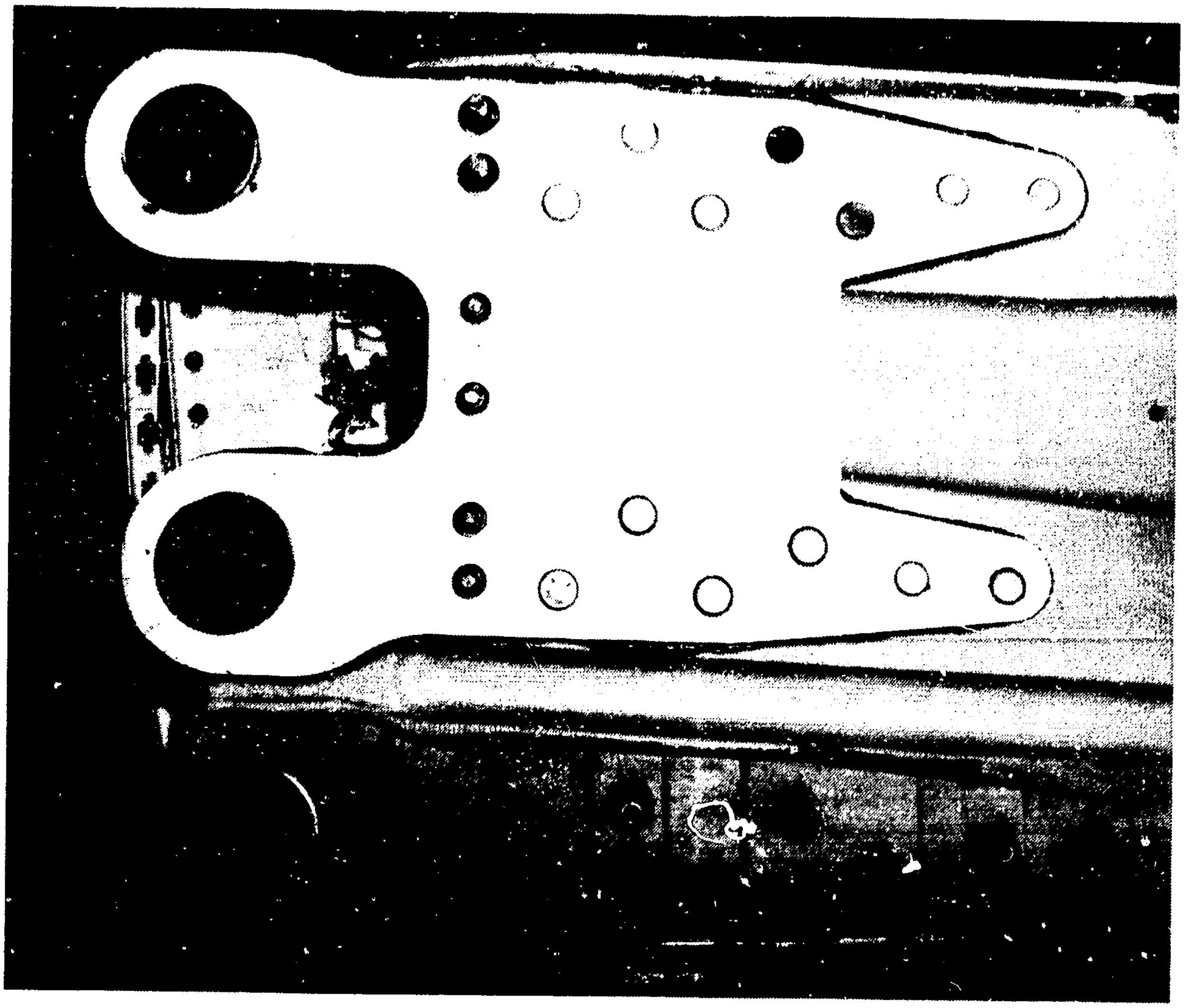

Figure 31. Rear-Spar Fail-Safe Steel Reinforcement Plate

3.3 FLIGHT TESTS

Flight tests were conducted to demonstrate flutter clearance and stability and control performance. The flight flutter test used a production model 737-200 with a graphite-epoxy horizontal stabilizer installed.

The airplane was flown at incrementally increasing speeds up to the airplane dive speed at three altitudes. The envelope of conditions flown is shown in Figure 35. Excitation of the stabilizer was performed by means of control surface impulses and an oscillating aerodynamic vane mounted on the left-hand stabilizer tip. The vane installation is shown in Figure 36. At each speed, subcritical damping and frequency calculations were made from measurements taken on the empennage. Control system power on and off, autopilot, and yaw damper operation were checked. Modal damping for all modes was high throughout the tests.

ORIGINAL PAGE
BLACK AND WHITE PHOTOGRAPH

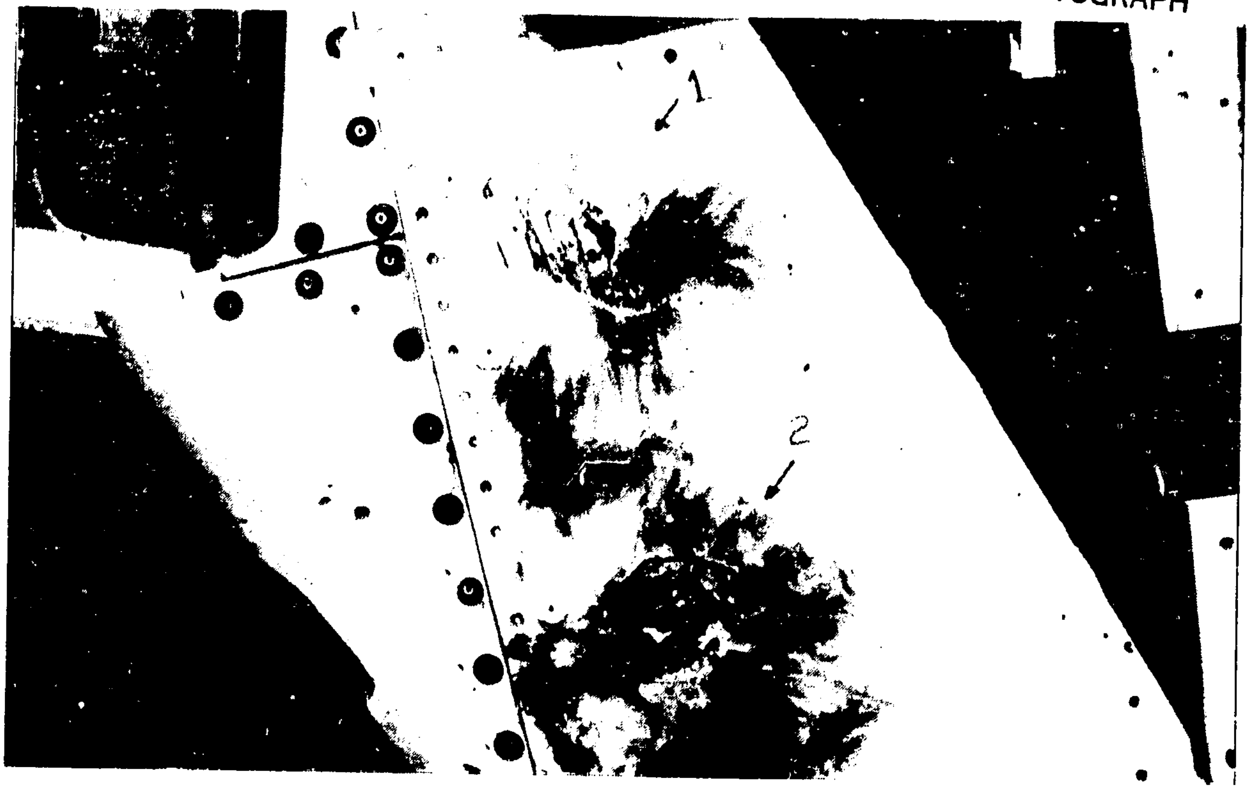

Figure 32. Lightning Discharge Damage (Tests 1 and 2)

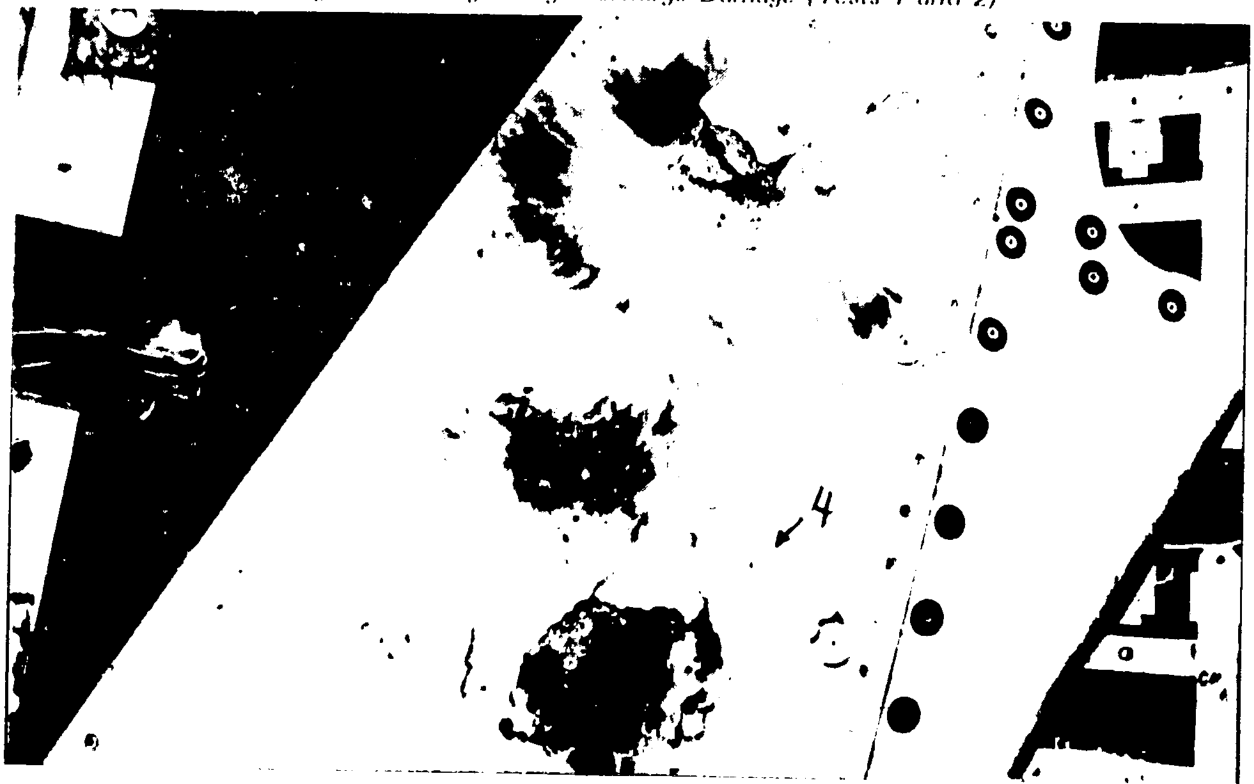

Figure 33. Lightning Discharge Damage (Tests 3 and 4)

ORIGINAL PAGE IS
OF POOR QUALITY

Table 4. Aluminum Versus Graphite-Epoxy Stabilizer Mode Comparison

Mode description	Hydraulic power on		Hydraulic power off	
	Composite frequency, Hz	Aluminum frequency, Hz	Composite frequency, Hz	Aluminum frequency, Hz
Body lateral bending/torsion Stabilizer spanwise bending	4.23 A	4.23	4.26 A	4.24
Stabilizer spanwise bending	5.66 A	5.70	5.69 A	5.57
Elevator rotation	5.94 A	5.99	5.97 A	5.97
Stabilizer bending/ elevator rotation	6.73 S	6.72	6.62	
Stabilizer spanwise bending	6.98 S	7.01	7.12	
Stabilizer chordwise bending	7.28 A	7.62	Not measured	Not measured
Elevator torsion	18.42 A		18.50 A	
Stabilizer chord/pitch	19.23 S	18.18	Not measured	Not measured
Elevator torsion	19.76 S	20.32	19.81 S	20.28
Stabilizer 2nd bending/torsion	24.53 A	24.78	24.80 A	

Note: A is antisymmetric; S is symmetric.

ORIGINAL PAGE IS
OF POOR QUALITY

ORIGINAL PAGE
BLACK AND WHITE PHOTOGRAPH

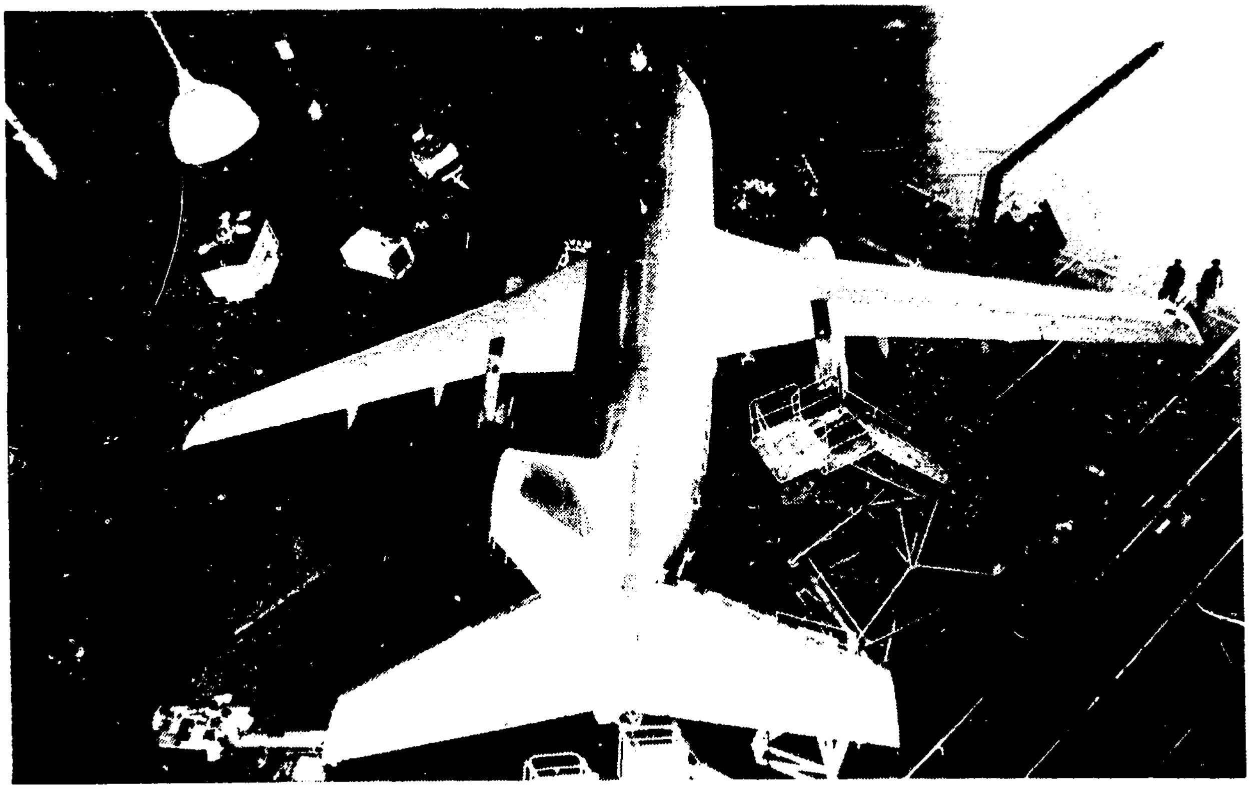

Figure 34. Ground Vibration Test Setup

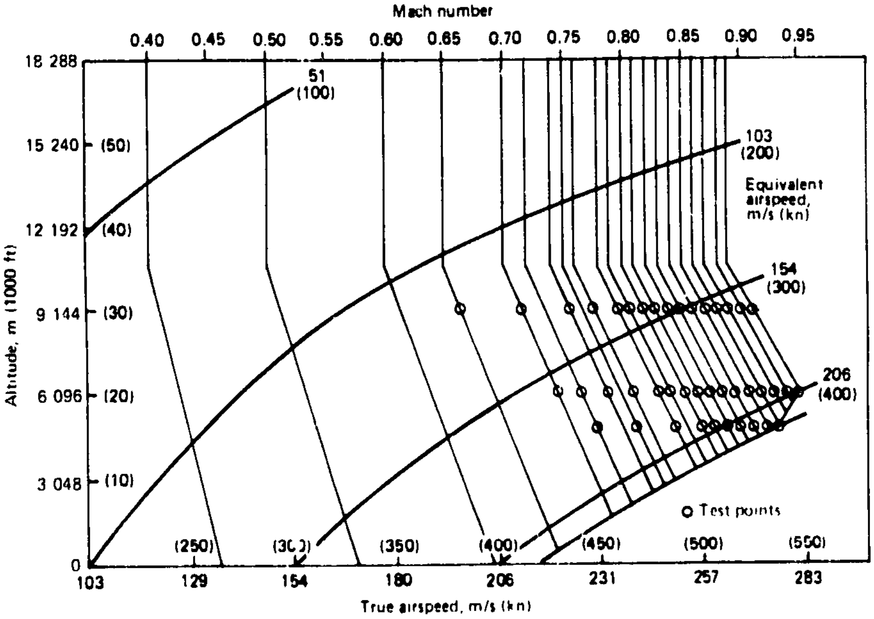

Figure 35. Speed and Altitude Test Points

ORIGINAL PAGE IS OF POOR QUALITY

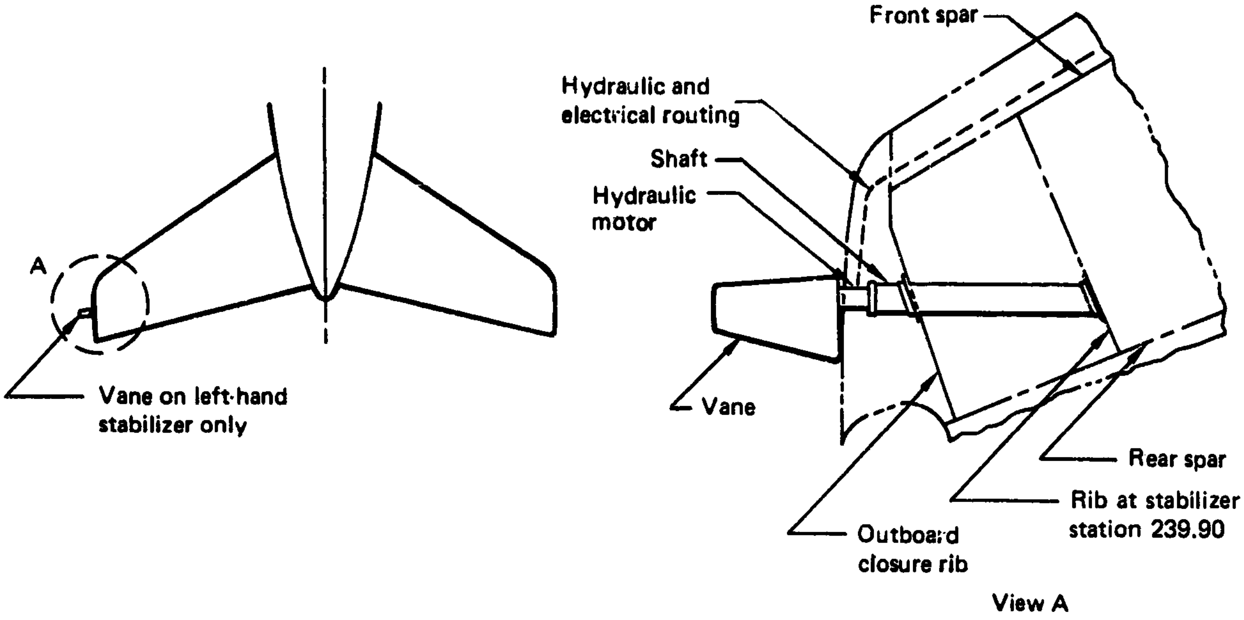
A
Vane on left-hand stabilizer only
Front spar
Hydraulic and electrical routing
Shaft
Hydraulic motor
Vane
Rear spar
Rib at stabilizer station 239.90
Outboard closure rib
View A

Figure 36. Flutter Vane Installation

Results of this testing with the graphite-epoxy stabilizer have demonstrated clearance to the V_D/M_D flight boundary and an equivalence to the aluminum stabilizer from a flutter standpoint.

Stability and control flight tests consisted of two phases. Phase I flight tests were conducted on a production aluminum stabilizer to establish baseline data. For phase II, the aluminum stabilizer was replaced by the graphite-epoxy stabilizer, and phase I flight tests were repeated.

Flight test maneuvers that placed the highest demands on the longitudinal control system were selected. These maneuvers, which were flown with both the aluminum and graphite-epoxy stabilizers for back-to-back comparison, included windup turns with hydraulic power on and off, stabilizer-elevator trades, mistrim dive recoveries, and simulated landings in manual reversion. In addition to the back-to-back testing, selected certification maneuvers also were flown to demonstrate further that the graphite-epoxy stabilizer produces no change in 737 handling characteristics. These certification maneuvers included flaps up and flaps 40 stall characteristics and longitudinal static stability in cruise at 9144m (30 000 ft) and 7010m (23 000 ft). The flight test airplane was flown by an FAA pilot as part of the stability and control and autopilot certification flight testing. Back-to-back flight test conditions demonstrate that there are no significant differences in observed flight characteristics when the aluminum stabilizer is replaced by the graphite-epoxy stabilizer. Flight test results show that the graphite-epoxy stabilizer is equivalent to the aluminum stabilizer and, therefore, will satisfy all handling qualities requirements of Federal Aviation Regulation 25 (FAR 25) for the model 737.

3.4 FAA CERTIFICATION

FAA certification was achieved by showing compliance with the requirements of FAR 25 and Composite Guidelines AC 20-107.

Compliance was demonstrated by structural analyses and supporting test evidence. The test program that produced the supporting data included a full-scale ground test, a flight test program, and an ancillary test program, all discussed in previous sections of this document and in References 2 and 3. Structural analyses included a finite element model analysis (ATLAS), an ultimate strength analysis, and a damage tolerance and fail-safe analysis. These analyses and supporting test data were submitted to and accepted by the FAA. Certification of the 737 graphite-epoxy horizontal stabilizer was issued in the third quarter of 1982.

3.5 WEIGHTS

3.5.1 Production Analysis

Weights were calculated based on production drawing configurations. The values were used to replace the evaluations derived from the extrapolation of the stub box design that comprised the preliminary weight comparison (table 35, ref. 3).

Completion of the production drawing evaluation resulted in an increase of 9.7 kg (21.1 lb). The predicted total weight of the graphite-epoxy inspar structure following this revision was 183.3 kg (404.1 lb) compared with the aluminum structure weight of 238.3 kg (525.4 lb), a reduction of 23%.

As production hardware became available it was weighed and compared with the respective predicted values. The front- and rear-spar weights were approximately 6% and 9% heavier respectively, and the lower skin panel exhibited a weight 7% lighter than predicted. A reevaluation of the production drawings revealed errors in calculations, which when corrected showed closer correlation between the actual and predicted weights. These predicted weight changes resulted in a net 0.4-kg (0.9-lb) weight increase.

The addition of plies to the front- and rear-spar webs to correct a negative margin of safety condition resulted in a 0.7-kg (1.4-lb) increase.

Stainless steel (15-5PH) was substituted for titanium (6Al-4V) for the front- and rear-lug straps (described in sec. 3.1.3.5 of ref. 3) because replacement titanium was not available within the timeframe of the contract schedule. This change is not reflected in the stabilizer weight status. Follow-on advanced composite horizontal stabilizer lug straps will be titanium in compliance with the released production drawing material callout.

Two production design changes were required late in the program to correct deficiencies occurring during final testing. The first test failure occurred during a lightning strike test. Penetration of the skin and delamination of the stringers required rework of the five shipsets by adding a stringer support rib. The production equivalent of this rework calls for the addition of a one-piece rib, installed in a similar manner to the rework rib.

Table 5. Metal and Graphite-Epoxy Horizontal Stabilizers— Inspar Structure Weight Comparison

Item	Baseline aluminum stabilizer structure, kg (lb)/airplane		Advanced composite stabilizer structure, kg (lb)/airplane		Weight difference, kg (lb)/airplane		ght erence, %
Front spar	31.3	(69.0)	21.2	(46.8)	−10.1	(−22.2)	−32.2
Rear spar	71.1	(156.8)	51.6	(113.7)	−19.5	(−43.1)	−27.5
Skins							
• Upper	36.2	(79.8)	39.0	(86.0)	+2.8	(+6.2)	+7.8
• Lower	36.2	(79.8)	40.2	(88.7)	+4.0	(+8.9)	+11.2
Ribs	60.9	(134.2)	34.1	(75.2)	−26.8	(−59.0)	−44.0
Corrosion protection	–	–	1.0	(2.2)	+1.0	(+2.2)	–
Lightning protection	–	–	0.0	(0.0) [1]	–	–	–
Access doors	0.7	(1.6)	0.0	(0.0)	−0.7	(−1.6)	−100.0
Gap cover support	1.9	(4.2)	0.0	(0.0) [2]	−1.9	(−4.2)	−100.0
Total stabilizer inspar structure per airplane	238.3	(525.4)	187.1	(412.6)	−51.2	(−112.8)	−21.5
Stabilizer TE/elevator interface thermal expansion provision	–	–	15.5	–	+15.5	–	–

[1] 1.0 lb included in skin panel weight.

[2] Gap cover support structure integral design of inboard closure rib installation.

The second test failure occurred on full-scale ground test article during the fail-safe maximum negative bending condition when the inboard rear spar web failed at 61% design ultimate load. The rework required on the five completed shipsets involved joining the aft fail-safe and lower lug strap by a web. The production equivalent is the localized addition of 4 plies of fabric to the spar web and chords and a material change from aluminum to steel for the inboard closure rib attach angle (65C17828-3). These two changes added 0.1 kg (0.2 lb) and 0.8 kg (1.8 lb) respectively to the horizontal stabilizer inspar structure weight. A plot depicting the weight trend throughout the program is shown in Figure 37.

3.5.2 Conclusions

The final weight status detailed in Table 5 shows a production graphite-epoxy component weight of 187.1 kg (412.6 lb). This is 51.2 kg (112.8 lb) lighter than the comparable aluminum structure, a weight reduction of 21%.

ORIGINAL PAGE IS
OF POOR QUALITY

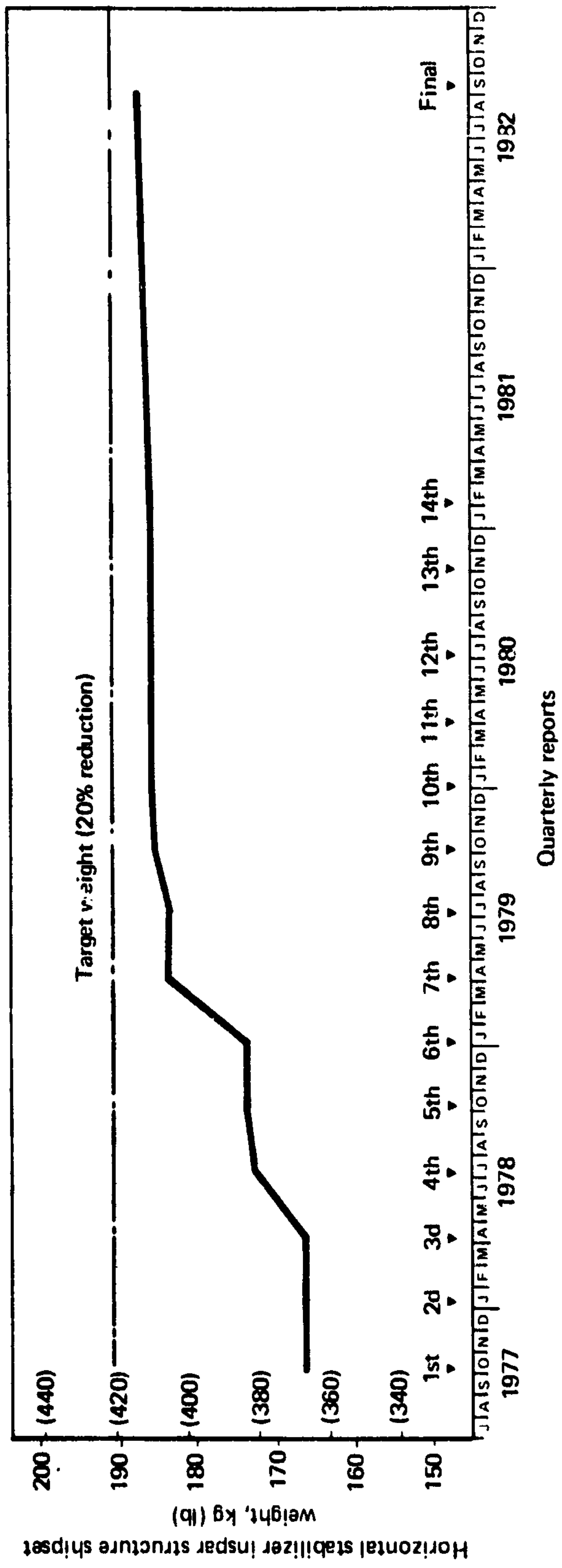

Figure 37. Weight and Time History

Table 6. Predicted and Actual Composite Stabilizer Inspar Structure Component Weights

Component	Predicted values	Actual weights per shipset									
		No. 1		No. 2		No. 3		No. 4		No. 5	
		LH	RH	LH	RH	LH	RH	LH	RH	LH	RH
Front spar, kg (lb)	9.8 (21.5)	9.7 (21.3)	9.8 (21.6)	9.8 (21.5)	9.8 (21.6)	9.9 (21.8)	9.8 (21.6)	10.1 (22.2)	10.8 (23.7)	10.0 (22.1)	10.0 (22.0)
Rear spar, kg (lb)	22.3 (49.3)	22.5 (49.5)	21.9 (48.2)	22.6 (49.9)	22.4 (49.4)	22.6 (49.9)	22.9 (50.4)	22.5 (49.5)	22.6 (49.9)	22.7 (50.0)	22.6 (49.9)
Skin panel–upper, kg (lb)	17.8 (39.3)	17.8 (39.2)	17.9 (39.5)	18.1 (40.0)	18.4 (40.6)	17.6 (38.9)	17.6 (38.9)	17.4 (38.4)	17.6 (38.9)	17.7 (39.0)	18.2 (40.2)
Skin panel–lower, kg (lb)	18.8 (41.4)	19.1 (42.1)	19.1 (42.2)	19.3 (42.6)	19.4 (42.7)	19.0 (41.8)	19.3 (42.5)	19.0 (41.8)	19.0 (41.8)	19.0 (41.8)	19.3 (42.5)
Rib details, kg (lb)	9.3 (20.5)	9.6 (21.1)	9.6 (21.2)	9.9 (21.9)	9.6 (21.1)	9.5 (21.0)	9.7 (21.4)	9.9 (21.8)	9.4 (20.8)	9.8 (21.6)	9.8 (21.6)
Totals, kg (lb)	78.0 (172.0)	78.7 (173.2)	78.3 (172.7)	79.9 (175.9)	79.6 (175.4)	78.6 (173.4)	79.3 (174.8)	78.9 (173.7)	79.4 (175.2)	79.2 (174.6)	79.9 (176.2)
Difference, %	–	+0.7	+0.4	+2.3	+2.0	+0.8	+1.6	+1.0	+1.9	+1.5	+2.4

Because of the assembly sequence for the horizontal stabilizer, it was not possible to weigh the inspar structure in the configuration as reported in the predicted weight statement (table 6). Therefore, components weighed under the actual weight program were tabulated to the appropriate shipset and compared with the predicted values. The total predicted weight of the subject components per shipset is 156 kg (344 lb) or 83% of the total inspar structure. The remaining 31.1 kg (68.6 lb) comprises installation fasteners, non-graphite-epoxy components, small graphite-epoxy angles, corrosion protection provisions, and rework changes not incorporated at the time of actual weighing.

This tabulation (table 6) shows weight differences of 0.4% to 2.4% over the predicted values for the five shipsets and an average overweight of 1.4%.

It would be expected that in a full-scale production mode, the percentage overweight would be reduced because the actual component weights include liaison fixes to salvage rejected parts. The defects occasioning the liaison rework would be greatly reduced on a production run.

PRECEDING PAGE BLANK NOT FILMED

4.0 PRODUCTION

4.1 DETAIL TOOLING

Detail tools for the fabrication of composite components were designed and constructed to production standards and used for fabrication of verification hardware. Because the test box built for verification encompassed only 304.8 cm (10 ft) of the stabilizer, a number of tools were tried for the first time at the startup of production operations. Also only those portions of the large skin panel and spar tools that were contained within the test box had prior tryout. As a result, some tool development was necessary during production of the full-size article, but there were no major deviations from original concepts based on prior fiberglass tooling experience.

Both male- and female-configured layup tools were used. Male tooling was preferred and most commonly used because tool fabrication and layup and bagging operations were less costly. Female tools were used wherever necessary to avoid having honeycomb core against the tool surface.

Layup mandrels were designed and fabricated for multiple use wherever possible; i.e., the tool was capable of producing both left- and right-hand components.

Aluminum, steel, and fiberglass materials were used for the tools. Material selection was based on part size and complexity. Although lower thermal expansion made steel the desired material, its weight and low heat-up rate were factors that led to the selection of aluminum for large parts such as skin panels and spars. Shrink factors were developed for both metals to account for tool thermal expansion during 182°C (350°F) cure cycles. Laminated fiberglass had limited usage.

4.2 ASSEMBLY TOOLING

New tools were designed and fabricated for stabilizer assembly operations. These tools are similar to existing metal stabilizer tools, but are fewer in number because the major assembly work is accomplished in one stage. The reduced number of internal structural members and one-piece cover panels for composite units allowed a one-stage operation. These features and other engineering design variances disallowed using existing tool designs and constructing dual-purpose tools for stabilizer production. Tooling consisted of left- and right-hand units for rear spar, front spar/leading edge, and major assembly operations. The rear spar and trailing edge were joined in a tool common to production. Existing master tooling was used as a control medium to ensure interchangeability at the stabilizer/elevator hinge centerline.

Conventional tooling methods were used to design and construct all tools, but unique features were included to accommodate the special equipment developed for drilling and trimming composite parts. This equipment included such items as high-speed (18 000 r/min) tapered drills, diamond-coated router bits, and dust collection systems. For the latter, vacuum nozzles adapted to drill motors and router units were used in conjunction with portable vacuum canisters.

Index holes sized to the drill motor vacuum nozzle diameter were used in assembly tool drill plates to provide positive dust management during drilling operations, as well as proper hole location and drill alignment. Restricted access prevented use

44 NALLY BL

of this system in some areas of the spars and major assemblies. In these areas, a hand-held vacuum hose was used.

The tool tryout conducted during assembly of the left-hand test stabilizer and shipset 1 identified some modification necessary to improve tool use, but for the most part, the conventional tool approach worked quite effectively.

4.3 COMPONENT MANUFACTURING

Production facilities at Boeing's Fabrication Division in Auburn, Washington, were selected to produce advanced composite components and certain new metal components. The facilities were modified as necessary to accommodate the unique processing requirements of the composite materials. To support the composite program, systems and procedures in use for ongoing commercial airplane manufacturing were employed for release of engineering drawings, production plans, part fabrication orders, and schedule compliance. Personnel assignments were made from the pool of production workers already engaged in normal fiberglass and metal manufacturing operations.

The fabrication of composite parts for the Advanced Composite Stabilizer program was performed to the requirements of a Boeing process specification using the method for no-bleed material. The procedure is basically the same for laminate or honeycomb parts. The fabrication can be divided into two operations: layup and bagging (fig. 38) and curing (fig. 39).

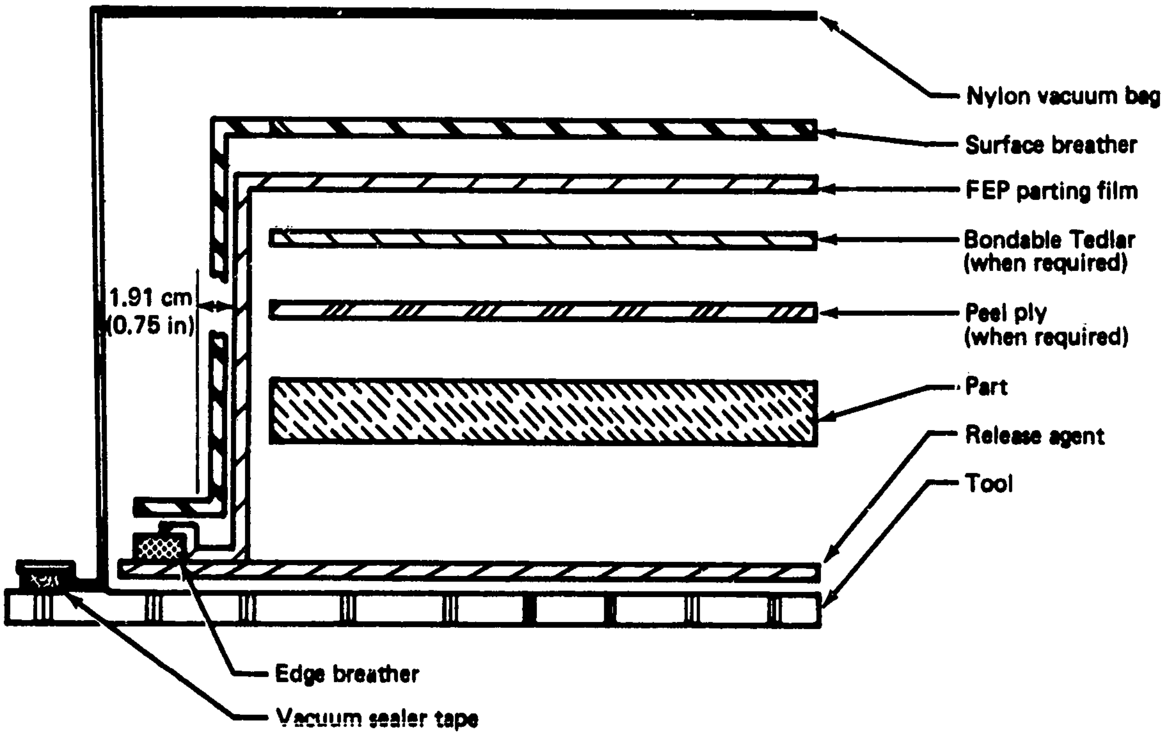
Nylon vacuum bag
Surface breather
FEP parting film
Bondable Tedlar
(when required)
Peel ply
(when required)
Part
Release agent
Tool
1.91 cm
(0.75 in)
Edge breather
Vacuum sealer tape

Figure 38. Bagging Procedure—No-Bleed Material

ORIGINAL PAGE IS
OF POOR QUALITY

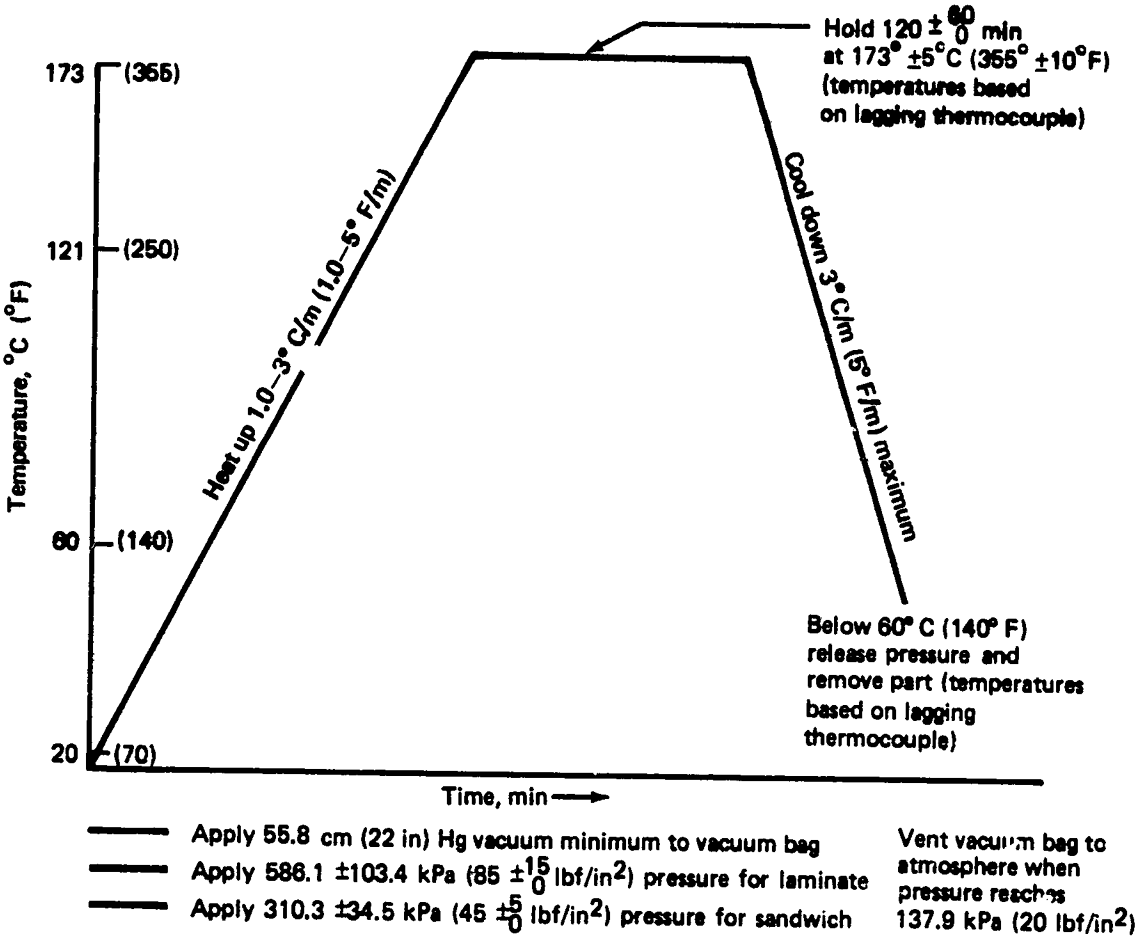

Figure 39. Cure Cycle—No-Bleed Material

Layup and bagging began with preparation of the laminating tool. The tool surface was cleaned with methyl ethyl ketone (MEK), and a mold release agent, Frekote FR 33, was baked on the clean surface for 30 min at 121°C (250°F). The tool was then ready for layup. The graphite prepreg was laid on the tool in the directions specified on the engineering drawings and cut to shape. After every two to three plies, the laminate was compacted by placing a temporary vacuum bag over the laminate and drawing a minimum vacuum of 55.88 cm (22 in) of mercury. After the layup was completed, peel ply or bondable Tedlar was placed over the laminate as required. (Peel ply is used on surfaces that are secondarily bonded or painted. Bondable Tedlar is used on all honeycomb components as a moisture barrier and on solid laminates to isolate the graphite laminate from aluminum elements.) A fiberglass edge breather with a vacuum connection fitting then was placed around the periphery of the part. A minimum of 1.91 cm (0.75 in) was required between the part edge and inside edge of the edge breather. A single fiberglass yarn was placed between the base of the layup and edge breather to evacuate air from the layup. (Additional yarns may be used at the discretion of the shop to provide adequate removal of trapped air.) Thermocouples were located in the excess area

ORIGINAL PAGE IS
OF POOR QUALITY

of the part to monitor the curing temperatures. A 2-mil FEP parting film was laid over the part and extended to the centerline of the edge breather. An Airweave SS surface breather was placed over the part and extended to connect with the edge breather. Finally, the part was bagged with 2- or 3-mil nylon vacuum bag material. The bag was sealed to the tool with high-temperature-resistant extruded sealing tape. A minimum vacuum of 55.88 cm (22 in) of mercury was applied to the vacuum bag, which then was checked to ensure that it conformed to the part shape. The bag also was checked for leaks by disconnecting the vacuum line and monitoring the vacuum drop.

After verifying the bagging step, the part was ready for curing. Still under full vacuum, it was placed in an autoclave, and the vacuum connection was coupled to an outside vent line. Immediately upon closing the autoclave, pressure and heat were applied. When the pressure reached 137.9 kPa (20 lbf/in^2), the vacuum bag was vented to the outside atmosphere. (For solid laminates, the maximum pressure is held between 586.1 to 689.5 kPa (85 to 100 lbf/in^2). For honeycomb parts, the maximum pressure is between 275.8 to 344.8 kPa (40 to 50 lbf/in^2).) The part was heated at a rate of 1 to 2.8°C/min (1 to 5°F/min) to a maximum temperature between 174 to 185°C (345 to 365°F). This temperature, based on the lowest thermocouple reading, was held for 120 to 180 min before cool-down was started. (The cool-down rate is a maximum 2.8°C/min [5°F/min].) When the highest thermocouple reading reached 58°C (140°F), the pressure was released from the autoclave, and the part was removed. After the bagging material was removed, the part was ready for trim and final finishing.

4.3.1 Component Statistics

The magnitude of the stabilizer program is illustrated by the number of components used: graphite components, 280; graphite components and assemblies shipped for assembly buildup, 122; and nongraphite components, 268.

The major graphite component assemblies used for each right- and left-hand stabilizer final assembly were:

- Upper skin panel
- Lower skin panel
- Front spar
- Rear spar
- Trailing-edge beam
- Seven inspar ribs
- Inboard closure rib
- Outboard closure rib
- Lightning strike support rib (rework)

4.3.2 Skin Panel Fabrication

The stabilizer skin panels were fabricated as a cocured unit that incorporated both the I-stiffeners and the skin layup. The I-stiffeners were laid up over mandrels, debulked, and then positioned on the skin ply layup for cocuring (figs. 40 through 43). Because of the warp in the stub box panels, the extent of spanwise and cross-section warpage that would occur when producing full-length panels was a concern.

ORIGINAL PAGE
BLACK AND WHITE PHOTOGRAPH

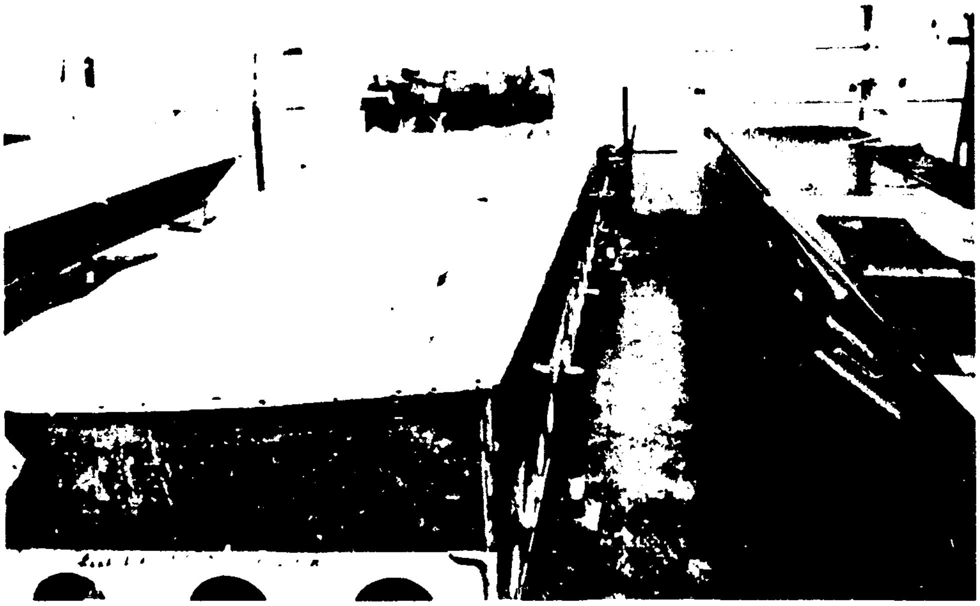

Figure 40. Stabilizer Skin Panel in Layup

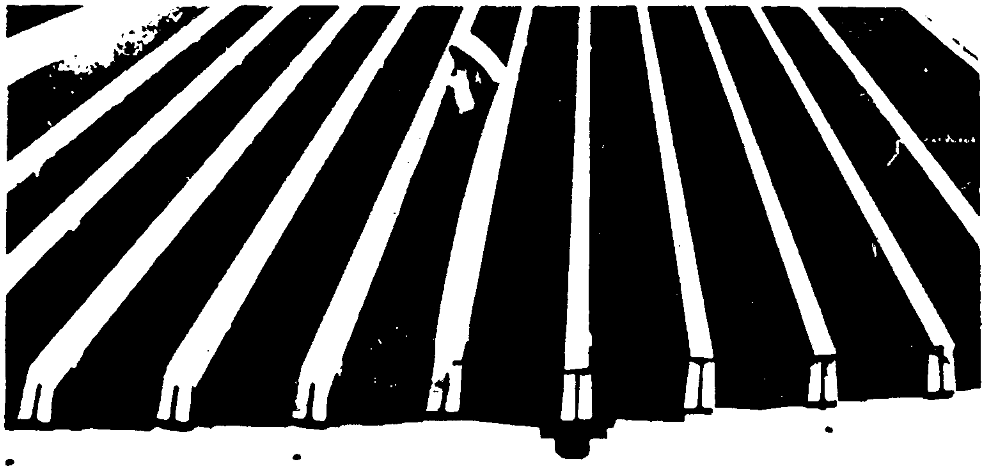

Figure 41. Closeup of I-Stiffeners Located on Skin Layup

ORIGINAL PAGE
BLACK AND WHITE PHOTOGRAPH

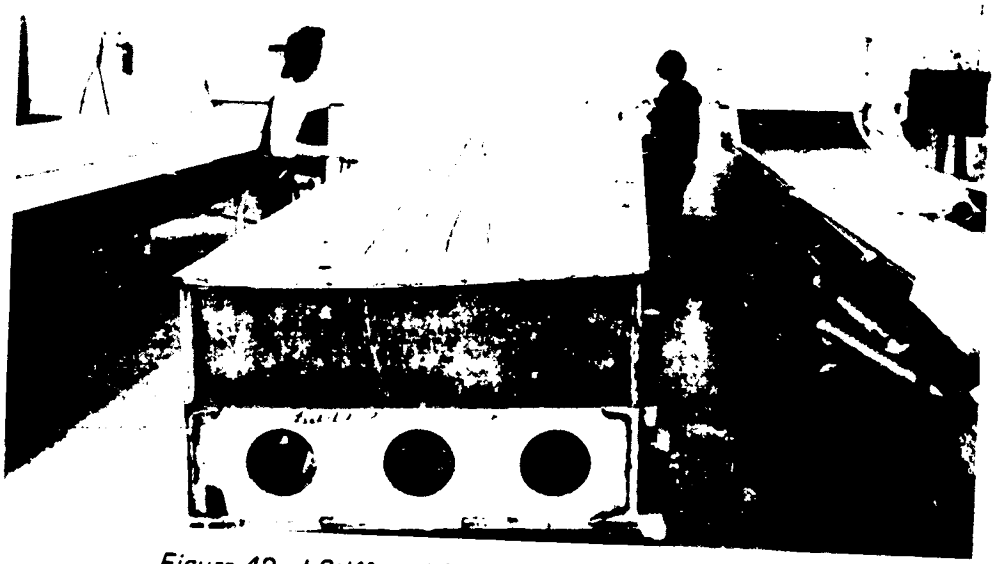

Figure 42. I-Stiffened Skin Panel in Fabrication

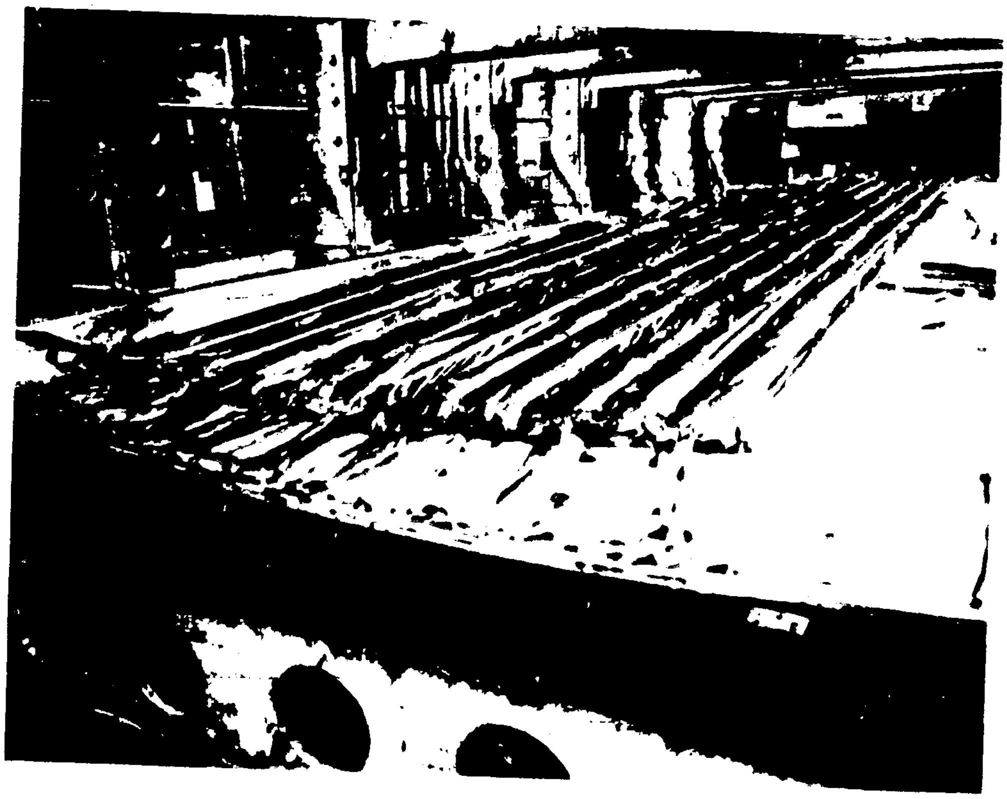

Figure 43. I-Stiffened Skin Panel After Cure

ORIGINAL PAGE
BLACK AND WHITE PHOTOGRAPH

The full-length panels showed both spanwise and cross-section warps in the cured state (fig. 44). To determine the early consequence of this condition on later assembly operations, a plywood simulation of the inspar ribs was constructed to check the assembled panel-to-rib interface. It was determined that the pressure required to place the panels in correct contour position relating to the inspar structure was not excessive, but the pressure necessitated assembly tool features for maintaining fitup during drilling and fastening operations. The panels were accepted as fabricated and were delivered for assembly.

4.3.3 Spar Fabrication

Both front and rear spars were fabricated in a two-stage bonding operation. Spars have two-channel cross sections and laminate spar caps that were fabricated, precured, and then bonded together (figs. 45 through 56). Completed spar halves and spar caps showed negligible warpage, and the first-stage bonding of the spar

Figure 44. I-Stiffened Skin Panel Showing Spanwise Warp

ORIGINAL PAGE
BLACK AND WHITE PHOTOGRAPH

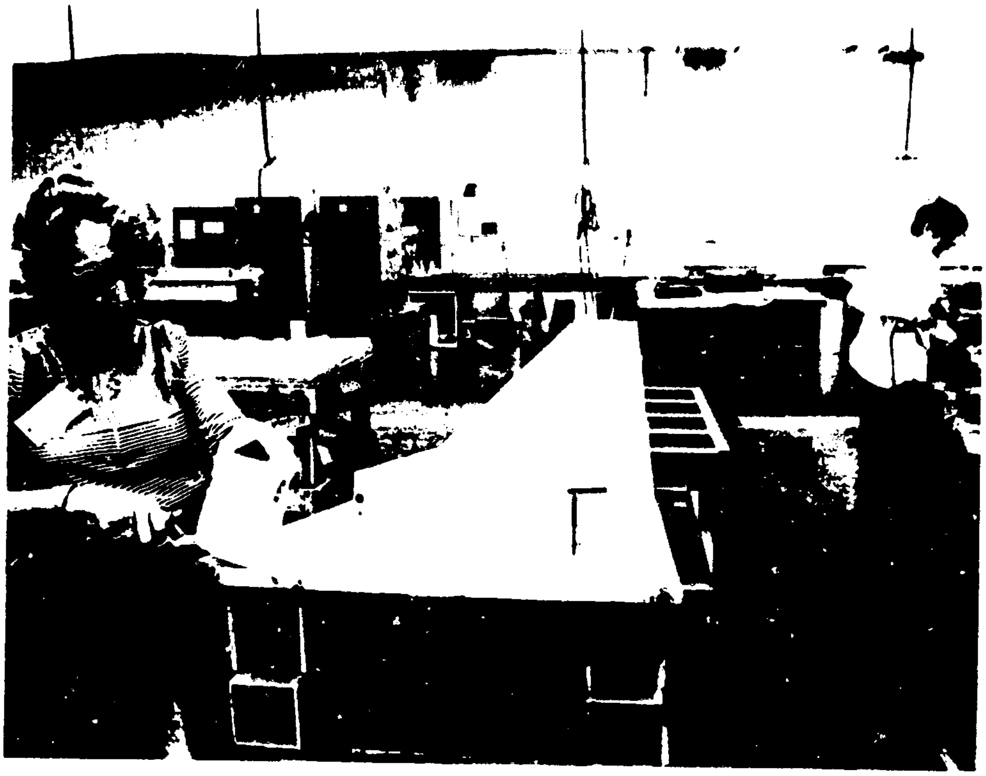

Figure 45. Front-Spar Channel Layup Mandrel

Figure 46. Front-Spar Layup of Fillers in Lug Area

ORIGINAL PAGE
BLACK AND WHITE PHOTOGRAPH

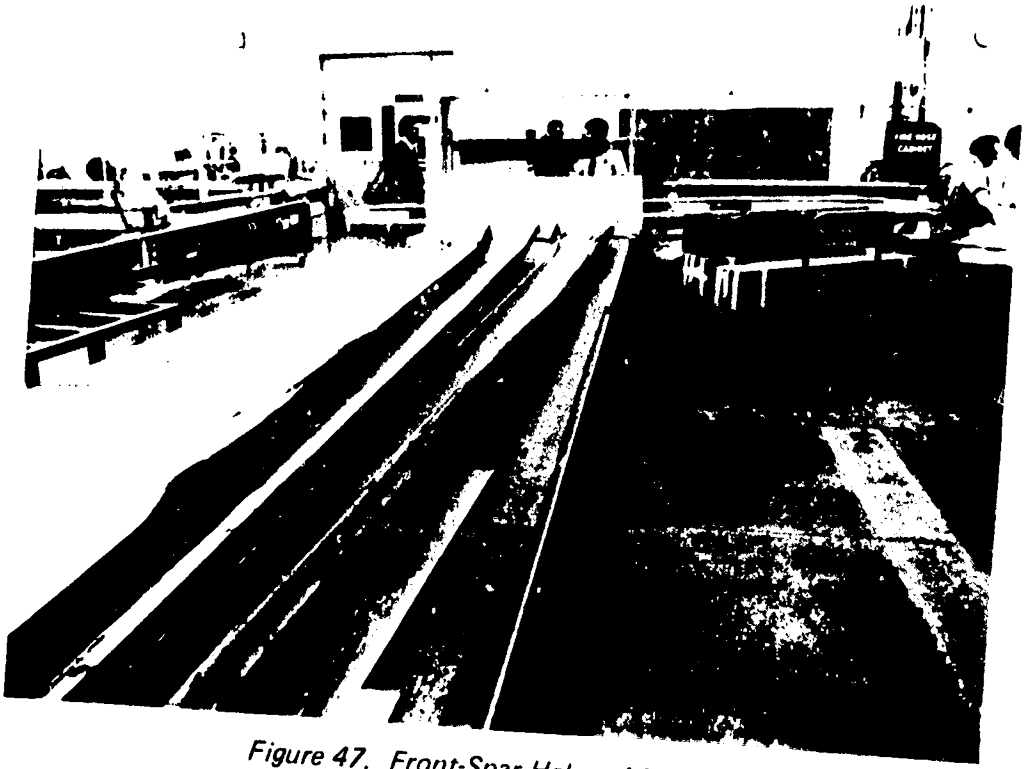

Figure 47. Front-Spar Halves After Cure

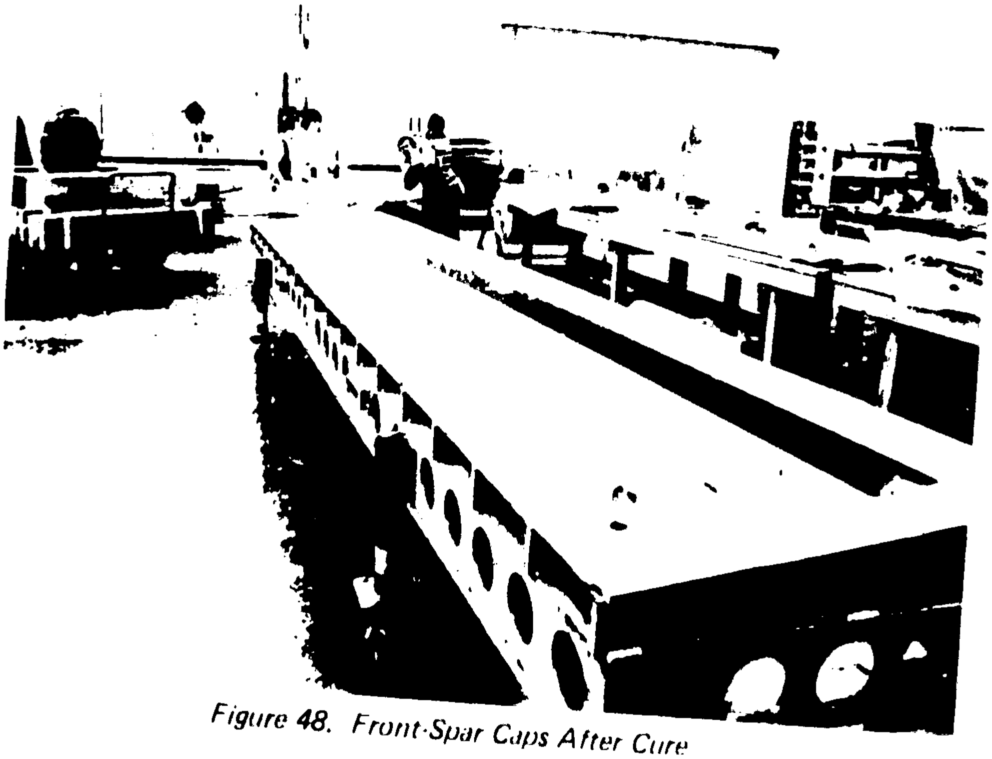

Figure 48. Front-Spar Caps After Cure

ORIGINAL PAGE
BLACK AND WHITE PHOTOGRAPH

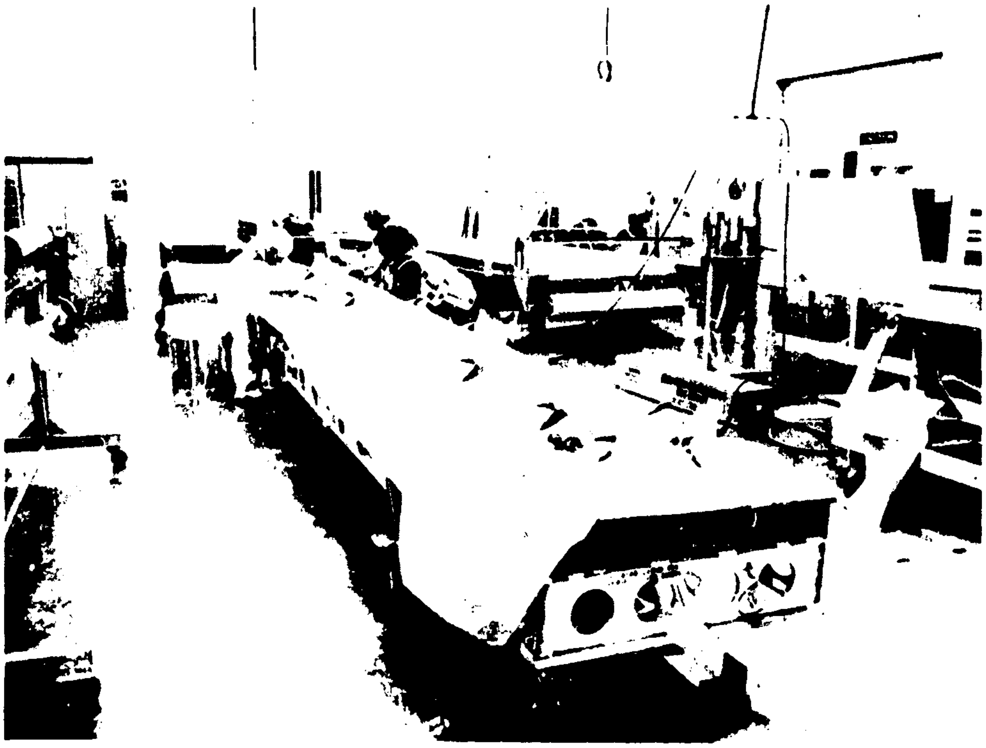

Figure 49. Front-Spar Final Bond Preparations

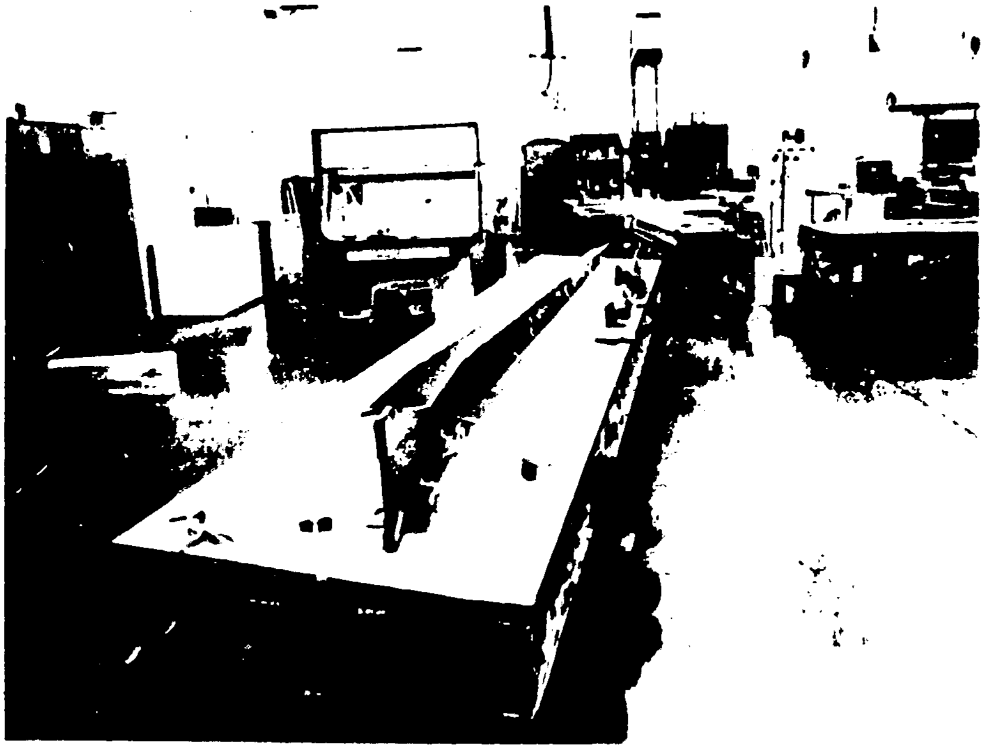

Figure 50. Front Spar After Final Bond

ORIGINAL PAGE
BLACK AND WHITE PHOTOGRAPH

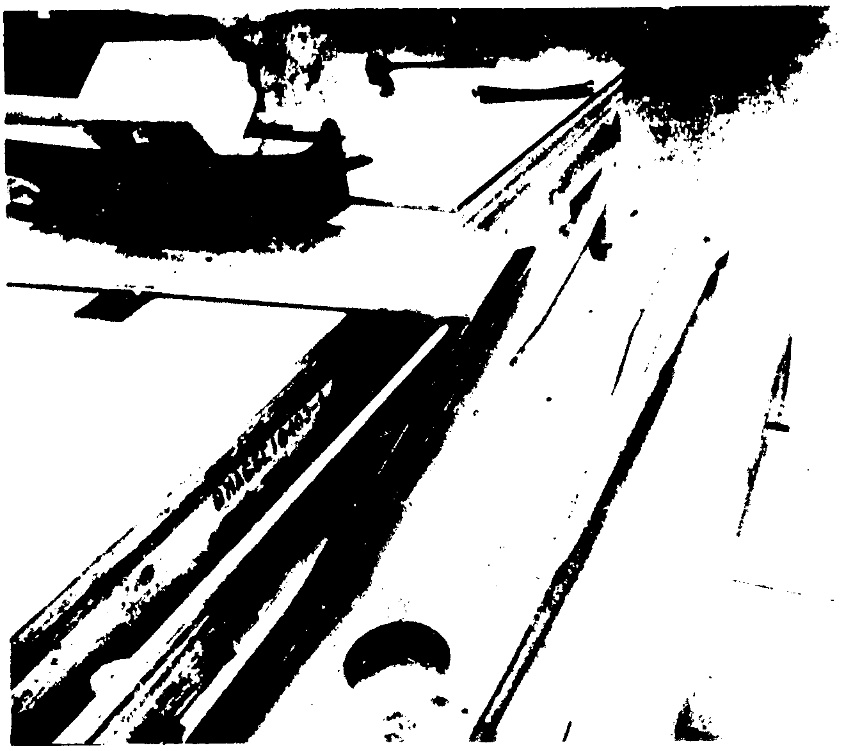

Figure 51. Front-Spar Inboard End After Trim

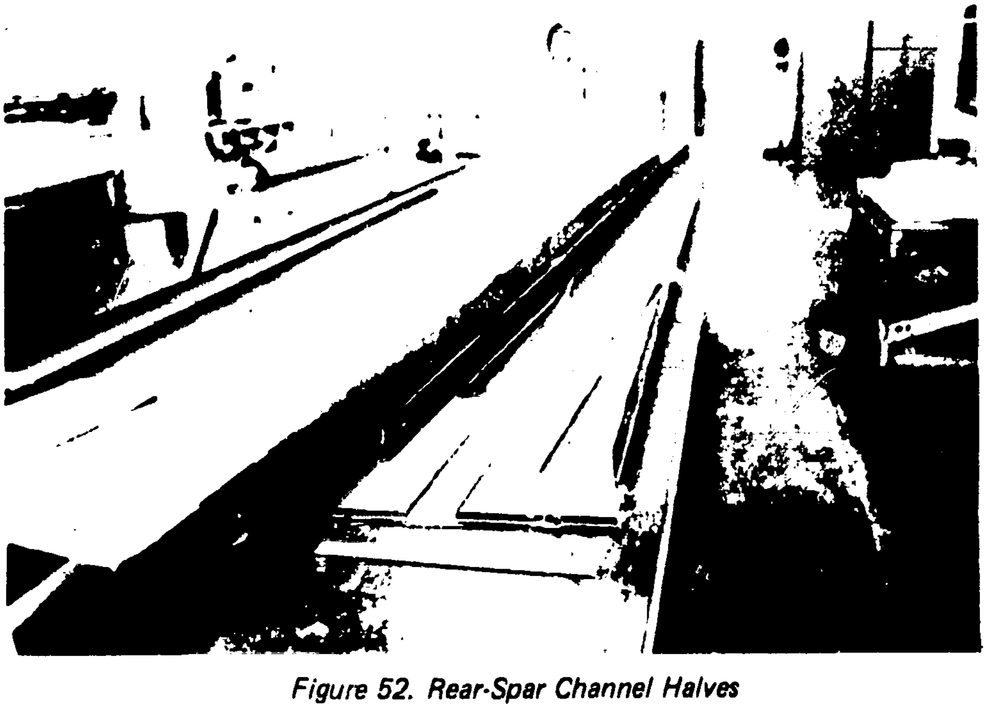

Figure 52. Rear-Spar Channel Halves

ORIGINAL PAGE
BLACK AND WHITE PHOTOGRAPH

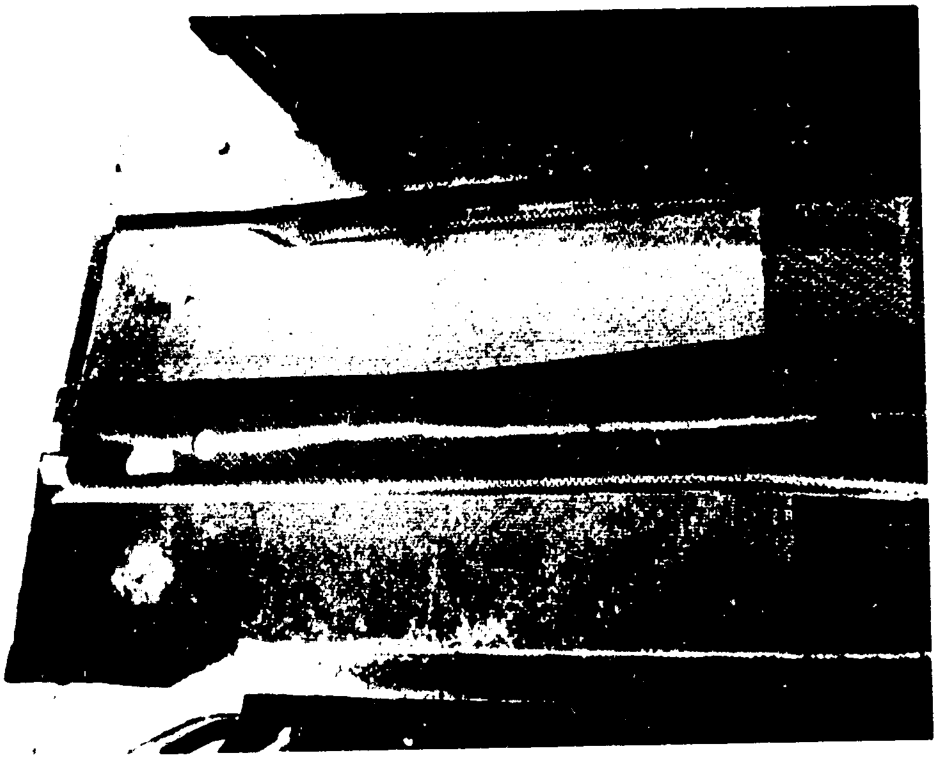

Figure 53. Rear-Spar Closeup of Lug Area

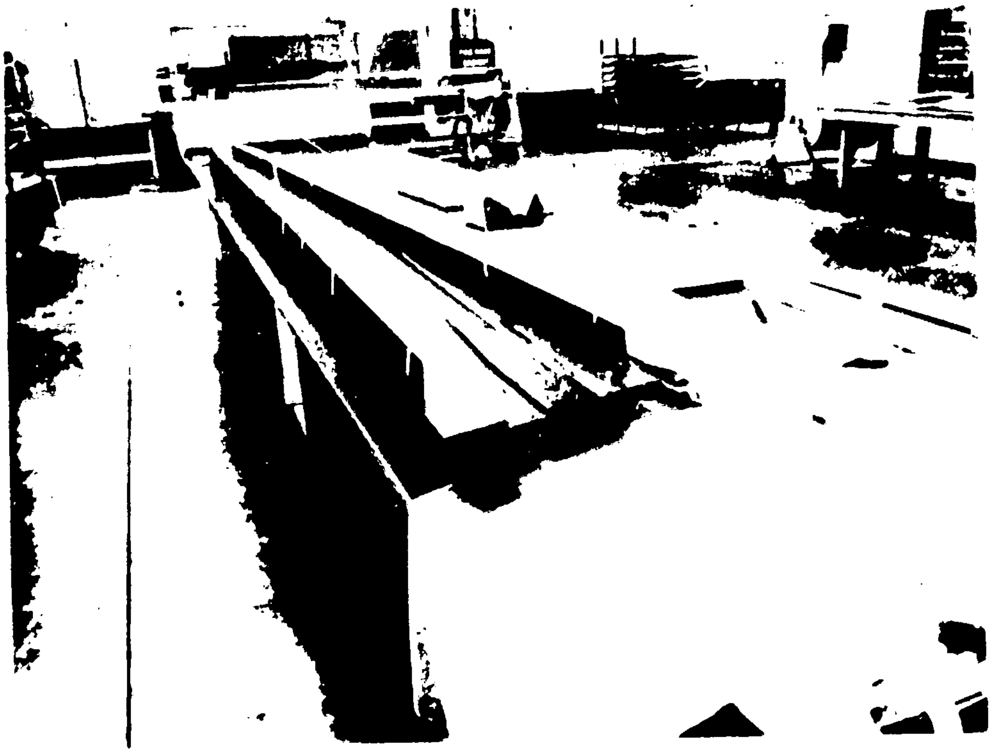

Figure 54. Rear-Spar Preparation for Final Bond

ORIGINAL PAGE
BLACK AND WHITE PHOTOGRAPH

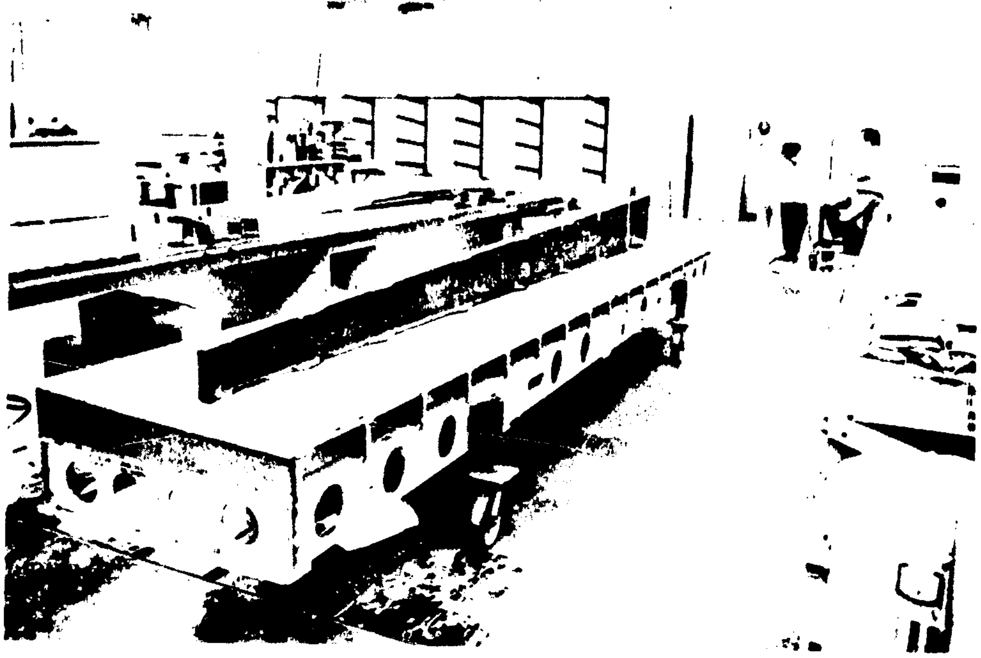

Figure 55. Rear-Spar After Final Bond and Chord Trim

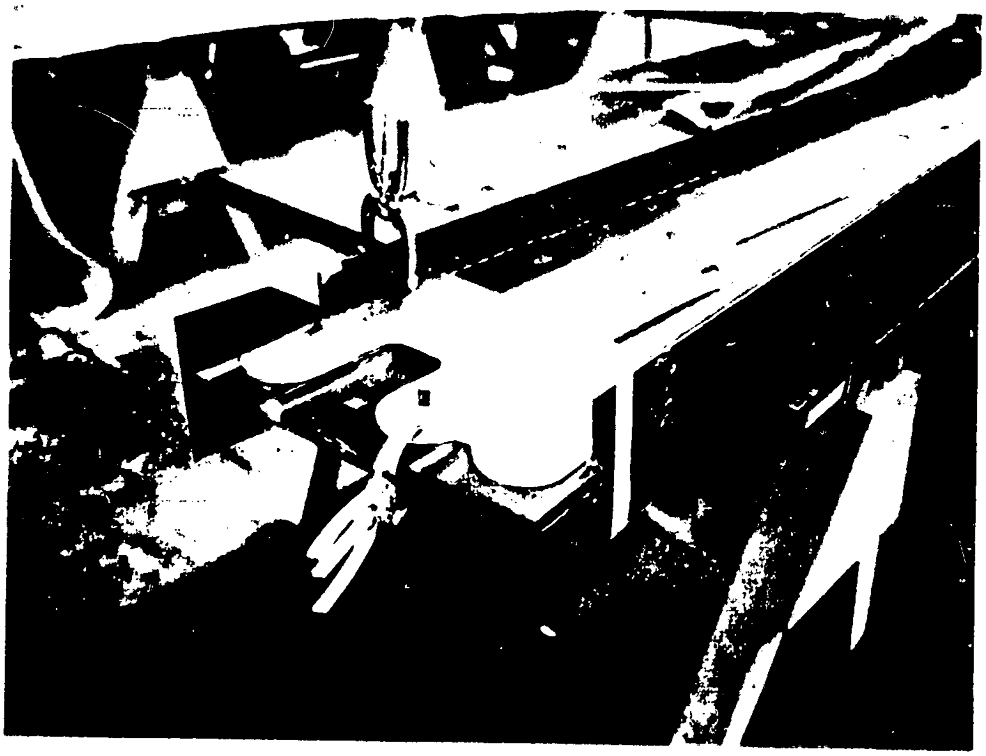

Figure 56. Rear-Spar Preparation for Inboard End Trim

ORIGINAL PAGE IS
OF POOR QUALITY

ORIGINAL PAGE
BLACK AND WHITE PHOTOGRAPH

halves was satisfactory. After bonding the spar caps to the channel section, however, both spars exhibited spanwise warp away from the bond tool (fig. 57). Subsequent net trimming of the caps and cutting of access holes relieved the condition in the front spar to the point where light hand pressure could place it in proper fitup to the bonding tool. The rear spar had a greater amount of warp; however, and these operations did not relieve conditions enough to avoid having to provide tooling assist in the assembly stages to hold it in proper contour position.

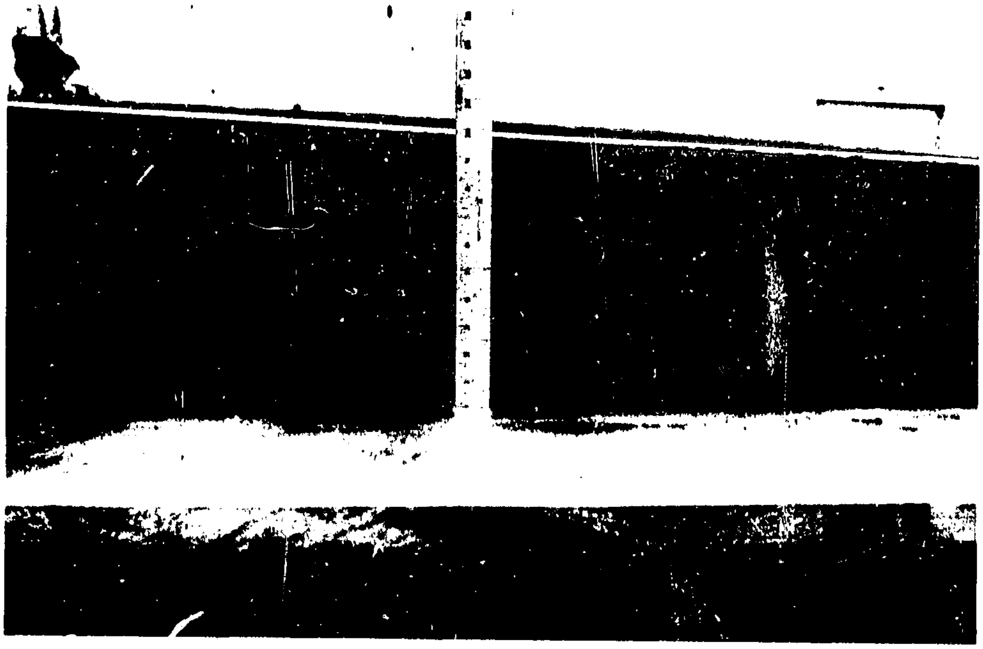

Figure 57. Spar Warpage

4.3.4 Fabrication Problems and Solutions

Overall, the production problems for the five stabilizer shipsets were minimal and only occasionally caused setbacks in the production schedules. The predominate problems experienced were:

Delamination Shipset 1, Right-Hand Upper Skin Panel—Component fabrication for shipset 1 was completed on schedule except for the right-hand upper skin panel. Completion of this panel was delayed by an unexpected problem caused by delamination of some of the stringer caps after the cure cycle. This production article exhibited delamination in five stringers (fig. 58).

Two sets of test panels were constructed to determine the cause of the problem. The first panel was five stringers wide and 152.4 cm (5 ft) long. Suspected factors tested were material age, bagging techniques, caul-strip buckling, and bond-line contamination. This panel showed no delamination. The age of the material was ruled out as a contributing factor, but it was determined that a full-length panel test was required to fully assess other probable causes. The second panel was six stringers wide, each with a different layup and bagging technique for capping the stringer ends, tying down the aluminum caul strips, and for resin bleeding.

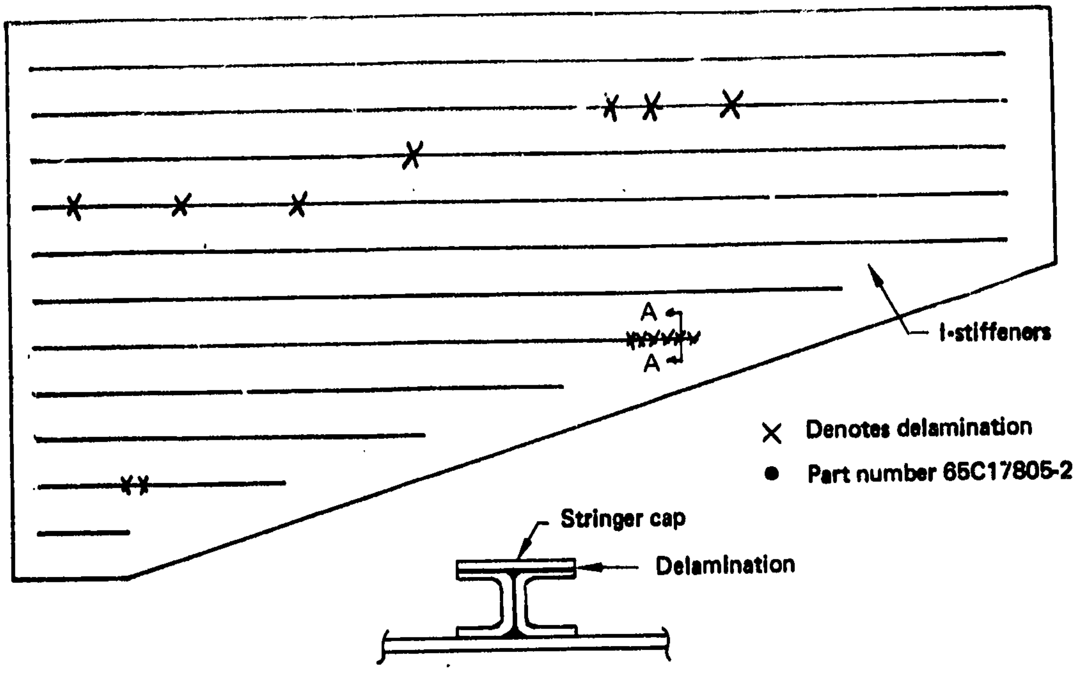
A
A
I-stiffeners
X Denotes delamination
● Part number 65C17805-2
Stringer cap
Delamination
View A-A rotated 90 deg, no scale

Figure 58. Delamination in Stabilizer Upper Skin Panel

The full-length test panel showed no delamination and established the need for revisions in present layup and bagging techniques to ensure that the condition would not recur. As a result, the full-size production panel was remade with the following changes (fig. 59):

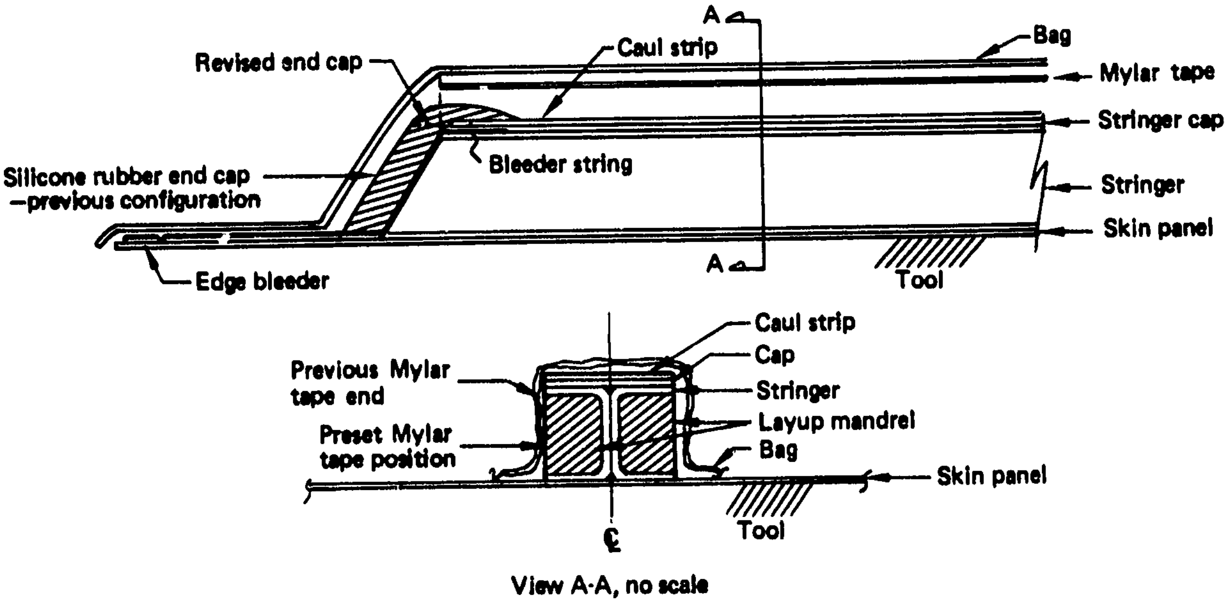
A
Bag
Caul strip
Revised end cap
Mylar tape
Stringer cap
Bleeder string
Silicone rubber end cap
—previous configuration
Stringer
Skin panel
A
Edge bleeder
Tool
Caul strip
Cap
Previous Mylar tape end
Stringer
Layup mandrel
Preset Mylar tape position
Bag
Skin panel
Tool
℄
View A-A, no scale

Figure 59. Stabilizer Typical Skin Panel/Stringer Layup

- Caul strips were shortened and refinished with Teflon to provide less friction and prevent buckling.

- Mylar tape used to hold caul strips in place was extended to tie into the stringer mandrels.

- String was added at the ends of stringers to provide a bleeder path to the edge bleeder.

The first two changes were made to prevent interference between the caul strips and the rubber caps during caul-strip expansion and, thus, eliminate potential buckling of the strips. The taping was altered to ensure positive tiedown of the caul strips, and the bleeder string was added to control and reduce resin bleedout. The remade panel exhibited no delamination.

Warpage Rear-Spar Assembly—Spanwise warpage was a problem in producing the spars for the left-hand test unit. Programs instituted to correct the problem were successful, and spars for shipset 1 were within engineering tolerances.

Evaluations of the fabrication processes used during production of the left-hand units and developmental test programs showed that there were three primary reasons for warpage: temperature differential between the tool-side spar cap and the upper spar cap, interface friction between the tool and the part, and cool-down rate. To correct these conditions, processing changes were made:

- **Temperature differential.** Two plies of style 1597 fiberglass were placed over the upper spar cap as an insulation blanket to balance the temperature between the upper and lower cap during autoclave cure (fig. 60).

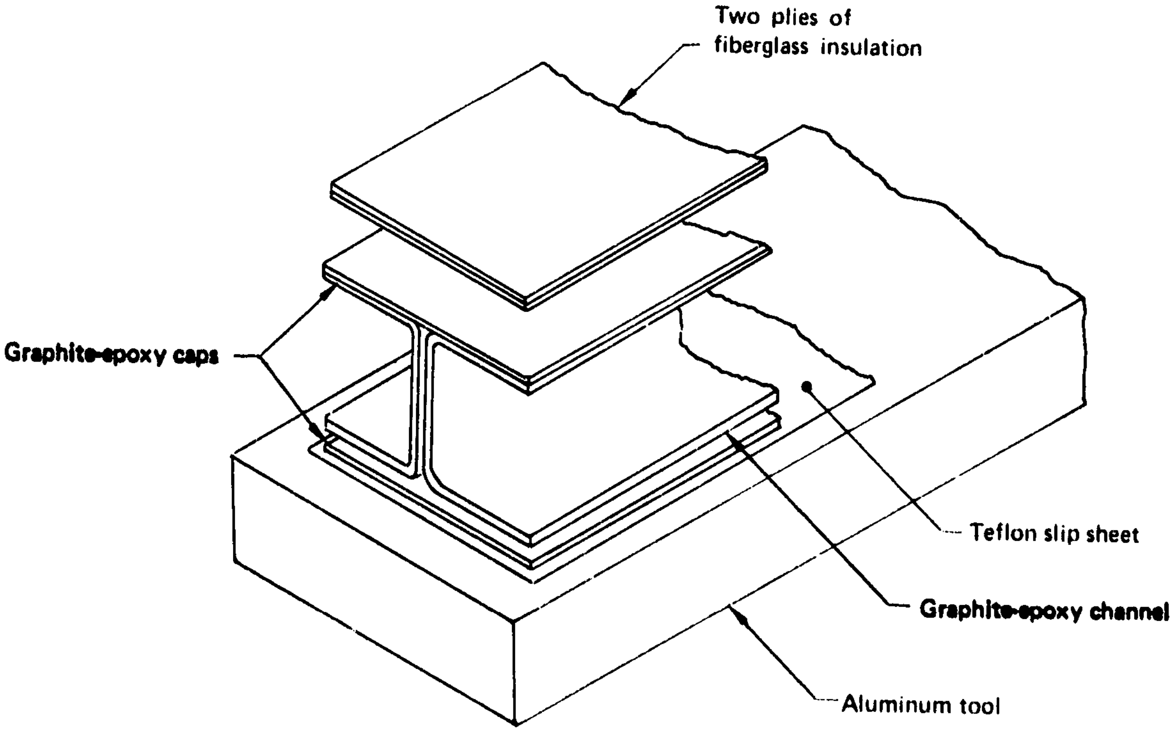

Note: Use of fiberglass insulation and
Teflon slip sheet to reduce warpage

Figure 60. Spar Bonding

- **Spar/tool interface friction.** A Teflon slip sheet was applied between the tool surface and the part to allow expansion and contraction of the tool without inducing stress buildup in the part (fig. 60).
- **Cool-down rate.** The rate was controlled to a maximum of 1°C/min (2°F/min) rather than to the allowable 3°C/min (5°F/min).

Resin-Starved Areas—Work was suspended on advanced composite components for shipsets 2 through 5 while engineers assessed methods to eliminate local areas of the resin-starved surface appearance. The assessment indicated that only the ribs and skin panels presented a problem and that a design change to replace 3K-70-P fabric with grade-95 tape on the tool sides of these parts would correct the conditions. The change was tried on a test rib and skin panel, which showed a marked improvement in surface quality. Drawings were subsequently revised to reflect the change in design, beginning with shipset 3. Another concern was the potential for fiber breakout by drills exiting through rib flanges. To correct this condition, one layer of 120-fiberglass fabric was added over the graphite-epoxy tape plies (tool side of the part) on the rib flanges and surfaces of the ribs common to the rear-spar attach angles.

Bonding Failure—The shipset 3 left-hand rear-spar and trailing-edge beam were scrapped and had to be remade because of bonding failure. An electron spectroscopy study of the bonded surfaces disclosed traces of silicon, and chemical analysis of the Frekote release agent showed the same silicon compounds. It was determined that the most probable cause of Frekote contamination of the bonded surfaces was either the wiping cloths or the MEK cleaning fluid. The latter was more probable, since the two liquids are identical in appearance and were kept in identical containers. The entire bonding procedure was subsequently reviewed, and appropriate procedures were implemented to prevent this recurrence.

4.4 ASSEMBLY OPERATIONS

The first major assembly step was the buildup of the rear-spar/trailing-edge area. Buildup consists of the rear-spar assembly (figs. 61 and 62), elevator hinge support ribs, trailing-edge beams, inboard and outboard closure ribs, and the upper and lower trailing-edge skin panels (figs. 63 through 66). The assembly tool provided tooling assistance for holding the warped spar in position. Shims were not needed for fitup of the metal ribs to the spar.

Boeing Wichita Company performed a fit check of the production elevator/balance panels on the left-hand test unit (fig. 67). The fit check uncovered minor interference problems between the elevator skin fasteners and the trailing-edge beam of the stabilizer, and it also determined that the installation time was approximately three times longer than for production line units. The primary

ORIGINAL PAGE
BLACK AND WHITE PHOTOGRAPH

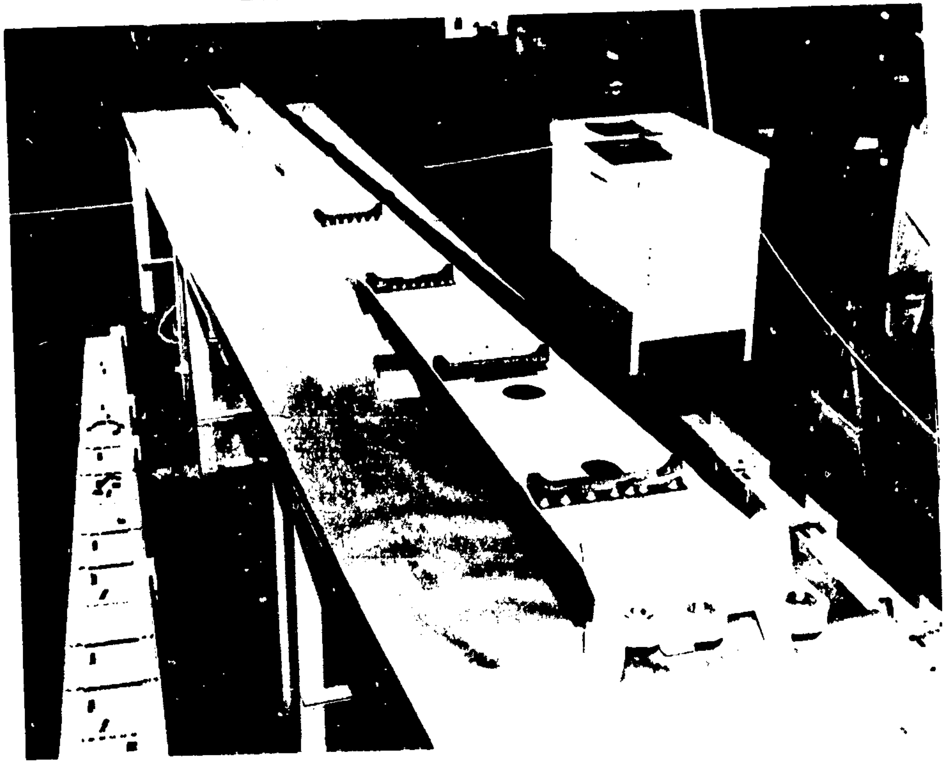

Figure 61. Left-Hand Rear-Spar Assembly—Aft Side View

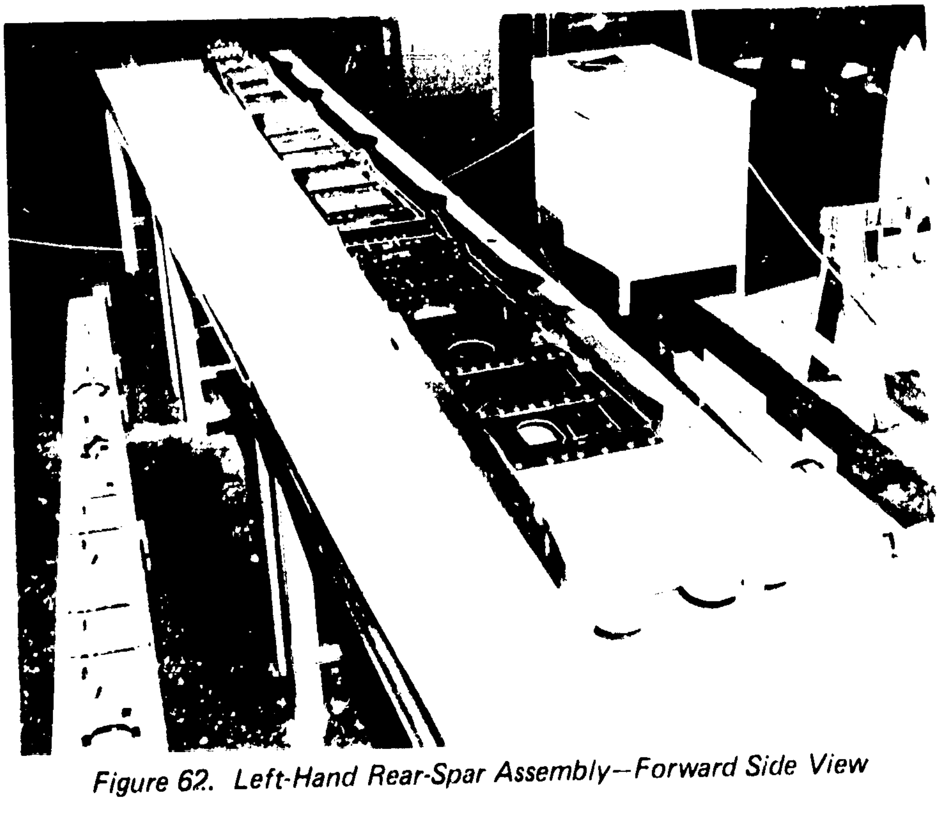

Figure 62. Left-Hand Rear-Spar Assembly—Forward Side View

ORIGINAL PAGE
BLACK AND WHITE PHOTOGRAPH

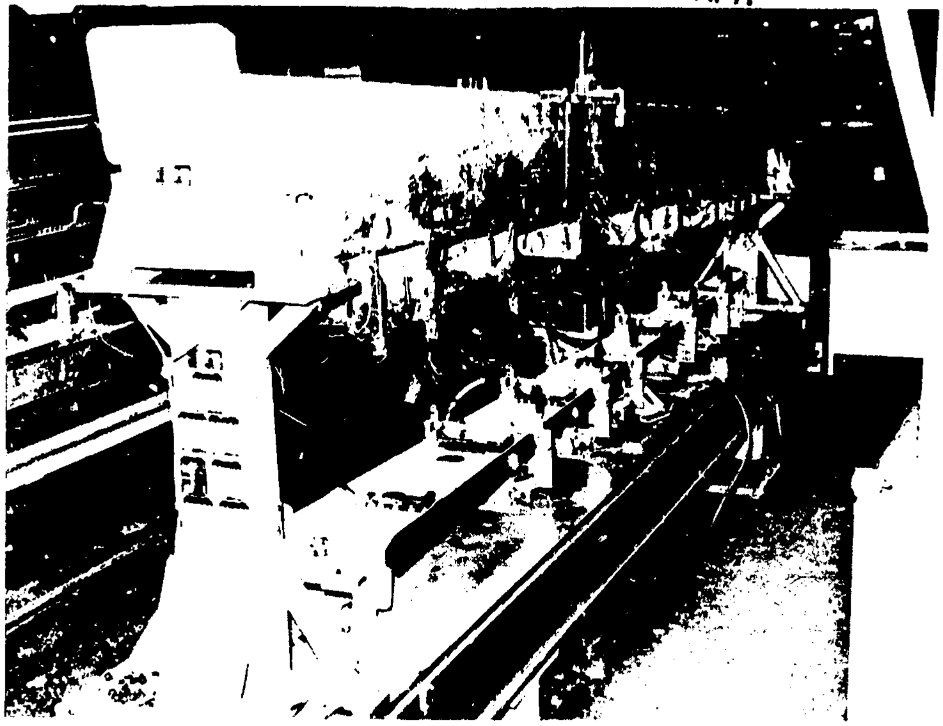

Figure 63. Left-Hand Rear-Spar Located in Trailing-Edge Assembly Tool

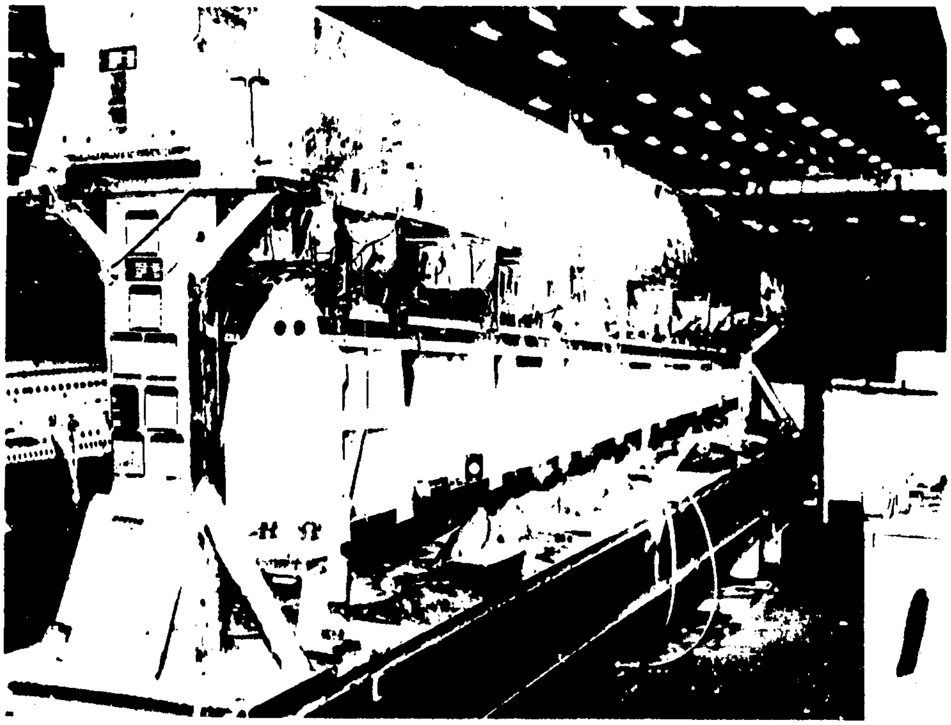

Figure 64. Left-Hand Rear-Spar/Trailing-Edge Assembly

ORIGINAL PAGE
BLACK AND WHITE PHOTOGRAPH

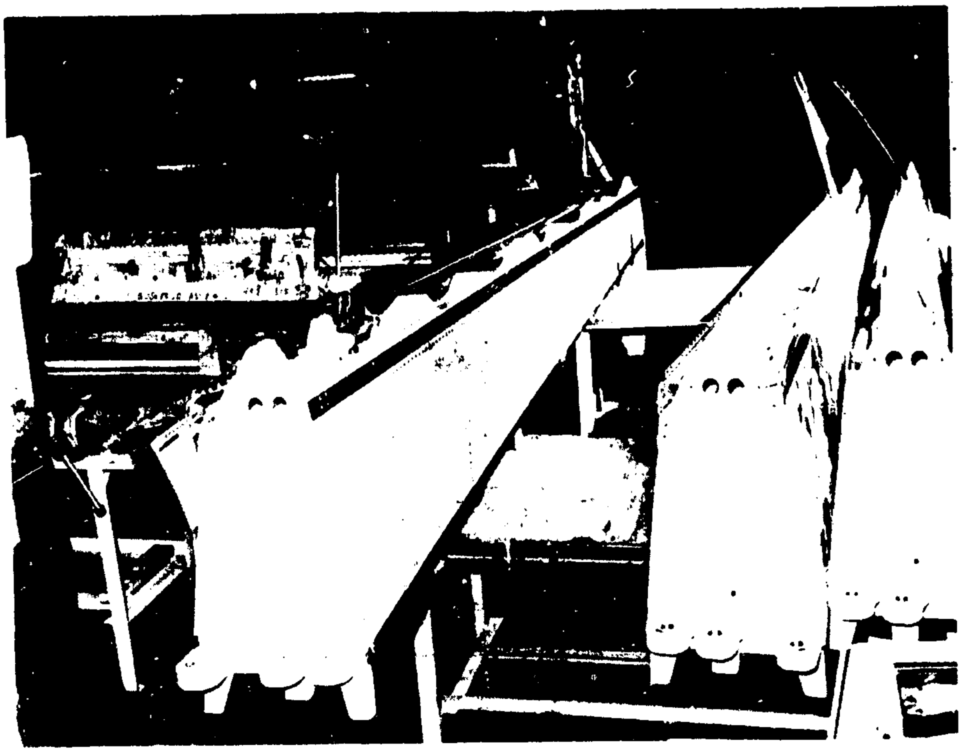

Figure 65. Left-Hand Rear-Spar/Trailing-Edge Assemblies—Inboard End View of Advanced Composites (Left) and Metal (Right)

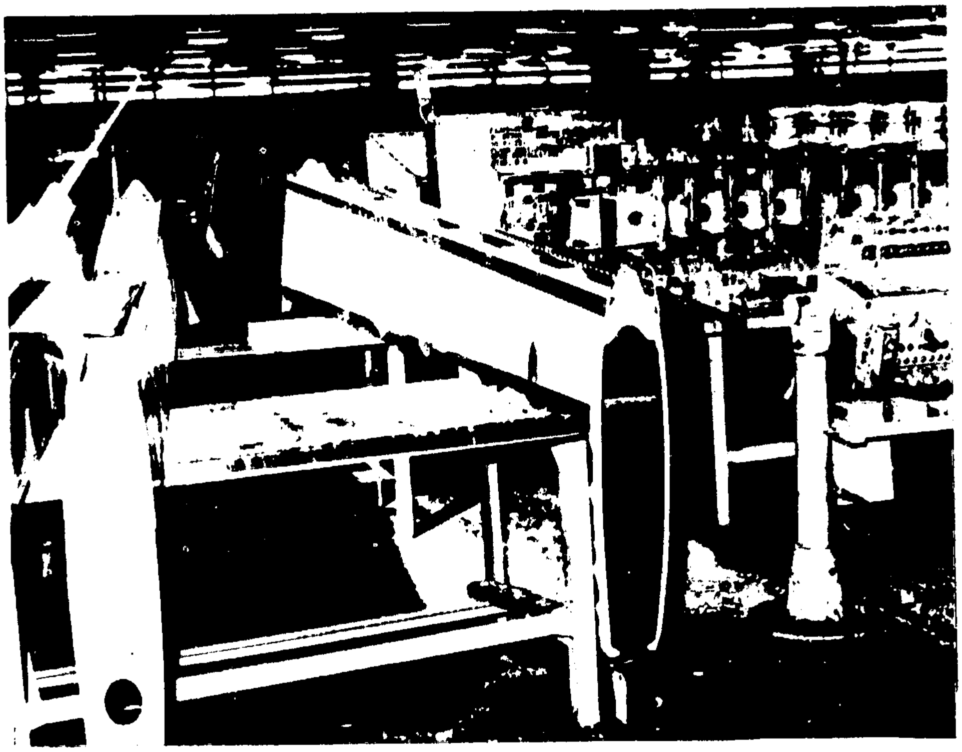

Figure 66. Left-Hand Rear-Spar/Trailing-Edge Assemblies—Outboard End View of Advanced Composites (Right) and Metal (Left)

ORIGINAL PAGE
BLACK AND WHITE PHOTOGRAPH

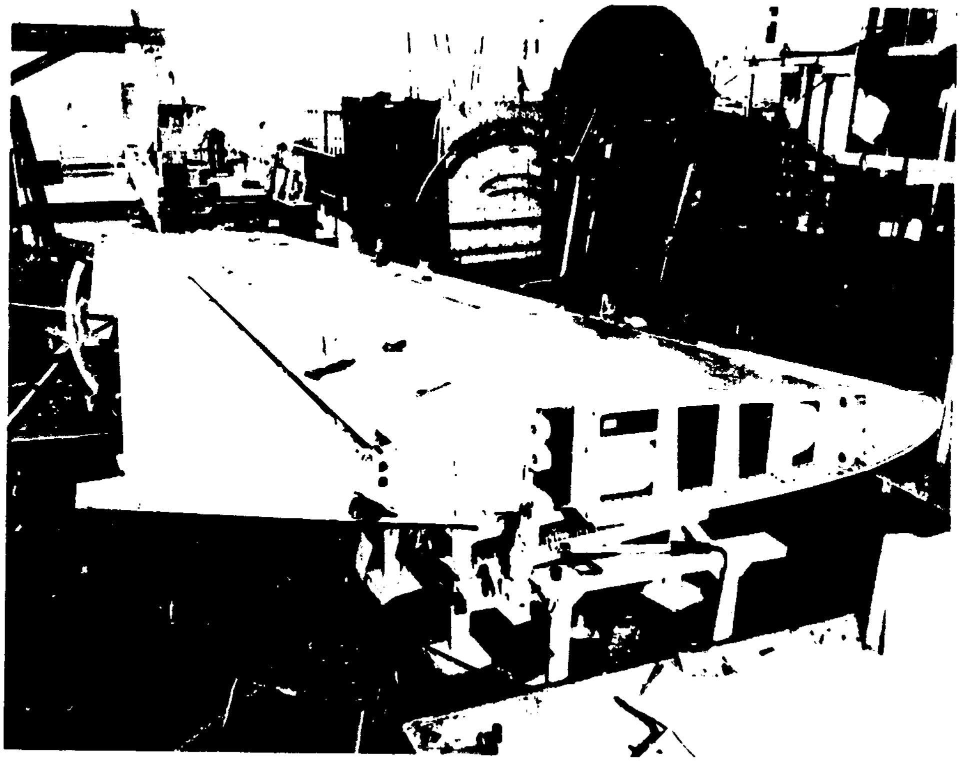

Figure 67. Stabilizer During Fit Check to Production Elevator/Balance Panels

reason for the latter condition was the extra time required to convert to the elevator hinge attachments that allow for thermal expansion differences between the advanced composites stabilizer and the metal elevator. Engineering design revisions corrected the interference problem.

The stabilizer box was fabricated by joining the rear-spar/trailing-edge assembly, front-spar assembly, inspar ribs, and skin panels. Production problems associated with the advanced composite components were minimal. Drilling and countersinking were readily accomplished, and part fitup was good. Skin panel warpage, as noted in Section 4.3.2, did not present the problem that had been anticipated.

The panels conformed to contour with hand pressure, and the original tooling provisions thought necessary for that purpose were not required. Sequential fastening was used to install the panels, assisted by Cleco clamping to hold contact at the rib locations. As experienced on the model 727 elevator, the nutplate installation for the closeout (upper) panel was time consuming, and some titanium bolts galled and prematurely torqued out in the crimped steel nutplates. The Visu-lok blind fastener, which was substituted for nutplates and bolts on the elevator, was not used on the left-hand stabilizer because of the requirement to bond a washer to the interior surface. Alternative blind fasteners ("Bigfoot") were examined for use on shipsets 1 through 5.

ORIGINAL PAGE
BLACK AND WHITE PHOTOGRAPH

Figures 68 through 71 depict the sequence of production buildup of the major assembly. Completed stabi~~lizers~~ are shown in Figure 72.

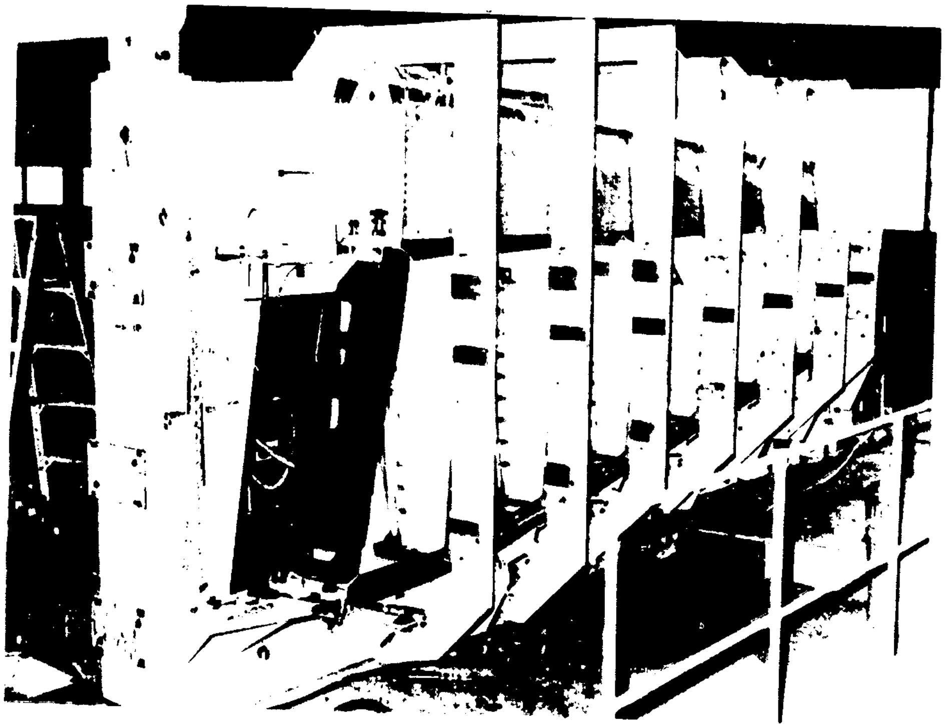

Figure 68. Left-Hand Trailing Edge, Front Spar, and Inspar Ribs in Major Assembly Tool—Inboard End View

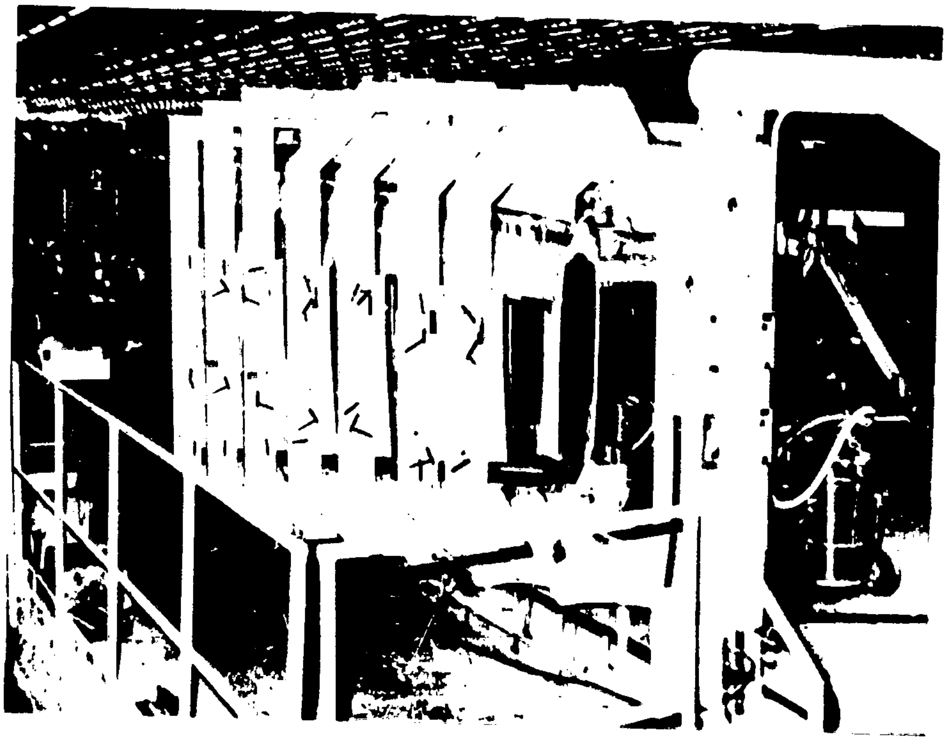

Figure 69. Left-Hand Trailing Edge, Front Spar, and Inspar Ribs in Major Assembly Tool—Outboard End View

ORIGINAL PAGE
BLACK AND WHITE PHOTOGRAPH

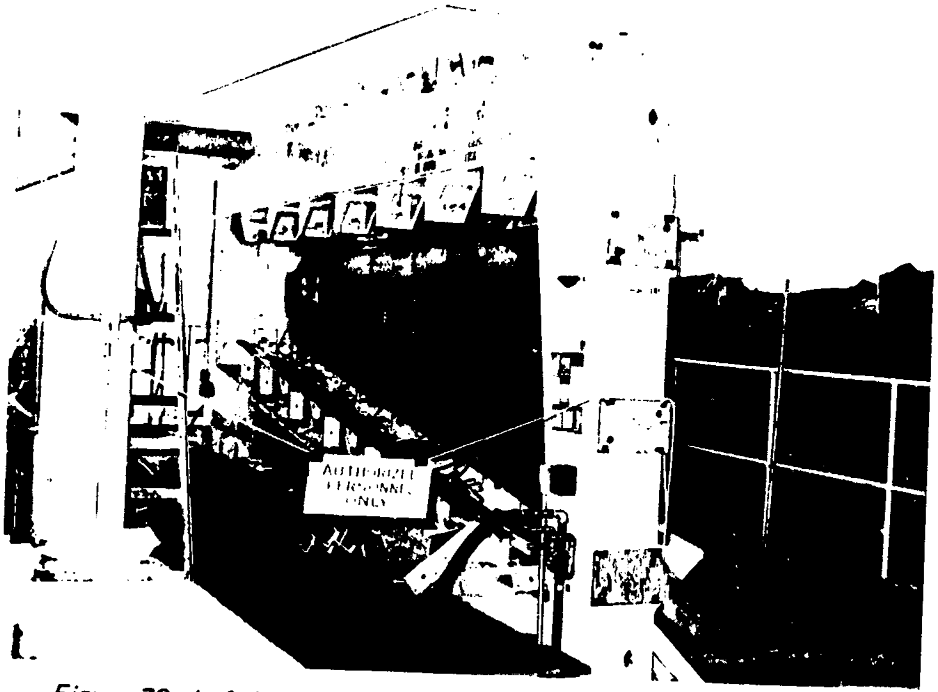
AUTHORIZED
PERSONNEL
ONLY

Figure 70. Left-Hand Stabilizer Box With Lower Skin Panel in Place

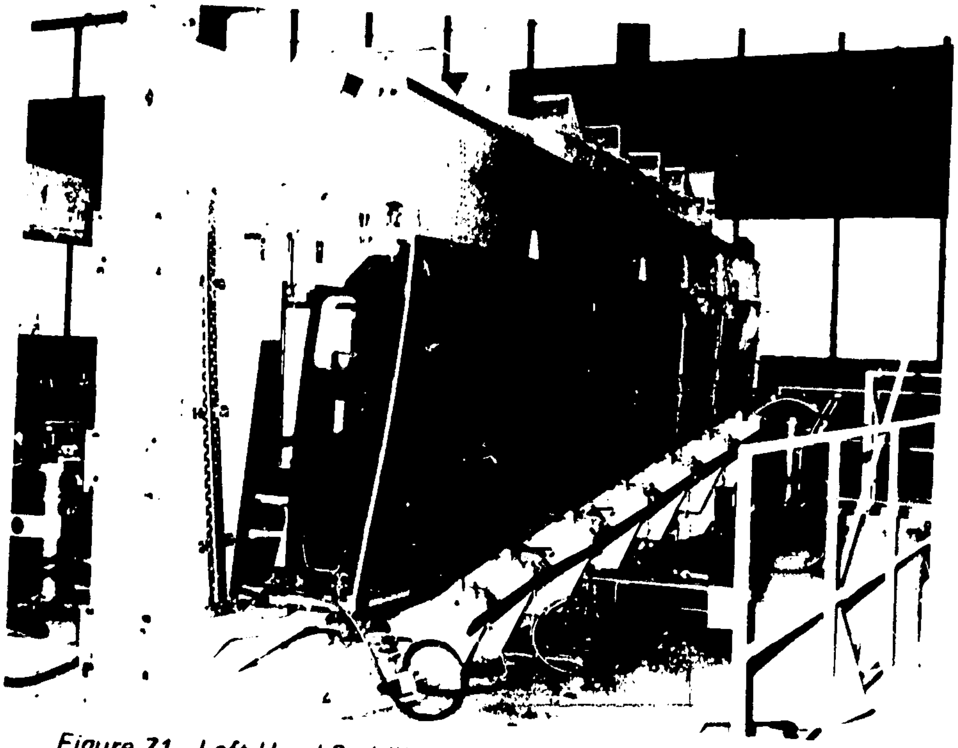

Figure 71. Left-Hand Stabilizer Box With Upper Skin Panel in Place

ORIGINAL PAGE
BLACK AND WHITE PHOTOGRAPH

ORIGINAL PAGE IS
OF POOR QUALITY

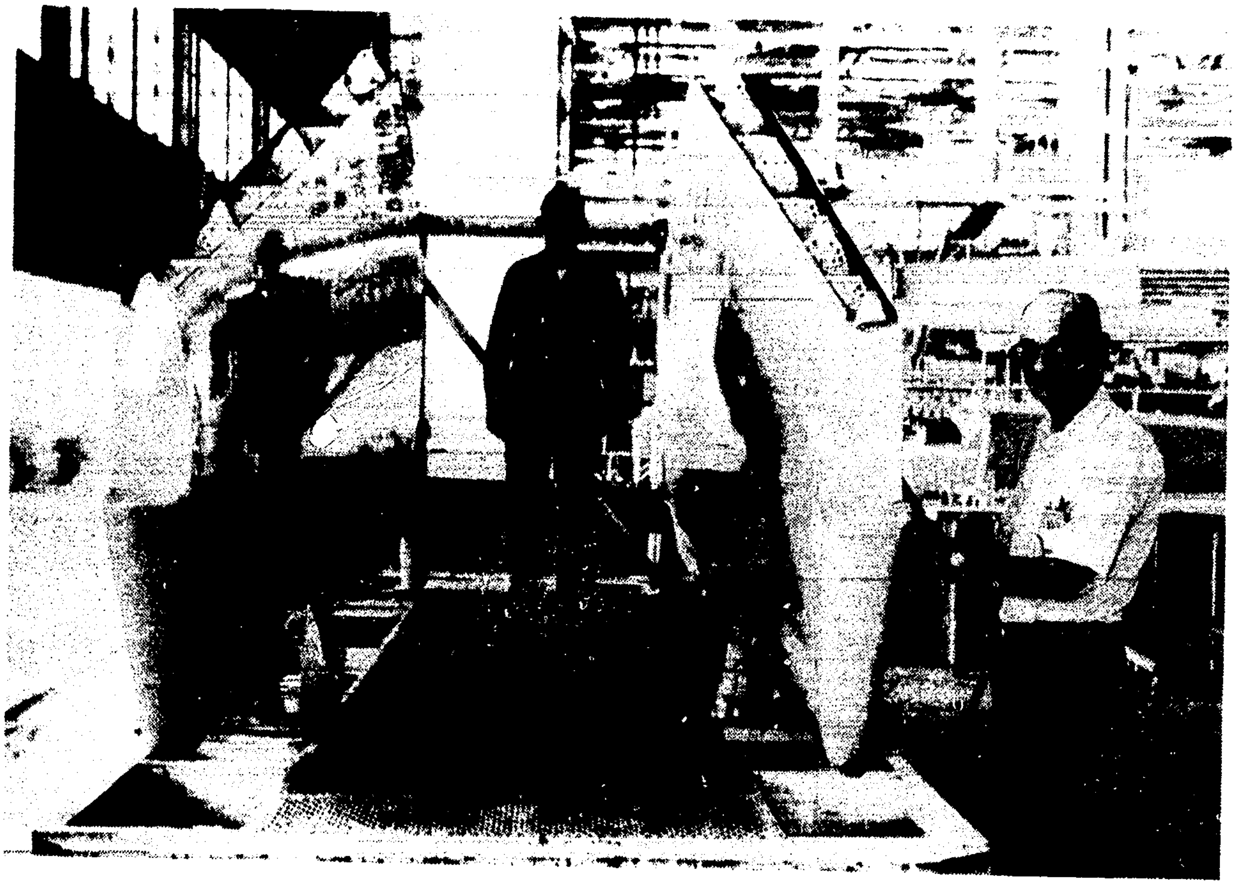

Figure 72. Completed Stabilizers

4.4.1 Assembly Schedules

Nine major assembly positions were scheduled for each assembly:

- Front spar
- Rear spar
- Rear-spar and trailing-edge join
- Stabilizer major assembly
- Stabilizer mill and bore
- Stabilizer—floor pickup position
- Stabilizer—seal
- Stabilizer—paint
- Stabilizer—shipping preparation

The total five-and-one-half shipset program was accomplished on schedule with minimal disruptions. Figure 73 shows the program master schedule.

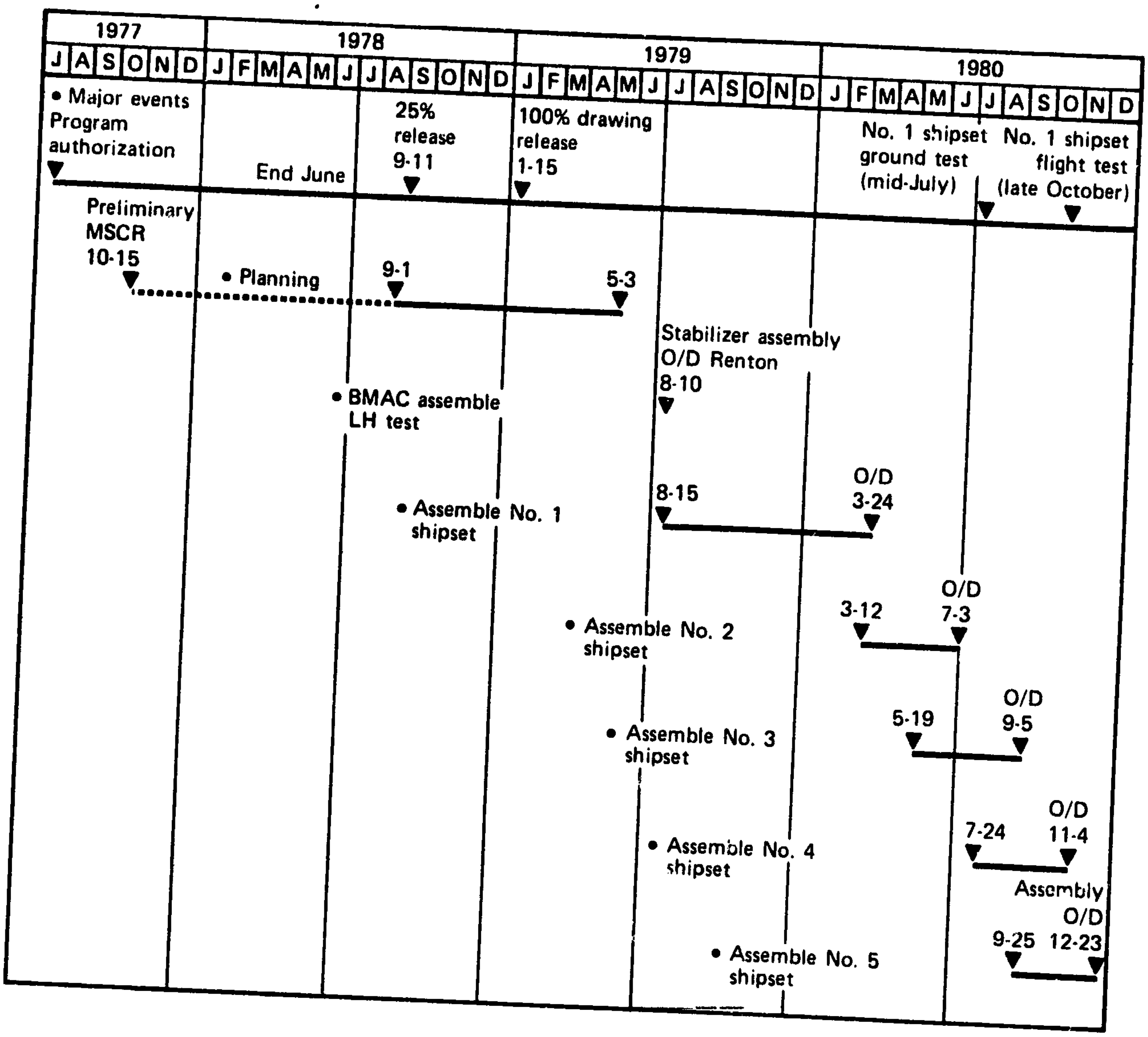

Figure 73. Operation Phasing Summary

4.4.2 Assembly Problems

The Bigfoot blind fastener used in the shipset 1 skin panel installation required excessive labor hours to shave inconel pins that broke off up to 25 mm (0.10 in) from flush.

The problem was resolved on shipset 2 by using the Bigfoot fastener with an A286 steel pin. The change reduced shaving time 70% on shipset 2, or 44 labor hours per airplane.

Hole breakout was encountered on shipset 3 when drilling unidirectional-tape-finished skins. The problem was reduced but not eliminated by priming the skin surface and using wooden and phenolic blocks as backup. In the event of a follow-on program, it would be beneficial to develop a template to be spotted on the outer-skin surface.

ORIGINAL PAGE IS
OF POOR QUALITY

PRECEDING PAGE BLANK NOT FILMED

5.0 COST ANALYSIS

This section presents the analysis of production cost data for the five-and-one-half-shipset production run. It addresses only those costs directly incurred in producing five-and-one-half shipsets of 737 advanced composite stabilizers using the methods and techniques developed during the preproduction phases of the program. Manufacturing process, assembly, and tool development considerations, and their production applications are discussed in detail in Section 5.0 of Reference 3 and Section 4.0 of this report.

Total production program costs shown in Figure 74 reflect the fabrication and manufacturing processes used in a semiproduction environment for the five-and-one-half-shipset program. Tooling and component manufacturing percentages are relative to overall costs in dollars; engineering costs are not included.

Work was performed in production shops by employees whose experience and skill levels represented a cross section of the shop work force. Component fabrication was performed with hand cutting and layup of broadgoods, ply-by-ply inspection, and hand trimming. Tooling was designed for extended production; however, the tool rework and improvement effort was restricted to the five-and-one-half-shipset contract.

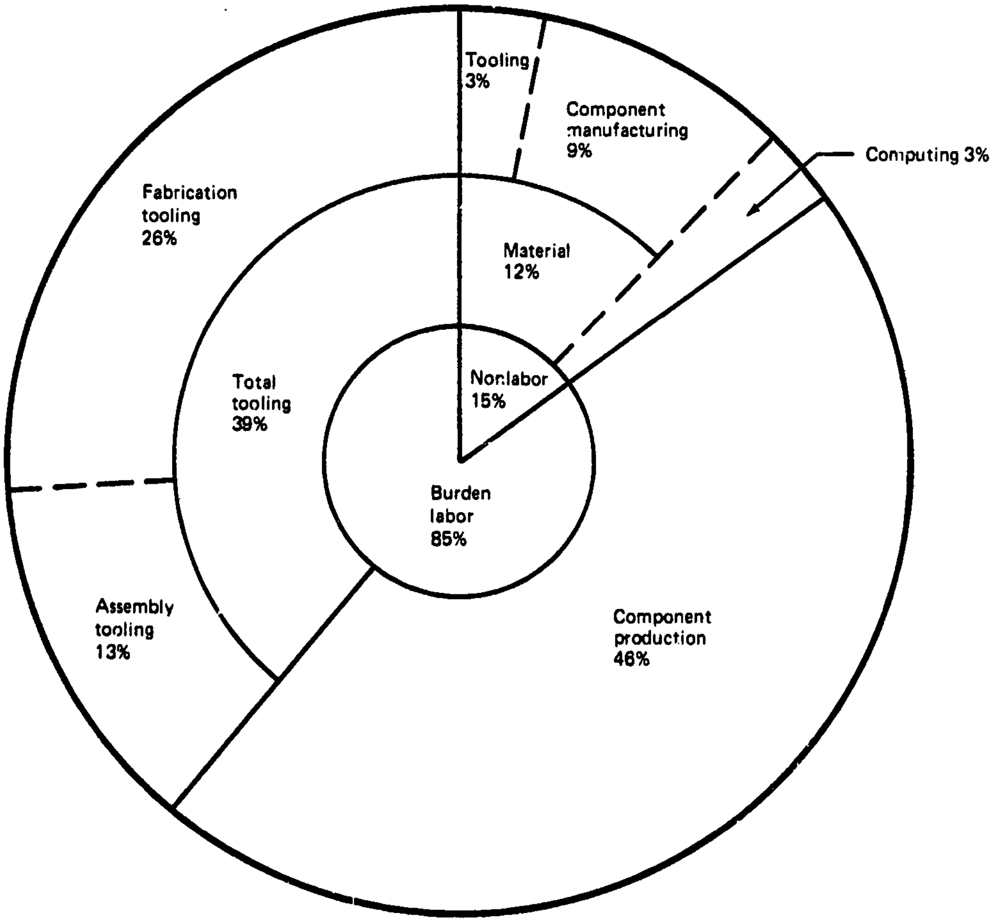

Figure 74. Total Recurring and Nonrecurring Production Costs by Major Element—5½ Shipsets

PAGE 70 INTENTIONALLY BLANK

ORIGINAL PAGE IS
OF POOR QUALITY

These activities were representative of the production processes that would, insofar as practical, be used to produce a large number of stabilizers. It is likely, however, that by adopting improved manufacturing processes, the per-unit cost of stabilizers produced in a regular production environment would be significantly lower. Projections of production cost trends are discussed in Section 5.3.

5.1 LABOR COSTS

Total recurring labor costs by shipset are detailed in Table 7. Separate costs are recorded for the larger process assembly items (i.e., cover panels, ribs, spars, and beam assemblies) because they are produced from single unit orders. Costs of lot-time items are prorated equally among the shipsets and are included in the unit costs.

Table 7. Recurring Labor Hours– 5 Shipsets

Description	Total	Left hand					Right hand				
		1	2	3	4	5	1	2	3	4	5
Front spar	7 817	862	①1030	753	667	712	817	② 614	853	633	③876
Rear spar	9 240	1068	853	1195	735	829	877	⑤1240	829	800	814
Ribs	5 201	401	437	624	④664	526	372	464	589	628	496
Beam assembly	3 492	331	357	441	326	392	357	350	297	210	431
Upper skin panel	3 578	273	261	⑥ 7	400	323	⑦ 604	⑧ 592	239	⑨ 607	272
Lower skin panel	3 273	266	464	305	251	279	342	279	340	328	⑩419
Graphite components	32 601	3201	3402	3325	3043	3061	3369	3539	3147	3206	3308
Nongraphite and blanket time	2 092 2 870	215 282	291 299	175 293	173 268	193 269	215 296	290 312	175 277	173 283	192 291
Manufacturing Engineering, Planning	2 025	203	202	202	202	202	203	203	203	202	203
Quality control	7 590	745	792	774	708	713	784	824	732	747	771
Fabrication recurring	47 178	4646	4986	4769	4394	4438	4867	5168	4534	4611	4765
Unit time assembly (CC5)	7 445	875	816	681	731	660	946	724	650	724	638
Nongraphite fabrication (CC40)	5 538	651	607	507	544	491	704	538	483	539	474
Subassembly (CC42)	5 399	634	592	494	530	478	686	525	472	525	463
Allocables	7 397	869	811	677	726	655	940	719	647	719	634
Quality [illegible]	2 066	243	226	189	203	183	263	201	180	201	177
Planning/Engineering/ Finance, direct	831	97	91	76	82	74	105	81	73	81	71
[illegible]	500	59	55	45	49	44	64	49	43	49	43
Recurring Wichita assembly	29 176	3428	3198	2669	2865	2585	3708	2837	2548	2838	2500
Engineering/MR &D/ Planning/QA liaison sustaining	3 579	351	373	365	334	336	370	389	346	352	364
Total recurring	79 933	8425	8557	7803	7593	7359	8945	8394	7427	7801	7629

① 93 scrap
② 126 scrap
③ 129 scrap
④ 109 scrap
⑤ 342 rework
⑥ Changed to tape and funded by Boeing/516 hr
⑦ 133 rework, 93 scrap
⑧ 263 scrap
⑨ 269 scrap
⑩ 129 scrap

ORIGINAL PAGE IS
OF POOR QUALITY

Nongraphite parts common to both the composite and metal stabilizers required rework of the tools to accommodate differences in configuration. The costs of fabrication of these nongraphite parts have been segregated and are identified in Table 7 and Figures 75 and 76.

Figure 75 and Table 8 show the total recurring and nonrecurring component production labor expenditures excluding tooling. The data provide a breakdown of the labor expenditures into the categories of component fabrication, Manufacturing Research and Development (MR&D), and assembly. The MR&D effort was liaison support to the fabrication and assembly work. Figure 75 shows that 64% of the total labor was for component fabrication including planning. This compares to only 30% for assembly including planning and 6% for liaison support. For aluminum, an average based on 200 shipsets experienced 64% of total labor for fabrication and 36% for assembly.

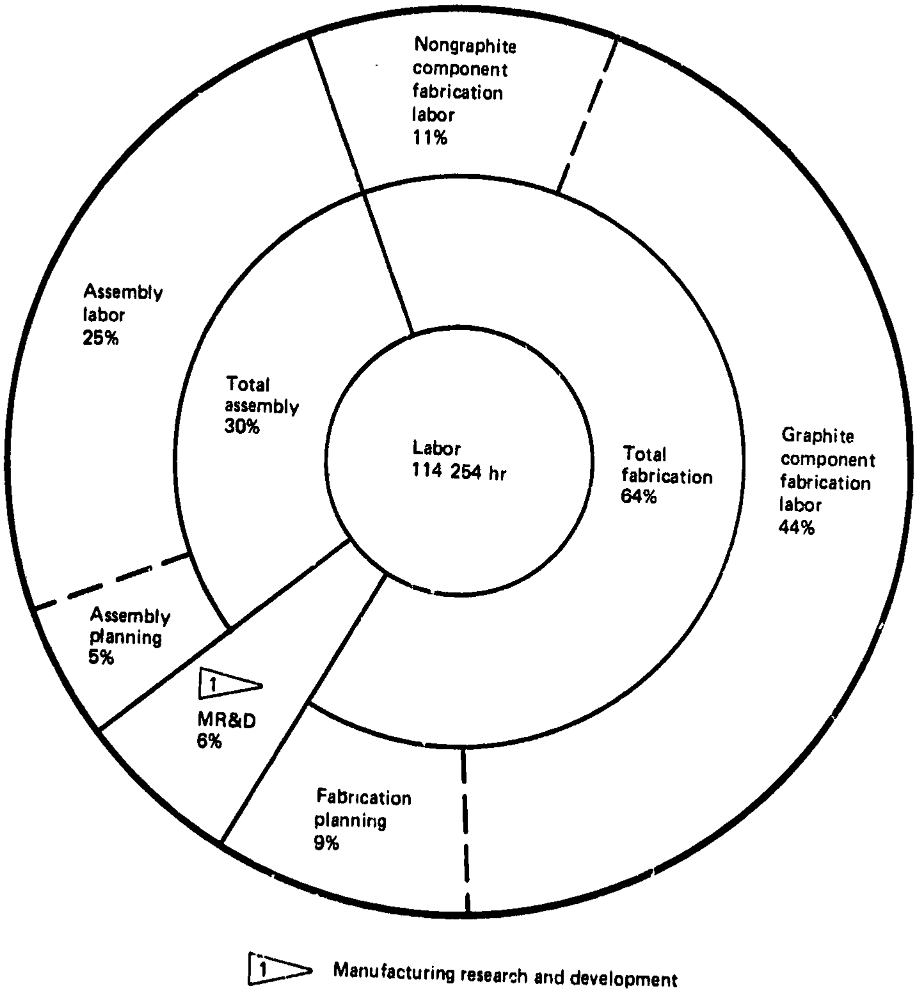

Figure 75. Total Recurring and Nonrecurring Component Production Labor Hours--5½ Shipsets

ORIGINAL PAGE IS
OF POOR QUALITY

Table 8. Component Production Labor Expenditures—Total Recurring and Nonrecurring (Excludes Tooling and Engineering)

	Labor hours		
	Ground test unit	Five shipsets	Totals
Recurring			
● Fabrication (excluding planning)	–	51 876	51 876
● Fabrication planning	–	2 058	2 058
• Subtotal fabrication	–	53 934	53 934
● Assembly (excluding planning)	–	21 123	21 123
● Assembly (planning)	–	225	225
• Subtotal assembly	–	21 348	21 348
● Manufacturing research and development (MR&D)	–	745	745
• Subtotal MR&D)	–	745	745
• Total recurring	–	76 027	76 027
Nonrecurring			
● Fabrication (excluding planning)	11 061	–	11 061
● Fabrication (planning)	6 658	1 886	8 544
• Subtotal fabrication	17 719	1 886	19 605
● Assembly (excluding planning)	6 962	–	6 962
● Assembly (planning)	3 194	2 541	5 735
• Subtotal	10 156	2 541	12 697
● Manufacturing research and development (MR&D)	2 804	3 121	5 925
• Subtotal MR&D	2 804	3 121	5 925
• Total nonrecurring	30 679	7 548	38 227
Total recurring and nonrecurring	30 679	83 575	114 254

ORIGINAL PAGE IS
OF POOR QUALITY

Figure 76 provides a further breakdown of the recurring component fabrication labor hours. The primary cost element is layup, which accounts for 32% of the total fabrication labor. Graphite component fabrication (including layup, kitting, bag and cure, and trim) accounted for 57% of the total labor expenditures. Nongraphite fabrication accounted for 15% of the expenditures.

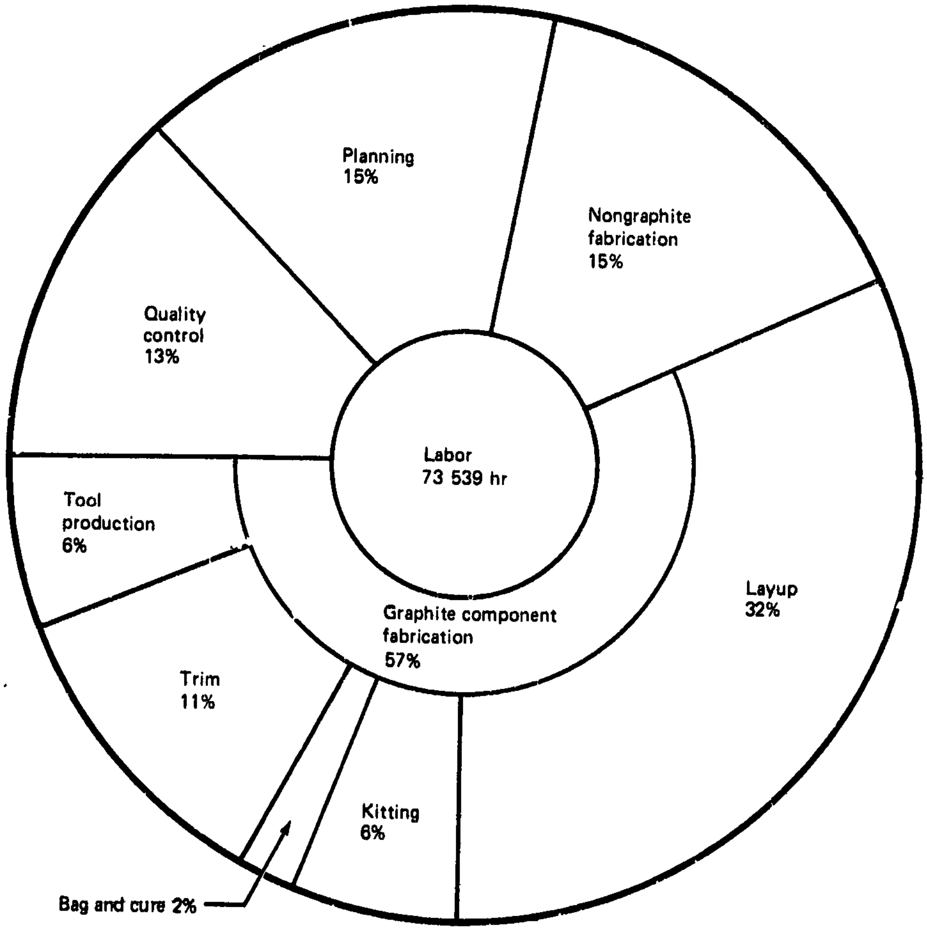

Figure 76. Total Recurring and Nonrecurring Fabrication Labor Hours

Table 9 shows total production tooling hours. Fabrication tooling labor hours were 66%, while assembly tooling labor hours were 34%. Recurring tooling labor hours were only 2%, while nonrecurring tooling hours, which included all left-hand test article tooling, were 98%.

Table 9. Production Tooling

	Labor hours		
	Design	Fabrication	Total
Recurring			
● Fabrication tools	127	827	954
● Assembly tools	–	500	500
• Subtotal	127	1 327	1 454
Nonrecurring [1]			
● Fabrication tools	3 087	58 562	61 649
● Assembly tools	168	31 779	31 947
• Subtotal	3 255	90 341	93 596
Total recurring and nonrecurring	3 382	91 668	95 050

[1] All left-hand test article tooling is nonrecurring

Figure 77 provides a breakdown of the total recurring and nonrecurring labor expenditures for component assembly. The primary cost element is assembly labor, which comprises 75% of the total. The balance consists of planning (17%) and quality control (8%).

Figure 78 shows the percentage breakdown of the recurring direct labor hours for the 737 composite stabilizer component fabrication and assembly. The MR&D effort, which is included in Figure 78, was expended in support of fabrication and assembly work and was not expended in the developmental hardware programs. Planning that occurred before 1980 was considered nonrecurring and was not included. Kitting, layup, bag and cure, and trim were based on hours generated by the applicable shops associated with those functions.

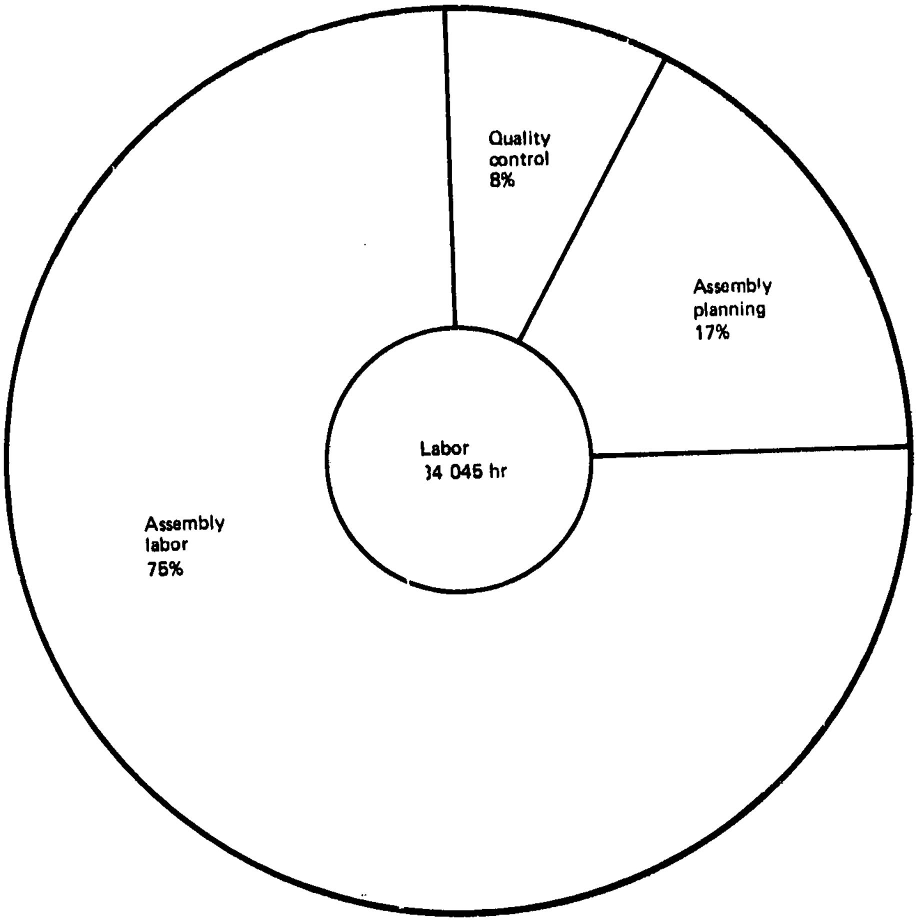

Figure 77. Total Recurring and Nonrecurring Assembly Labor Hours—5½ Shipsets

5.2 USAGE FACTORS

Usage factors experienced for graphite-epoxy materials were 0.78 kg (1.8 lb) of tape and 1.22 kg (2.8 lb) of fabric for each pound of graphite-epoxy flyaway weight in the finished stabilizer. This included indirect usage for receiving tests, kitting trim loss, process test panels, process and miscellaneous rejections, and layup trim loss. It is estimated that these usage factors could be reduced to 1.5 and 2.0 lb, respectively, over a 200-shipset program with more uniform quality materials, revised handling methods, and improved manufacturing processes. With automated material cutting/part nesting and new layup and processing technology, these factors would be further reduced.

ORIGINAL PAGE IS
OF POOR QUALITY

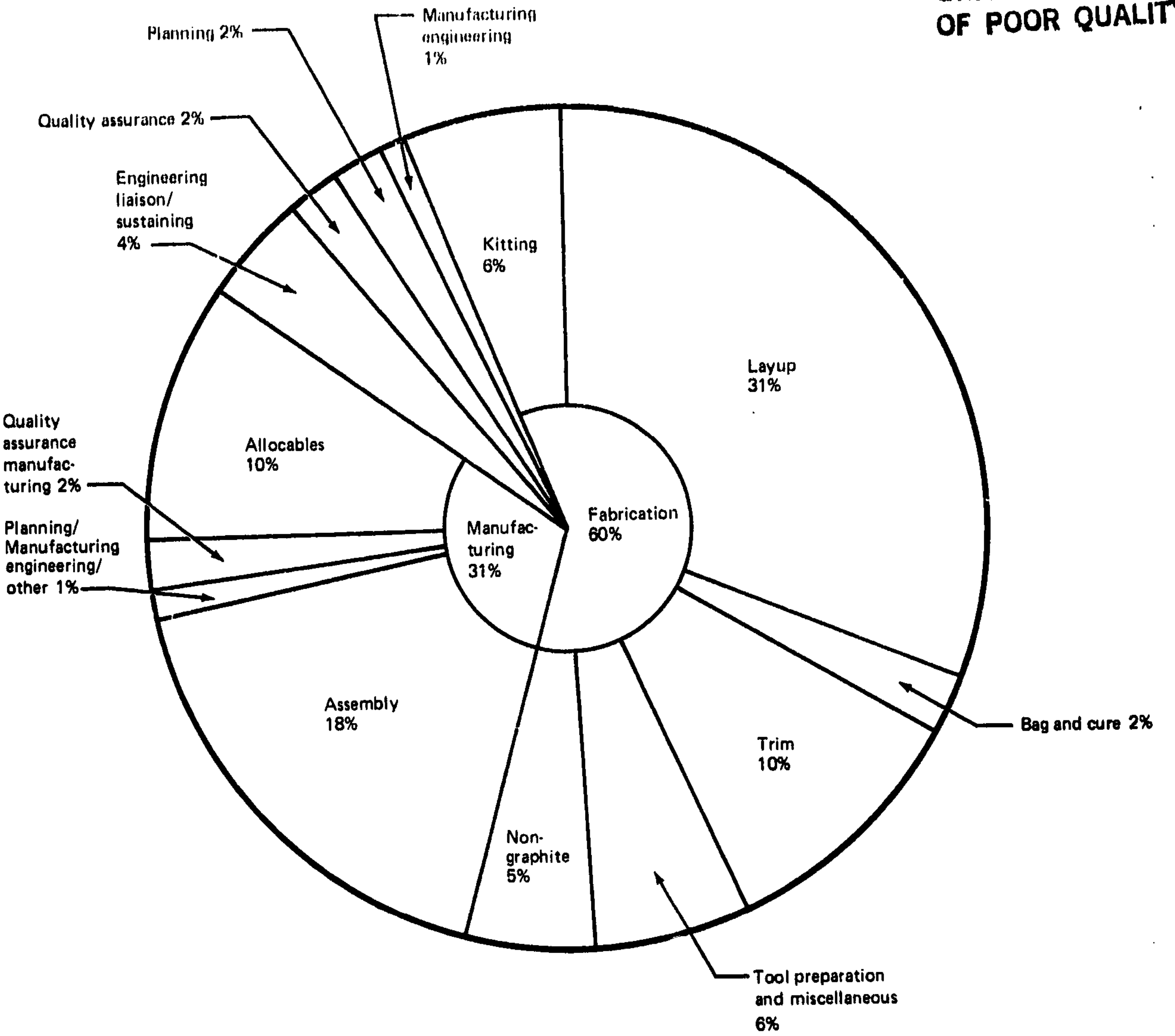

Figure 78. Fabrication and Assembly Recurring Costs (Percentage of Labor Hours)—5 Shipsets

Based on costs incurred in producing the five-and-one-half shipsets of the composite stabilizer, recurring costs for 200 shipsets are estimated at \$40.3 million, using the NASA baseline. This figure is derived from \$10.8 million in Wichita labor, \$0.7 million in Wichita material, \$22.1 million in Auburn labor, and \$6.7 million in Auburn material.

The effect of improved technology on the trend of competitive cost averages for the initial 200-shipset quantities of the model 737 composite stabilizer is depicted in Figure 79. This figure shows that the present costs could be reduced by 25% with improved automated methods. Further optimization of the design would be expected to produce additional cost benefits.

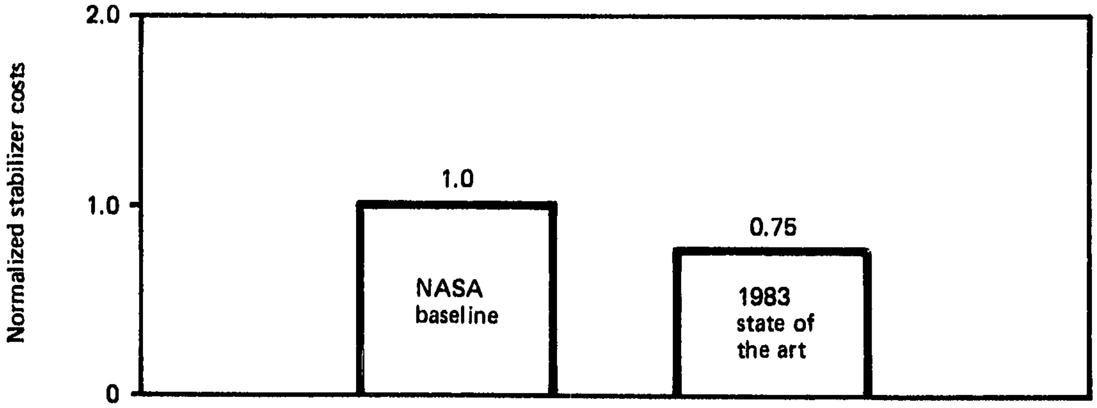

Figure 79. Relative Composite Stabilizer Cost Comparison—Initial 200 Shipsets

Ground rules for the cost projection of 200 shipsets of the composite stabilizer shown in Figure 79 are based on:

- Cost projection is the scoping level.
- Costs are recurring only for 200 shipsets.
- Costs reflect 1981 commercial pricing rates and do not include profit or contingency.
- Part count and weights are assumed to be the same as the NASA stabilizer.
- Auburn and Wichita labor hour estimates have been adjusted to reflect 1983 state of the art.
    - MR&D has defined 1983 state of the art to include automated tape laminators, automated ply cutters, vacuum compacting tables, improved fasteners, and laminated shims.
    - Designs will be revised as required to allow automated manufacturing methods.
- Graphite material costs are based on supplier quotations.
- Graphite epoxy usage factors: tape 1.5 lb, fabric 2.0 lb.
- Automation will radically change the ratio of tape versus fabric in the design.

5.3 CONCLUSIONS

It is projected that advanced composite material waste will be reduced with the implementation of advanced manufacturing technology and more uniform quality material. It also is projected that cost per pound of advanced composite material will decrease 20% as industry usage of the material increases. Based on these projections, the production experience gained during this program and assumptions of other cost-reducing factors as detailed in Section 5.2, the cost of advanced composite stabilizers will become comparable to the cost of similar metal components.

When the increasing value of weight reduction is considered together with the adoption of innovative manufacturing methods and engineering designs, the economic justification for advanced composite aircraft structure is ensured.

6.0 CONCLUSIONS

NASA established a program for primary composite structures under the Aircraft Energy Efficiency (ACEE) program. As part of this program, Boeing has redesigned and fabricated the horizontal stabilizer of the 737 transport using composite materials. Five shipsets were fabricated, and FAA certification has been obtained. Airline introduction will follow.

Key program results are:

- Weight reduction greater than the 20% goal has been achieved.
- Parts and assemblies were readily produced on production-type tooling.
- Quality assurance methods were demonstrated.
- Repair methods were developed and demonstrated.
- Strength and stiffness analytical methods were substantiated by comparison with test results.
- Cost data were accumulated in a semiproduction environment.
- FAA certification has been obtained.

The program has provided the necessary confidence for the company to commit use of composite structure in similar applications on new generation aircraft and has laid the groundwork for design of larger, more heavily loaded composite primary structure.

PRECEDING PAGE BLANK NOT FILMED

7.0 REFERENCES

1. Aniversario, R. B.; Harvey, S. T.; McCarty, J. E.; Parsons, J. T.; Peterson, D. C.; Pritchett, L. D.; Wilson, D. R.; and Wogulis, E. R.: Full-Scale Testing, Production, and Cost Analysis Data for the Advanced Composite Stabilizer for Boeing 737 Aircraft. Volume I—Technical Summary. NASA CR-3649, 1983.

2. Aniversario, R. B.; Harvey, S. T.; McCarty, J. E.; Parsons, J. T.; Peterson, D. C.; Pritchett, L. D.; Wilson, D. R.; and Wogulis, E. R.: Design, Ancillary Testing, Analysis, and Fabrication Data for the Advanced Composite Stabilizer for Boeing 737 Aircraft. Volume I—Technical Summary. NASA CR-3648, 1983.

3. Aniversario, R. B.; Harvey, S. T.; McCarty, J. E.; Parsons, J. T.; Peterson, D. C.; Pritchett, L. D.; Wilson, D. R.; and Wogulis, E. R.: Design, Ancillary Testing, Analysis, and Fabrication Data for the Advanced Composite Stabilizer for Boeing 737 Aircraft. Volume II—Final Report. NASA CR-166011, December 1982.

4. Federal Aviation Regulations, Part 25, Airworthiness Standards: Transport Category Airplanes. Department of Transportation, Federal Aviation Administration, December 1978.

PAGE 82 INTENTIONALLY BLANK

APPENDIX

FATIGUE SPECTRUM

PRECEDING PAGE BLANK NOT FILMED

FIGURES

		Page
A-1	Test Spectrum General Loading Sequence	A-5
A-2	Maneuver Alternating Load Levels	A-7
A-3	Gust Alternating Load Levels	A-8

TABLES

A-1	Alternating Load Occurrence Summary	A-9
A-2	Flight Type Definition	A-9
A-3	Alternating Load Allocation for Climb, Cruise, and Descent Test Phases	A-10

PAGE A-2 INTENTIONALLY BLANK

PRECEDING PAGE BLANK NOT FILMED

ORIGINAL PAGE IS
OF POOR QUALITY

FATIGUE SPECTRUM

The selection of a base mission for spectrum definition was made by reviewing the original 737 fatigue analysis and the 10 years of service history since the 737 was introduced. Existing fleet service utilization data were investigated. This information showed that there will be approximately 50 000 flights in 20 years for the median utilized aircraft with an average flight length between 463 km (250 nmi) and 741 km (400 nmi). The 463-km (250-nmi) range was selected as the base mission, based on the fact that metallic fatigue damage per flight for the 737 spectrum has been constant between the 463-km (250-nmi) and the 741-km (400-nmi) missions.

The 463-km (250-nmi) flight profile defined in the existing 737 fatigue analysis consists of 24 segments, each with 1g gust and maneuver loads. The total flight profile has been reviewed. The test flight profile was reduced to six major flight phases defined as taxi, takeoff, climb, cruise, descent, and landing. The taxi, takeoff, and landing phase alternating loads are of a relatively small magnitude and are represented by single excursions of the 1g load plus the secondary cycle excursion. Significant alternating load activity exists during climb, cruise, and descent phases, so these test phases will contain an appropriate number of alternating load peaks about the 1g load levels. The load sequence has been developed to be similar to the European standard spectra TWIST and FALSTAFF (refs. A-1 and A-2), in which flight conditions of varying severity are applied with more and larger load peaks in severe flights than in lesser flights. The resulting general load sequence is shown in Figure A-1.

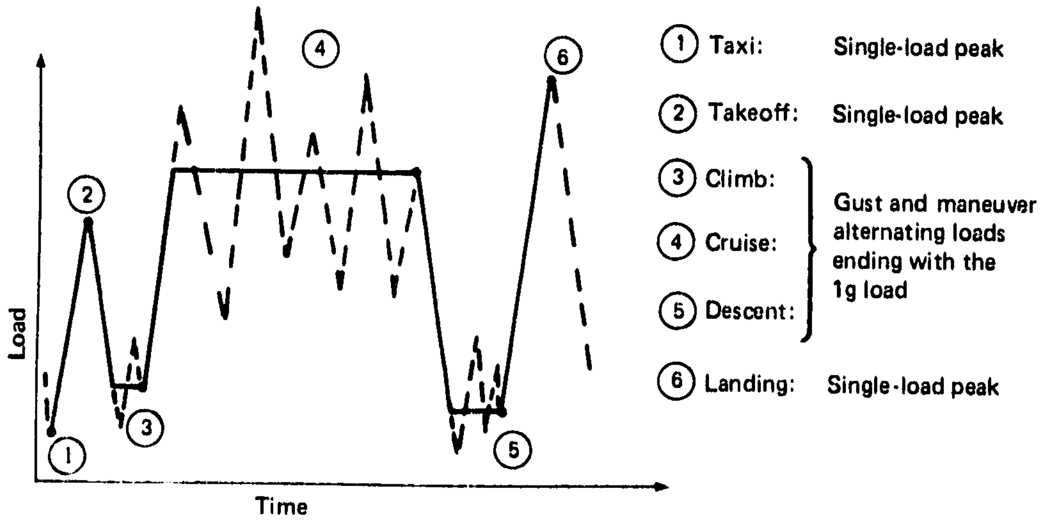
Load
Time
①
②
③
④
⑤
⑥
① Taxi: Single-load peak
② Takeoff: Single-load peak
③ Climb:
④ Cruise:
⑤ Descent:
Gust and maneuver alternating loads ending with the 1g load
⑥ Landing: Single-load peak

Figure A-1. Test Spectrum General Loading Sequence

PAGE A-4 INTENTIONALLY BLANK

ORIGINAL PAGE IS
OF POOR QUALITY

Prior to selecting the number and magnitude of alternating load peaks, the importance of small-cycle omission and large-cycle truncation was investigated. In previous graphite-epoxy fatigue testing, Schutz and Gerharz (ref. A-3) used an omission level of 6% of ultimate as a baseline and found that further omission resulted in life increase. Based on this testing, the omission levels were set at 6% of ultimate for maneuver and 3% of ultimate for gust. This resulted in an average of 10 maneuver and 7 gust load cycles per test flight, or an average of 20 load cycles per test flight including the secondary GAG cycles.

Truncation load levels were examined according to the standard spectrum TWIST (ref. A-1), which truncates at the load level exceeded 10 times per lifetime. Schutz and Gerharz showed that truncation of the highest test spectrum loads to 90% had virtually no effect on the fatigue life of graphite-epoxy.

Based on this examination, truncation levels were conservatively set at the load exceeded five times per lifetime, which corresponds to approximately 90% of the load exceeded once in two lifetimes. Therefore, based on the previously defined 50 000 flights per lifetime, the test spectrum will be constructed from 10 000-flight blocks.

Eight gust and eight maneuver alternating load levels were defined, resulting in the stepped exceedance curves shown in Figures A-2 and A-3. Table A-1 lists the resulting occurrences of gust and maneuver incremental loads to be applied in one 10 000-flight block.

Many of the alternating loads contained in the test spectrum occur less than once per flight, necessitating several test flight types with different severities and frequencies. Test flight severity levels were defined in a similar manner to those defined in TWIST, (ref. A-1). Eight flight types were defined to produce an array in which each succeeding flight includes a larger load level. The resulting frequency and cyclic load content of the eight flight types are shown in Table A-2.

The distribution of gust and maneuver loads between climb, cruise, and descent test phases in each test flight type was made to match the overall distribution for 10 000 flights shown in Table A-1. The resulting gust and maneuver load allocation for these three test phases is shown in Table A-3. The sequence of flight types in the 10 000-flight block will be controlled to result in a uniform distribution of flight types.

ORIGINAL PAGE IS
OF POOR QUALITY

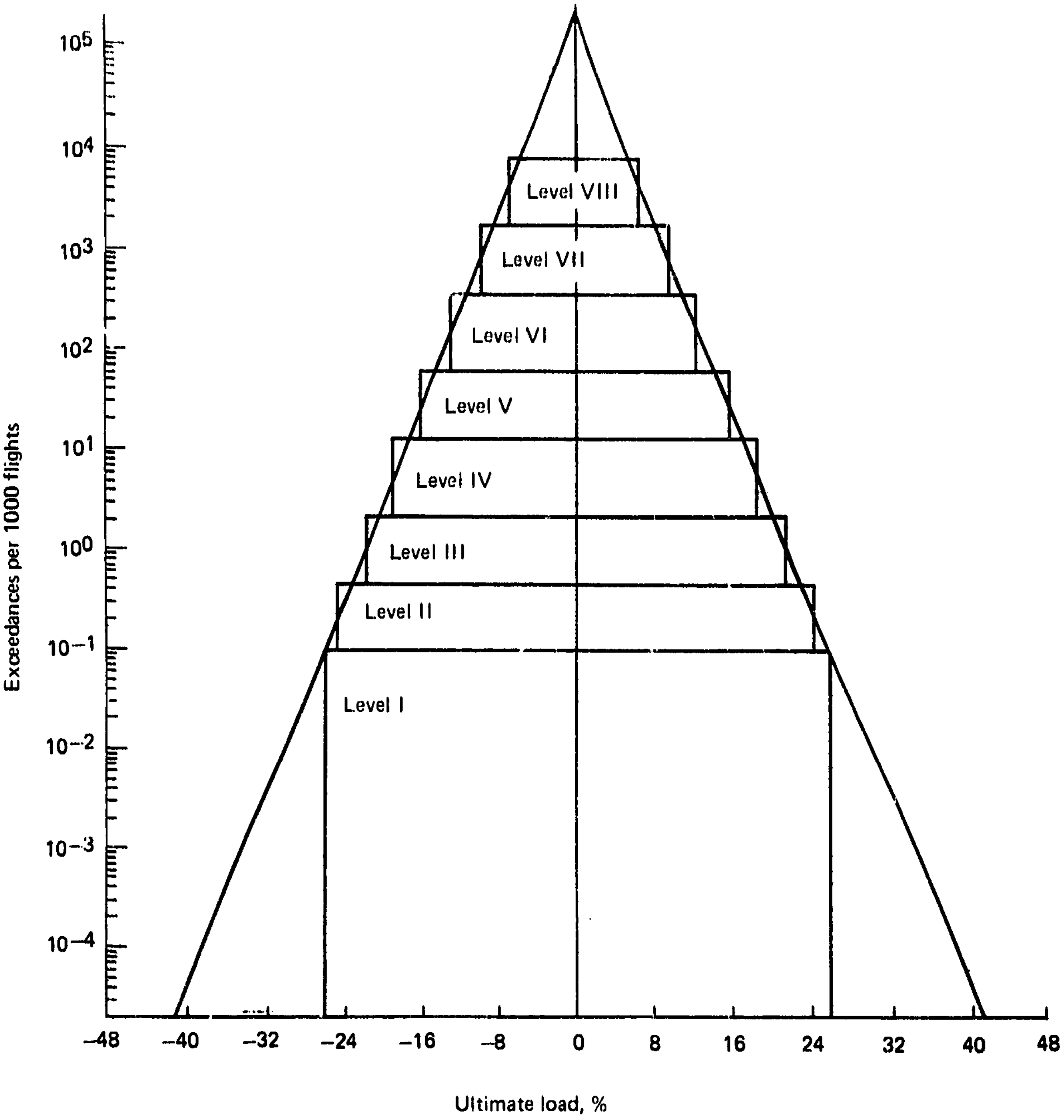

Figure A-2. Maneuver Alternating Load Levels

ORIGINAL PAGE IS OF POOR QUALITY

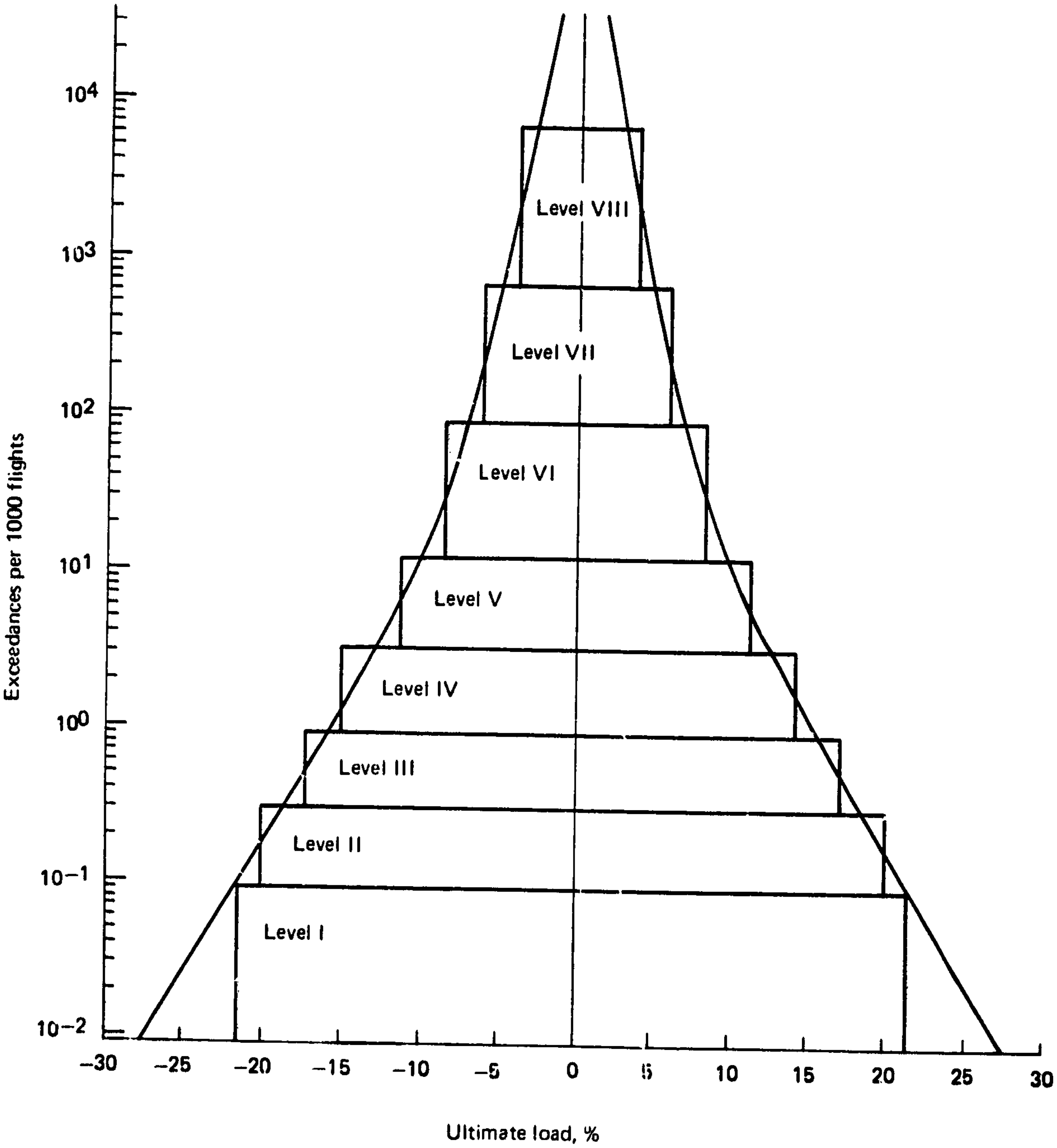

Figure A-3. Gust Alternating Load Levels

C-7

ORIGINAL PAGE IS
OF POOR QUALITY

Table A-1. Alternating Load Occurrence Summary

Load type	Load level	Load cycle occurrences in 10 000 flights			
		Climb	Cruise	Descent	Total
Gust	VIII	8 797	40 548	13 966	63 311
	VII	718	3 955	1 128	5 801
	VI	87	575	138	800
	V	8	74	13	95
	IV	2	18	2	22
	III	1	5	1	7
	II	0	2	0	2
	I	0	1	0	1
Maneuver	VIII	11 040	55 722	14 896	81 658
	VII	2 152	10 122	2 699	14 973
	VI	426	1 875	497	2 798
	V	85	350	92	527
	IV	17	67	17	101
	III	3	12	3	18
	II	1	2	1	4
	I	0	1	0	1

Table A-2. Flight Type Definition

Flight type [1]	Number of gust load cycles at eight amplitude levels								Number of maneuver load cycles at eight amplitude levels								Number of load points in one flight
	I	II	III	IV	V	VI	VII	VIII	I	II	III	IV	V	VI	VII	VIII	
A 1	1	1	2	2	6	14	112	766	1	3	5	2	7	3	2	3	1866
B 1		1	1	2	6	10	91	655		1	3	3	7	2	2	2	1578
C 5			1	1	2	2	39	468			2	8	7	3	1	5	1084
D 14				1	1	2	14	166				4	12	8	6	7	448
E 62					1	2	4	73					5	13	10	15	252
F 620						1	3	15						3	8	10	86
G 3100							1	6							3	8	42
H 6200								4								8	30

[1] Number of flights in a 10 000-flight block

**ORIGINAL PAGE IS
OF POOR QUALITY**

Table A-3. Alternating Load Allocation for Climb, Cruise, and Descent Test Phases

Flight type [1]	Climb gust Number of load cycles at 8 amplitude levels								Cruise gust Number of load cycles at 8 amplitude levels								Descent gust Number of load cycles at 8 amplitude levels							
	I	II	III	IV	V	VI	VII	VIII	I	II	III	IV	V	VI	VII	VIII	I	II	III	IV	V	VI	VII	VIII
A 1			1	1	1	2	14	109	1	1	0	0	4	9	73	489			1	1	1	3	25	168
B 1				1	1	2	11	91		1	1	0	4	6	60	419				1	1	2	20	145
C 5					1	1	3	65			1	1	1	0	28	300					0	1	8	103
D 14						1	0	24				1	0	0	10	107					1	1	4	35
E 62						1	1	8					1	0	1	51						1	2	14
F 620							1	2						1	1	9							1	4
G 3,100								0							1	5								1
H 6,200								1								2								1

Flight type [1]	Climb maneuver Number of load cycles at 8 amplitude levels								Cruise maneuver Number of load cycles at 8 amplitude levels								Descent maneuver Number of load cycles at 8 amplitude levels							
	I	II	III	IV	V	VI	VII	VIII	I	II	III	IV	V	VI	VII	VIII	I	II	III	IV	V	VI	VII	VIII
A 1		1	2	1	3	1	1	0	1	1	1	0	1	1	1	2		1	2	1	3	1	0	1
B 1			1	1	2	1	1	0		1	1	1	1	0	1	1			1	1	4	1	0	1
C 5				3	2	2	0	2			2	2	2	0	0	3				3	3	1	1	0
D 14					5	3	3	4				4	2	1	1	2					5	4	2	1
E 62						6	4	7					5	0	3	8						7	3	0
F 620							3	2						3	1	4							4	4
G 3,100								1							3	7								0
H 6,200								1								5								2

[1] Number of flights in a 10,000-flight block